

2 Estimation of ground movements

Estimation of settlement caused by the withdrawal of subsurface support is a much more imprecise operation than the estimation of settlement caused by surface loading. The latter has benefited from analytical examination and field observation over a period of many years, but there is as yet no analytical solution for the former. Either some more-or-less empirical assumptions have to be made about ground behaviour, or numerical solutions must be sought. Whichever method is adopted, there is a requirement for tunnel designers to reassess their estimates carefully in the light of their own experience and that of others. Designers should ask whether their estimates seem sensible, whether the assumptions (for example, of transverse settlement symmetry) are really valid in the field circumstances that apply, and whether their specification of input conditions is overcautious. Experience suggests, in fact, that there is a tendency to err rather too much on the side of caution when specifying the input parameters for estimation. Of course, a major requirement is for good site investigation information on ground conditions; knowledge of adjacent building foundations; and knowledge of the location, construction and condition of buried pipelines that could be affected by the tunnel excavation. These matters are discussed later in the book.

To aid ground movement estimation, a body of settlement case history data is included in Table 2.1. This was originally published by Attewell (1978a), updated by Tsutsumi (1983) and further extended for this book. It includes information on tunnel size and depth, maximum settlement, settlement trough width, volume and slope, ground description, geotechnical properties and method of working.

2.1 Volume loss parameter, V_t

For any attempt at analysis it is convenient to distinguish between cohesive clay soils and non-cohesive granular soils, while recognizing that not all soil materials likely to be tunnelled fall comfortably into these categories. It is also necessary to recognize that the thrust of the analyses in this book relates to soils which, when relaxed, deform under a degree of self-control. Such soils usually possess some cohesion through the presence of clay minerals and/or a more amorphous cementing agent and/or moisture under suction (negative)

Table 2.1 Case history data on some tunnels and tunnelling conditions. Information is compiled, with additions, after Peck (1969), Attewell (1978a), Tsutsumi (1983), where detailed references should be sought. z_0 is usually taken as tunnel axis depth, c_u is the undrained shear strength of the ground and γ is its bulk unit weight; $\frac{V_s}{c_u} \cdot c_u$ is the stability ratio; V_t is the excavated volume expressed per unit advance distance; V_s is the surface settlement volume expressed per unit tunnel advance distance; V_s° expresses V_s as a percentage of V_t ; i is the distance from the tunnel centre line to the point of inflection on an assumed normal probability form of transverse surface settlement trough; w is the 'practical' half-width of the transverse surface settlement trough; β is the angle formed to the vertical by a line tangent to the tunnel extrados and joining the point $y = 3i$ or $2.5i$; an asterisk against any value denotes an estimated quantity.

Tunnel	Maximum recorded surface settlement	Tunnel data	Ground geotechnical properties	Volumes	Settlement trough width	Tunnelling method and soil conditions								
						Dia- meter $2R$ (m)	$\frac{z_0}{2R}$ (m)	w (mm)						
						c_u (kN/m ²)	$\frac{V_s}{c_u}$ (m ³ /m)	V_t (m ³ /m)						
						V_s (%)	i (m)	i/R (m)						
							$3i$	$w = 2.5i$ (m)						
1. London Transport Fleet Line, Green Park (Attewell and Farmer, 1974 a, b)	29.3	4.15	7.06	6.17	270	2.1	13.52	0.199	1.4	12.6	6.1	37.8	32.0	Shield construction. Cast iron lining, 7 segments per ring, erected in shield tail. Annulus behind rings contact grouted every stope. Stiff, fissured, overconsolidated London Clay. Tunnel horizon blue clay overlain by weathered brown clay.
2. N.W.A. Sewerage Scheme, Hebburn, Tyneside (Attewell <i>et al.</i> , 1975)	7.5	2.01	3.9	7.86	75	2.02	3.17	0.077	2.42	3.9	3.71	11.7	9.75	Shield construction. 5-segment precast concrete lining per ring erected in shield tail. Annulus behind rings contact grouted every 3 rings. Laminated clay overlain by stony clay.
3. N.W.A. Sewerage Scheme, Willington Quay Syphon, Contract 32 (Attewell <i>et al.</i> , 1978)	13.375	4.25	3.15	81.5	33	9.4	24.37	1.86	13.1	9.1	4.28	27.3	22.7 ($\beta = 57^\circ$)	Shield construction. Compressed air pressure 90 kN/m ² . 7-segment precast concrete lining per ring erected in shield tail. Annulus behind rings contact grouted every 3 rings. Silty alluvial clay with sand and gravel lenses containing water at artesian pressure.

Table 2.1 (Contd.)

Tunnel	Maximum recorded surface settlement							Ground geotechnical properties			Settlement trough width			Tunnelling method and soil conditions	
	Depth (m)	Dia. (m)	$\frac{z_0}{2R}$ (mm)	w (mm)	c_u (kN/m^2)	$\frac{\gamma z_0}{c_u}$ (m^3/m)	V_s (m^3/m)	$\frac{V_s}{V_s^0}$	i (m)	i/R (m)	$\frac{3i}{w} = 2.5i$ (m)				
4. N.W.A. Sewerage Scheme, Howdon, Tyneside (Glossop, 1978)	14.18	3.625	3.91	11.2	100	2.98	0.37	0.194	1.9	6.9	3.81	20.7	17.25 $(\beta = 47^\circ)$	Shieldless construction. 5-segment precast concrete lining per ring erected up to the face. Annulus behind rings contact grouted every three rings. Boulder/stony clay.	
5. London Transport Fleet Line, Regent's Park Northbound Tunnel (Barratt and Tyler, 1975)	20	4.15	8.2	7	230	1.70	13.52	0.18	1.3	10.3	4.96	30.9	25.75 $(\beta = 50^\circ)$	Shield construction. Expanded concrete segmental lining. Stiff fissured, overconsolidated London Clay.	
6. London Transport Fleet Line, Regent's Park, Southbound Tunnel (Barratt and Tyler, 1976)	34	4.15	8.2	5	230	1.7	13.52	0.19	1.4	15.2	7.32	45.6	38 $(\beta = 47^\circ)$	Shield construction. Expanded concrete segmental lining. Stiff fissured, overconsolidated London Clay.	
7. London Transport Experimental Tunnel, New Cross Boden and McCaull, 1976)	10	4.15	2.4	21.5	—	—	—	—	—	—	—	—	12.5 $(\beta = 46^\circ)$	Slurry (bentonite) shield. Sandy gravel.	
8. TRRL Tunnelling trials, Chinnor (Hignett and Boden, 1974; McCaull <i>et al.</i> , 1976)	8	5	1.6	8	—	—	—	—	—	—	7	3	21 $(\beta = 7^\circ)$	Full-face tunnelling machine; cruciform head with drag picks. Jacking against a two-section reaction ring. Lining comprised mining arches at 1 m spacing. Highly discontinuous Lower Chalk formation.	
9. Washington D C Metro, Lafayette Square (Butler and Hampton, 1975)	11.6	6.4	2.25	112.8	—	—	—	—	4.60	1.21	3.8	4.5	13.5 $(\beta = 35^\circ)$	Shield construction with bucket digger. Primary liner of steel ribs and hardwood lagging boards expanding during and after the shove. Sand-cement-bentonite grout injected originally through liner but later through shield at the front. Sand and gravel, interbedded silty sand, sand and clay.	
10. Washington D C Metro, Project A-2, 1st Tunnel C Line	14.6	6.4	2.3	152	75	4	—	—	—	—	—	—	11.25 $(\beta = 28^\circ)$	Shield construction with bucket digger. Primary liner of steel ribs and timber lagging expanded during and after the shove. Partial dewatering with wells 60 m apart on centre line. Medium dense silty sand and gravel, interbedded with sandy, silty clays.	
B Line	14.6	6.4	2.3	139	75	4	—	—	—	—	—	—	11 $(\beta = 28^\circ)$	Articulated shield with bucket digger. Steel segments erected in tailskins and grouted before shove.	
A Line	14.6	6.4	2.3	76	75	4	4.0	1.0	3.5	5.4	1.7	16.2	14 $(\beta = 36^\circ)$	Dense sand and gravel, very dense, slightly cemented sand.	
11. Washington D C Metro, Treasury Yard (Hansmire, 1975)	11.6	6.4	1.8	280	75	3	6.02	1.4	4.3	1.9	0.6	5.7 $(\beta = 9^\circ)$	Shield construction with ripper bucket digger. Primary liner of steel ribs (4 section) placed on 4 ft centres with full timber lagging. Lining expansion during and after shove. Medium dense silty sand and gravel interbedded with sand, silty clays.		
12. Washington DC 1st Tunnel Section A	20.9	6.4	3.3	6	—	—	—	—	—	—	0.1	5.1	1.6 $(\beta = 12^\circ)$	Articulated shield with bucket digger. Steel segments erected in tailskins and grouted before shove.	
Section B	23	6.4	3.6	3	—	—	—	—	—	—	0.1	0.3	—	Dense sand and gravel, very dense, slightly cemented sand.	

SOIL MOVEMENTS

Table 2.1 (Contd.)

Tunnel	Tunnel data	Diaphragm meter	Depth (m)	$\frac{z_0}{2R}$	w (mm)	c_u (kN/m ²)	$\frac{z_0}{c_u}$	V_t (m ³ /m)	V_s (m ³ /m)	V_o (%)	i (m)	$\frac{3i}{i/R}$ (m)	$w = 2.5i$ (m)	Settlement trough width	Tunnelling method and soil conditions
13. Frankfurt Shield, Fohrgasse (T-9) (Chambosse, 1972; Sauer and Lama, 1973; Breth and Chambosse, 1972)	12.4	6.5	1.9	70	—	—	2.23	0.86	2.6	4.9	1.5	14.7	1.2	Shield construction. Bolted concrete segments. Sand with some limestone and clay marl lenses.	
14. Frankfurt, Domplatz (Authors as in 13)	15	6.5	2.3	23	130— 550	0.6— (1.5 av.)	0.47	0.39	1.2	6.8	2.1	20.4	17 ($\beta = 42^\circ$)	Shield construction. Bolted concrete segments. Frankfurt clay marl with some limestone and sand lenses.	
15. Frankfurt Shield, Dominikanergasse (Authors as in 13)	10.3	6.5	1.6	140	—	—	5.58	1.36	4.1	3.9	1.2	11.7	10 ($\beta = 33^\circ$)	Shield construction. Bolted concrete segments. Sand with some limestone and sand lenses.	
16. Frankfurt No shield, Bauols 18a Tunnel 13 (Authors as in 13)	13.3	6.5	2.1	13	130— 550	0.6— (1.5 av.)	0.16	0.23	0.7	7.1	2.2	21.3	18 ($\beta = 48^\circ$)	Shieldless construction: heading and bench. Soil anchors; shotcrete and light steel ribs for support. Frankfurt clay marl with some limestone and sand lenses.	
17. Frankfurt No shield, Bauols 18a Tunnel 13 (Authors as in 13)	13.3	6.5	2.5	10	130— 550	0.6— (1.5 av.)	0.09	0.18	0.5	7.1	2.2	21.3	18 ($\beta = 43^\circ$)	Shieldless construction: heading and bench. Soil anchors; shotcrete and light steel ribs for support. Frankfurt clay marl with some limestone and sand lenses.	
18. Heathrow Cargo Tunnel (Wood and Gibb, 1971; Smyth-Osbourne, 1971)	13.3	10.9	1.2	12	72— 295	1.4— (2.5 av.)	0.04	0.19	0.2	6.5	1.2	19.5	16 ($\beta = 38^\circ$)	Shield construction and hand excavated. No tail to the shield-concrete segmental lining expanded behind shield. Upper part of London Clay with 3.6 m of clay cover under wet gravel.	
19. São Paulo Metro, Bôa Vista, Costa et al., 1974	11.8	5.5	2.2	70	—	—	6.0	1.2	5	6.9	2.5	20.7	17 ($\beta = 50^\circ$)	Shield construction with compressed air. Sand and clay lenses.	
20. Brussels Metro (Vinnel and Herman, 1969)	16	10	1.6	150	—	—	5.0	2.0	2.5	5.5	1.1	16.5	13 ($\beta = 26^\circ$)	Shield construction, hand excavated. Lining segments built in tail. Upper half of tunnel uniform cohesionless sand; lower half of tunnel clayey sand.	
21. Mexico City Syphon II, Gonzalez (Timajero and Vitelez, 1972)	11.7	2.9	4.0	105	40	5	78.9	2.1	38	7.8	5.4	23.4	20 ($\beta = 58^\circ$)	Shield with oscillating cutters. Steel lining. Lining grouted 8 m behind shield. Cutters offer support to three-quarters of face. Ground dewatering before tunnelling. Plastic lacustrine clay.	
22. Lower Market St, B.A.R.T., San Francisco (Kuesel, 1972)	19.0	5.5	3.4	36	40	14	1.73	0.64	2.7	6.9	2.5	20.7	17 ($\beta = 37^\circ$)	Shield with a rotating cutter wheel. Compressed-air support. Grouted segmental lining. Soft plastic clay.	
23. Washington DC, F2a-1 Route Tunnels (Cording et al., 1976)	1 IB	20.3	5.5	3.7	5	—	—	0.06	0.12	0.5	—	—	—	Articulated (3-segment) shield construction. Excavation by large, half-moon shaped, hydraulically-operated digger spade. Tunnelling below the water table, but ground dewatered by deep well pumping in advance of tunnel construction. Segmental steel lining erected in tail of shield. Series as both a primary and secondary or temporary support. Very variable medium stiff-to-hard clays; clayey sands—sandy clays; coarse sand and gravel.	
3 IB	20.3	5.5	3.7	3	—	—	0.02	0.07	0.3	—	—	—	—	—	
9 IB	22.5	5.5	4.1	8	—	—	0.16	0.2	0.8	8.52	3.1	25.56	21 ($\beta = 39^\circ$)		
10 IB	21.4	5.5	3.9	13	—	—	—	0.42	0.32	1.3	—	—	—	—	
11 IB	22.0	5.5	4.0	10	—	—	0.23	0.23	1.0	9.90	3.6	27.7	25 ($\beta = 45^\circ$)		

ESTIMATION OF GROUND MOVEMENTS

Table 2.1 (*Contd.*)

Tunnel	Tunnel data	Maximum recorded surface settlement	Ground geotechnical properties	Volumes	Settlement trough width	Settlement trough width	Tunnelling method and soil conditions
24. Mission Line, B.A.R.T., San Francisco (Peck, 1969)	Depth meter $z_0 = 2R$ (m) Dia. $\frac{z_0}{2R}$ (mm)	$w = \frac{z_0}{2R}$ (mm)	c_u (kN/m ²)	Σ_{t_0} (m ³ /m)	V_t (m ³ /m)	V_s (m ³)	i (m) i/R (m) $3i$ (m) $w = 2.5i$ (m)
25. Toronto Subway (Peck, 1969)	10.97	5.33	2.06	10.5 (9-12)	22.31	0.11	0.5 1.57 12.6 10.5 Mechanical shield tunnelling with 90 kN/m ² compressed air. Dense, silty fine sand (SPT N = 30) with occasional thin lenses of peat. Dewatering by deep wells.
26. Mission Line, B.A.R.T., San Francisco (Peck, 1969)	11.89	30.5 (13.41 10.36)			21.07	0.21	1.0 2.7 1.04 7.1 6.7 Shield tunnelling, hand excavation. Medium-to-fine uniform dense sand (SPT N-value = 40 to 60) above the water table.
27. Wilson Tunnel, Hawaii (Peck, 1969)	15.24	10.06	1.51	21.3			
28. Wilson Tunnel, Hawaii (Peck, 1969)	30.48	10.06	3.03	61.0			
29. Garrison Test Tunnel (Burke, 1957)	36.88	10.97	3.36	18.29 (6.1- 24.4)	958	0.77	94.51 79.48 Ribs and lagging support. Full-face blasting in a clay shale having an unconfined compressive strength of 958 kN/m ² . As for 27.
30. Subway Contract D.3, Chicago, (Peck, 1969)	23.47	7.31	3.2	36.6	38- 78	8.09	41.97 0.08 0.20 0.9 0.25 2.7 2.55 Hand-excavated, horseshoe-shaped cross-section tunnel. Face benched and tunnel supported by ribs and liner plates. Compressed air pressure of 30 kN/m ² . Bottom half of tunnel in hard clay. Stiff clay (unconfined compressive strength = 96-192 kN/m ²) for 3 m above crown. Soft-to-medium clay (u.c.s. = 36-96 kN/m ²) above that.
31. G.N.R.R., Seattle (Hussey <i>et al.</i> , 1915)	37.49	11.89	3.15	18.3	—	111.03	2.88 2.6 63.0 10.59 181.0 157.5 Hand-excavated using small drifts with a central core. Timbered support for hard clayey till. Raveling at the crown; pole bars used.
32. Kyoto, Tokyo, Subway (Shiraishi — personal communication to Peck)	22.55	7.01	3.22	12.2	77	5.85*	38.59 1.66 4.3 54.4 15.52 163.2 132 Hand-excavated sectional shield. Face breasted and lining segments erected in shield. Normally consolidated sensitive clay (u.c.s. = 72 kN/m ²) requiring no compressed air support.
33. B.A.R.T., San Francisco (Peck, 1969)	17.98	5.48	3.28	46.0	77	4.67*	23.67 1.02 4.3 8.9 3.24 26.7 22.2 Shield tunnelling with breasted face. Liner segments erected behind the shield. Moderately sensitive clay (u.c.s. = 77 kN/m ²) requiring no compressed air support.
34. Ottawa Sewer (Eden and Boozuk, 1968)	18.29	3.05	6.00	6.1	354	1.03*	7.31 0.12 1.6 7.9 5.18 23.7 19.7 Mechanical shield excavation. Liner segments erected behind the shield. Sensitive Leda clay (u.c.s. = 354 kN/m ²) required 28-34 kN/m ² compressed air support.
35. Toronto Subway (Matish and Cating, unpublished)	13.11	5.33	2.46	22.0 (13- 29)	67	3.91*	22.31 (0.13- 0.3) 0.95 3.8 1.42 11.4 9.5 Shield tunnelling, hand excavation. Air pressure of 69-83 kN/m ² . Silty clay (u.c.s. = 77 kN/m ²) at invert level.
36. Chicago D.5 (Peck, 1969)	11.89	6.10	1.95	39.6 (18.3- 61.0)	67	3.55*	29.22 (0.23- 0.3) 0.95 2.8 0.92 8.4 7.0 Hand-excavated bunched heading with rib and liner plate support. Glacial lake clay (u.c.s. = 57 kN/m ²) at axis level and 33 kN/m ² at 3 m depth. Nearer surface, ground is stronger.

Table 2.1 (Cont'd.)

Tunnel	Tunnel data		Maximum recorded surface settlement		Ground geotechnical properties		Volumes		Settlement trough width		Tunnelling method and soil conditions	
	Depth meter z_0 (m)	Dia- meter $2R$ (m)	$\frac{z_0}{2R}$	w (mm)	c_u (kN/m ²)	γz_0 (kN/m ²)	V_s (m ³ /m)	V_c (m ³ /m)	i (m)	i/R (m)	$3i$ (m)	$w = 2.5i$ (m)
37. Toronto Subway (Peck, 1969)	10.36	5.33	1.94	85	—	—	22.31	0.42	1.9	0.73	5.7	4.7
First Tunnel	13.41	5.33	2.52	140	—	—	22.31	0.85	3.8	2.4	9.2	6.0
Second Tunnel	30.48	2.74	11.12	204	—	—	5.9	2.97	50.39	5.8	4.2	17.4
38. São Paulo (Terzaghi, 1950)	—	—	—	—	—	—	—	—	—	—	—	—
39. Ayrshire Joint Drainage Scheme Tunnel (Eadie, 1976)	6.3	2.59	2.43	13.5	—	—	6.89	0.06	0.87	1.41	1.09	1.23
First Tunnel	6.2	2.59	2.39	16.0	—	—	6.89	0.06	0.87	1.60	1.23	4.80
Second Tunnel	—	—	—	—	—	—	—	—	—	—	—	—
40. Acton Grange Sewer, Warrington	5.75	2.44	2.36	19.9	—	—	6.16	0.086	1.37	1.73	1.42	5.19
Section C-C'	5.75	2.44	2.36	14.2	—	—	6.16	0.071	1.10	2.00	1.64	6.00
Section D-D'	(O'Reilly <i>et al.</i> , 1980)	—	—	—	—	—	—	—	—	—	—	—
41. White Mud Creek Tunnel, Edmonton, Alberta (Thomson and El-Mahhas, 1980) (authors as in 41)	15.25	6.05	2.52	—	—	—	—	—	—	—	—	—
42. 170 Street Tunnel, Edmonton, Alberta (authors as in 41)	21.5	2.56	8.40	12	—	—	—	—	—	—	—	—
43. Nagoya Subway (Kawamoto and Okuzono, 1977)	—	—	—	—	—	—	—	—	—	—	—	—
Section A	17.4	6.4	2.72	48	—	—	—	—	—	—	—	—
Section B	19.2	6.4	3.0	45	—	—	—	—	—	—	—	—
Section C	16.5	6.4	2.58	46	—	—	—	—	—	—	—	—
44. Stockton-on-Tees Stage 1 Interceptor sewer, Measurement Section D (McCaull, 1978)	6.28	1.26	4.98	43.7	30.5	2.7	1.25	0.38	30.4	3.48	3.47	5.51
45. Stockton-on-Tees Stage IV Interceptor sewer, Measurement Section D (McCaull, 1978)	5.86	1.26	4.65	56.3	41.7	2.2	1.25	0.52	41.5	41.7	3.68	5.84
46. New Cross L.T.E. Experimental Tunnel (Boden and McCaul, 1974)	10	4.15	2.4	21.5	—	—	13.52	0.27	2.0	5	1.82	15

Dense sand above ground water level.

Shield tunnelling, hand excavation through water-bearing raised beach sands of Clyde Estuary, Scotland. Timber bracing with face jacks. Internal pressure 1.4 to 1.6 atmospheres absolute. Non-expanding concrete lining segments with cement-bentonite grout injected into void at end of each 12h shift.

Slurry (bentonite) shield, machine excavated through a mixed face comprising mainly sand with some boulders but with a small proportion of Bunter Sandstone in the invert. Water-table level was partway up face. Bolted precast concrete segmental lining.

Two moles without shields (each 6.05 m diam.). Poorly indurated clay shale interbedded with thin sandstone strata. Bolted steel segmental ribs in temporary lining and replaced by plain concrete lining.

Mole with shield. Temporary lining consisted of segmental steel ribs and later replaced by plain concrete lining. Major portion of the tunnel excavated through till.

Shield tunnelling. Twin circular tunnels of 6.4 m diameter placed side by side. Tunnel constructed through the alluvium deposit.

Mini-Tunnel system. Hand excavation from shield. 3-segment, smooth, precast concrete lining. Soft, silty, sandy clay.

Table 2.1 (Contd.)

Tunnel	Maximum recorded surface settlement	Ground geotechnical properties	Volumes	Settlement trough width	Tunnelling method and soil conditions											
Tunnel data	Depth meter	Dia-meter	z_0	$2R$	w	c_u	γz_0	V_t	V_s	ψ_o	i	i/R	$3i$	w = 2.5i (m)		
47. Hamburg-Wilhelmsburg collector (Jacob, 1978)	19.24	4.48	4.3	0-10	—	—	—	—	—	—	—	—	—	Well-bedded, sharp sand and gravel (0.2-100 mm), boulders to 80 cm overlain by clay, peat and fill. Water table 1.6 m above invert. Hydro-shield. Reinforced concrete lining. Air pressure 1.6 atmospheres.		
48. Antwerp Metro (Jacob, 1978)	24	6.56	3.7	6-7	—	—	—	—	—	—	—	—	—	Hydro-shield. Reinforced concrete lining. Fine alluvial sand; interlayers of clay, overlying overconsolidated clay. Water table 12.1 m above invert, lowered to 10 m before tunnelling.		
49. Agasegawa Sewer Main No. 2, Katsushikaku, Tokyo (Eng. News Record, 1974)	av. 10	5.05	2.0	25-90	—	—	—	—	—	—	—	—	—	Slurry mole; concrete segmental primary lining. Mixed face of fine 'quick' sand and silt and clay, SPT N-value 20. Water table 7 m above crown.		
50. Takocho Water main, Suginami-ku, Tokyo (Miki et al., 1977)	27.8	3.55	7.8	21.9	max. 1.4 av.	—	—	—	—	—	0.3-0.6	1-2	4.38	1.41	13.13	10.95
51. Yotsugui Sewer Branch, Katsushikaku Tokyo (Miki et al., 1977)	7.4	2.40	3.1	20	—	—	—	—	—	—	—	—	—	Cemented dense sandy gravel (2-150 mm), SPT N-value 50, overlain by clay, sandy gravel and silt. Water table 11.5 m above crown.		
52. Chicago S-6 (Peck, 1969)	10.97	6.10	1.8	25.6 (15.0-36.6)	5-7	3.85*	29.22	0.15	0.5	2.3	0.75	6.9	5.7	Fully mechanized shield with full face and liner plate support. 83 kN/m ² compressed air support. Glacial late clay (uc.s. = 57 kN/m ²) at axis level and 33 kN/m ² at 3 m depth). Nearer surface, ground was stronger.		
54. Liner Plate Tunnel, Sabe SP, Brazil (Negro and Eisenstein, 1981)	8.0 appr.	3.6	2.22 av.	25.0	250	4.03	10.5	0.213	2.03	3.0	1.67	9.0	7.5	Full-face hand excavation with circular steel segmental lining plates erected immediately behind the face. Tertiary soft porous clay and clayey dense sand.		
55. Horseshoe Tunnel, Sabe SP, Brazil (Authors as in 54)	9.00 appr.	3.6	2.5	15.5	250	4.03	12.5	0.171	1.37	2.5	1.38	7.5	6.25	Same as 54 above.		
56. NATM Tunnel Sabe SP, Brazil (Authors as in 54)	8.5 appr.	3.96	2.14	5.0	250	4.28	12.8	0.048	0.37	3.0	1.52	9.0	7.5	Hand-excavated in three stages; heading, bench and invert. Shotcrete 10-13 cm thick, with 10 x 10 cm steel wire mesh. Soil conditions as 54 above.		
57. Anglian Water Authority Relief Sewer (O'Reilly and New, 1982)	(a) 8.0	2.7	2.96	95	12	13.4	5.73	0.905	15.8	3.8	2.81	11.4	9.5	Hand-excavated in shield; lined with concrete segments; compressed air applied about 20 days after excavation; lower 60% of face stiff story clay (Grimby Marine Warf) overlain with 2.5 m of stiff clay.		
	(b) 5.5	2.7	2.04	60	12	9.2	5.73	0.481	8.4	3.2	2.37	9.6	8.0			
	(c) 5.5	2.7	2.04	58	12	9.2	5.73	0.407	7.1	2.8	2.07	8.4	7.0			
	(d) 6.5	2.7	2.41	97	12	10.8	5.73	1.046	18.2	4.3	3.19	12.9	10.75			

Table 2.1 (Contd.)

Tunnel	Tunnel data	Maximum recorded surface settlement	Ground geotechnical properties	Volumes	Settlement trough width	Tunnelling method and soil conditions							
	Dia-meter	$\frac{z_0}{2R}$	$\frac{w}{R}$	$\frac{c_a}{(kN/m^2)}$	$\frac{V_s}{c_u} (m^3/m) (m^3/m)$	$\frac{V_s}{c_u} (\%)$	i (m)	i/R	$\frac{3i}{w} = 2.5i$ (m)				
58. Thames Water Authority, Sutton Sewer (O'Reilly and New, 1982)	(a) 17.1 (b) 3.4 (c) 4.9	1.78 1.78 1.52	9.61 1.91 3.22	3.8 3.7 7.1	180 90 9	1.89* 0.76* 1.09*	2.49 0.49 0.54	0.096 0.019 0.81	10.0 2.0 3.0	1.12 2.25 3.95	30.0 6.0 9.0	25.5 5.0 7.5	
59. Bristol City Engineers Dept. Avonmouth 2 Sewerage Scheme (Toombs, 1980)	6.0	3.4	1.76	20.0	18	6.67*	9.08	0.251	2.8	5.0	2.94	15.0	12.5
60. London Transport Interchange Subway at Kings Cross, London (West <i>et al.</i> , 1981)	14.06	4.13	3.4	4.0	230	1.22*	13.46	0.078	0.6	7.8	3.78	23.4	19.5
61. Thames Water Authority Oxford Trunk Outfall Sewer (O'Reilly and New, 1982)	11.7	2.82	4.15	2.2	200— 400	0.78*	6.24	0.028	0.44	5.0	3.55	15.0	12.5
62. WNTDC Lumb Brook Sewer (O'Reilly and New, 1982)	(a) 4.7 (b) 9.0 (c) 6.5 (d) 6.5 (e) 6.5	3.6 2.5 3.6 3.6 3.6	1.31 1.81 1.81 1.81 1.81	78.0 19.0 19.0 20.0 7.0	— — — — —	10.18 10.18 10.18 10.18 10.1	0.47 0.12 0.06 0.09 0.04	4.6 1.2 0.6 0.9 0.4	2.4 2.52 1.40 1.79 2.28	1.33 7.2 6.0 5.37 1.27	7.2 7.56 4.77 4.48 6.84	6.0 6.3 3.98 4.48 5.70	
63. North West Water Authority, Mersey Street to Howley Sewer (O'Reilly and New, 1982)	8.4	2.0	4.2	28.0	—	— 3.14	0.23 7.1	— 3.2	7.1 3.2	3.2 3.2	9.6	8.0	
64. Northumbrian Water Authority Sewerage Scheme, Ouseburn Valley (Spencer, 1978; Dobson <i>et al.</i> , 1979)	13.0	3.47	3.75	81.0	—	— 9.64	1.48 15.6	— 7.29	4.20 21.87	— 4.20	— 21.87	18.23	18.23
65. Budapest Metro (Ulrich, 1974)	(a) N-S Line (b) E-W Line	30	5.5 5.5	5.45 5.45	26 37	— —	23.76 23.76	0.83 2.2	0.29 0.11	9.23 30.25	3.35 11.00	27.66 90.75	23.05 75.62
66. Tyne and Wear Passenger Transport Executive, Running Tunnel, Eldon Square, Newcastle (O'Reilly and New, 1982)	14.2	5.21	2.73	7.5	200	1.4*	21.32	0.132	0.6	7.0	2.69	21.0	17.5

62. WNTDC Lumb Brook Sewer (O'Reilly and New, 1982)

Hand-excavated within shield; loose to medium sand with some gravel. Hand-excavated in medium to dense sand with some clay; cover of very stiff sandy clay. Partially stabilized medium dense sand and gravel with a little clay. Fully stabilized sand and gravel.

Hand-excavated within shield using compressed air; variable loose silty sand with some clay; tunnelling about 4 m below water table.

Shield tunnelling, hand-excavated in Oligocene clay overlain by sandy silt. Bolted concrete segmental lining.

Partial-face machine excavated in shield with compressed air. Glacial till, firm/stiff clay with some sand and gravel lenses.

Table 2.1 (Contd.)

Tunnel	Tunnel data	Maximum recorded surface settlement										Ground geotechnical properties				Settlement trough width				Tunnelling method and soil conditions				
		Dia-meter	$\frac{z_0}{2R}$	$\frac{z_0}{w}$	w	c_u	γz_0	V_t	V_s	i	i/R	$3i$	$w = 2.5i$											
67. Sewage Pipeline No. 352, Uchiku-cho Ibaraki (Miki <i>et al.</i> , 1977)	8.6	2.55	3.4	12.9	—	—	—	—	—	—	—	—	—	—	—	—	—	—	Slurry mole, segmental lining. Cemented fine (0.4 mm) clayey sand, overlain by sand, clay and silt. Water table 5.4 m above crown.					
68. Belfast Sewerage Scheme, Sydenham, Belfast. (Glossop and Farmer, 1977)	5	2.74	1.82	37.5	2.1	8.3	5.9	0.12	2.0	2.1	2.75	2.00	8.00	2.74 m diameter shield, 2 m long + 1 m tailskin. Compressed air spade excavation by hand. 41 kN/m^2 compressed air pressure for ground lining segments. 0.6 m long. Each ring grooved individually immediately after shield shove; 3–4 rings erected per shift. Belfast 'sleech'—soft organic silty clay with a high moisture content.										

pressure, noting that cohesion is enhanced by negative pore pressures. Granular soils without cohesion are more prone to collapse at the tunnel face, creating large vertical deformations which are less easily analysed and estimated for the purposes of support design at the tunnel (lining) and the protection of near-surface structures (buried pipelines and structural foundations). On this latter problem, reference may be made to Deere *et al.* (1969) and for a 'behavioristic' (*sic*) classification of various soils—ranging from cohesive to granular—see Figure 11.1, Appendix page 11–7 in that report.

2.1.1 Clay soil

It may be assumed that, during tunnelling in clay soil, the ground moves into the unsupported parts of the excavation at a constant rate. This particular problem was modelled by Attewell and Boden (1971) in the laboratory and is further described in Attewell (1978a). For shallow tunnels the overburden stress (on a depth times unit weight basis) can be regarded as supplying the driving pressure, and the rate of inward movement axially at the face proper is considered to be the same as that radially around the cut boundary. A laboratory-derived deformation rate of 0.0055 mm/min for London Clay was the same as that actually measured, using deep settlement probes, above the crown of a London Transport tunnel under construction (Attewell and Farmer, 1974a).

If clay soils tend to intrude into a tunnel at a constant rate for a given driving pressure, then it is obvious that the *rate of tunnel advance* can be a critical factor controlling ground loss. This rate of advance determines the time during which an element of soil at or near the opening is able to relax, and so the slower the rate of tunnel advance the greater is the total volume of soil intrusion at the tunnel for a material of particular rheological properties surrounding a tunnel of specified depth.

Referring to Figure 2.1, it is useful to consider the total ground loss V_t associated with open (hand) shield tunnelling, a bolted segmental lining constructed inside a tailskin welded to the rear of the shield body, and a cementitious contact grout injected behind newly-erected lining segments. These are the conditions that most frequently apply at present to British soft-ground tunnelling. The source contributions comprising the ground loss are as follows.

Face loss, V_f . This is the axial loss at the tunnel face proper. It contributes both to the transverse spread and to the extent of the forward longitudinal span of the surface settlement trough (see Figure 2.2).

Shield loss, V_p . This is the radial ground loss around the perimeter of a shield and its tail due to the presence of an overcutting bead or equivalent overcutting device installed to reduce ground friction with the extrados of the shield and to facilitate shield steering. There are also other losses V_y and V_x , discussed subsequently.

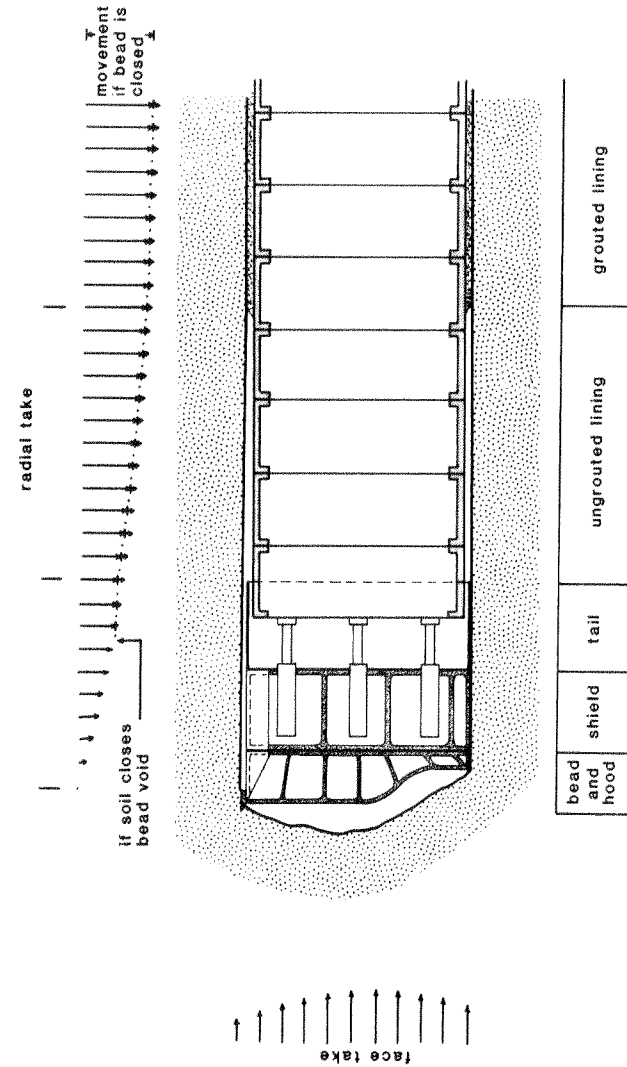


Figure 2.1 Simplified vertical cross-section along the centre line of a hand-driven shield-supported tunnel showing the likely zones of ground loss. For the purposes of clarity the possible deformations of the exposed soil surface are not shown within the cross-section but are indicated in exaggerated form outside the cross-section. Below the soffit, the radial movements will generally be somewhat smaller than those developing at the soffit.

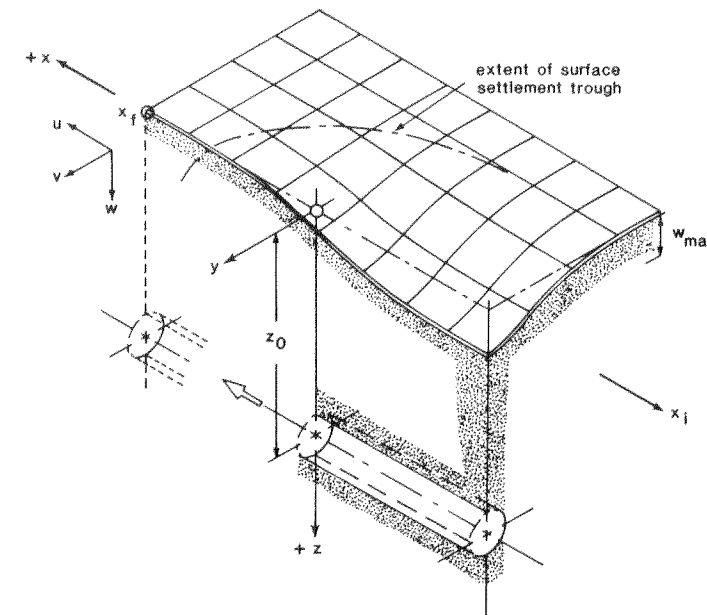


Figure 2.2 Tunnel face advancing in a $+x$ direction, creating a settlement (w) trough having a long axis of assumed cumulative probability form in the xz plane and a transverse axis of normal probability form in the yz plane. Axes x, y, z are orthogonal; $x = y = z = 0$ at ground surface vertically above the centre of the tunnel face. The tunnel start and final face positions are denoted by x_i and x_f , respectively. Ground displacements u, v, w , induced by tunnel excavation, occur in directions x, y, z , respectively.

Postshield/pregrout loss, V_u . This radial ground loss occurs behind the tailskin. It may be caused by uninterrupted continuous movement which began over the shield as a result of bead presence or, if the clay soil had encountered the shield, a reactivation of movement as the shield moves forward.

Postgrout loss, V_g . This radial loss occurs behind the tail of the shield until the set grout resists further inward movement of the ground.

The following parameters are used to analyse the problem.

m is the average amount of soil movement (displacement) at the tunnel and is more usefully expressed as dm/dt , the average rate at which the material moves unrestrained into the excavation. It is convenient to take, as an approximation, the same rate inwards axially at the face and radially over and behind the shield. Experimental work (Figure 2.3), specific to the problem, aimed at evaluating deformation rates in clay soils was performed by Attewell and Boden (1971) and others (see Attewell, 1978a, p. 871).

l is the tunnel advance distance, but again is more usefully expressed as dl/dt , an average rate of tunnel (and shield) advance.

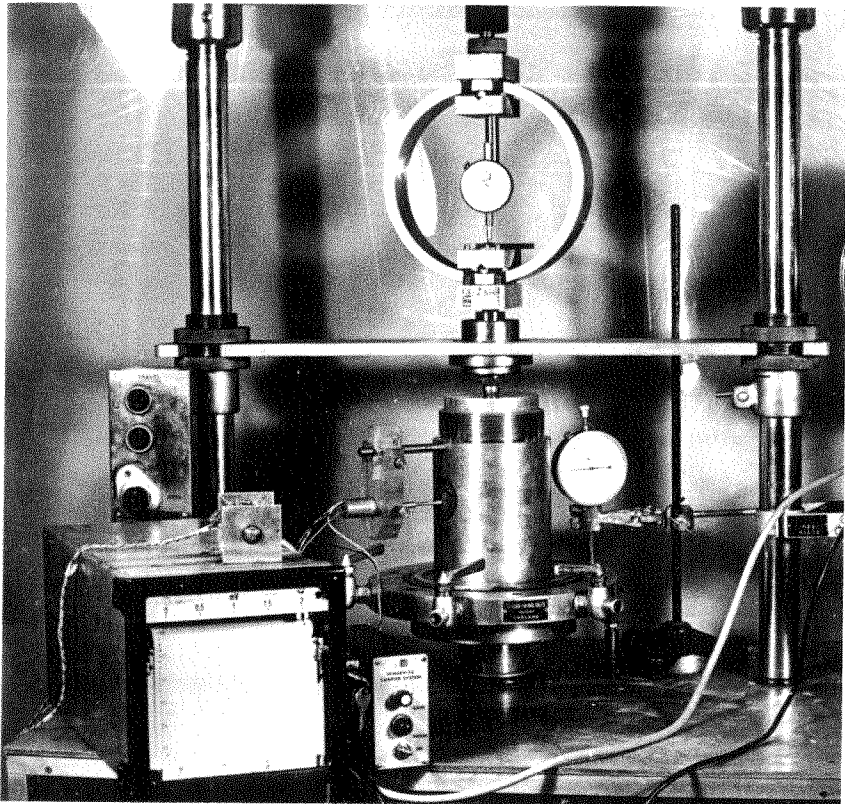


Figure 2.3(a) Equipment for estimating deformation rates in 100 mm undisturbed clay soil samples. The sample is extruded directly from a U100 tube into a brass cylinder and then compressed axially at a constant rate. Extrusion laterally through a hole of definable diameter is analogous to intrusion at a tunnel face, and is monitored by a linear variable differential transformer transducer.

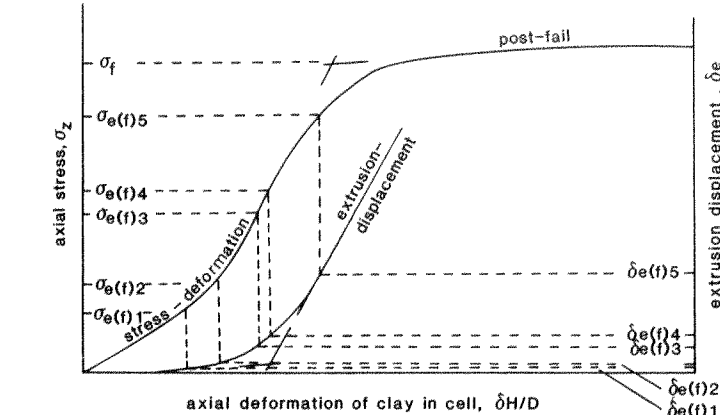
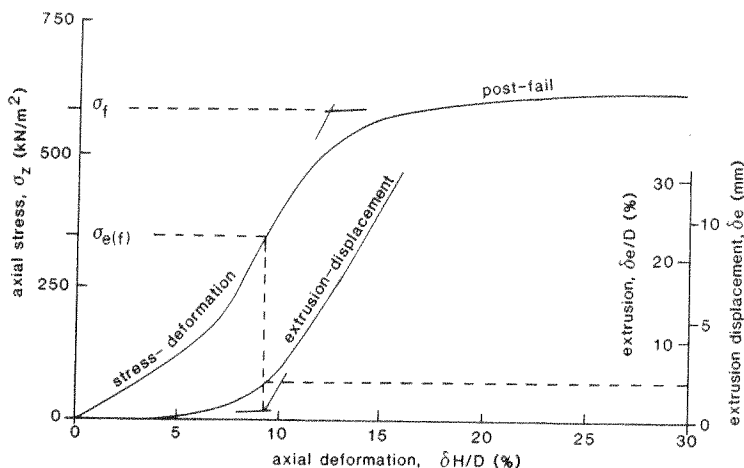


Figure 2.3(b) Result of a typical constant axial deformation rate test on a laminated clay (constant axial deformation rate of 0.593 mm/min). δH is the change in axial length of the sample in the cell under axial stress $\sigma_z (= \gamma z_0)$. Lateral extrusion δe occurs through hole of diameter D . Knowing the unit weight γ of the soil and the axis depth z_0 of the tunnel, rates of soil extrusion (tunnel face intrusion) can be assessed for different overburden pressures.

Surface situation	Critical overburden pressure	Definition of critical overburden pressure
<i>Super-critical</i> (e.g. important surface structures very sensitive to differential settlement)	$\sigma_z = \sigma_{e(f)1}$	Onset of extrusion acceleration—end of pre-acceleration 'linearity'
<i>Critical or near-critical</i> (e.g. less important surface structures, much less sensitive to differential settlement)	$\sigma_z = \sigma_{e(f)2,3,4}$	Range of $\sigma_{e(f)}$ values defined by the following lines constructed from point of intersection of pre- and post-acceleration curve:
	$\sigma_z = \sigma_{e(f)2}$	Horizontal back-projection (sub-maximum d^2e/dt^2)
	$\sigma_z = \sigma_{e(f)3}$	Angular bisector (approx. $d^3e/dt^3 = 0$)
	$\sigma_z = \sigma_{e(f)4}$	Vertical projection (Post maximum d^2e/dt^2)
<i>Sub-critical</i> (e.g. in an urban environment, under housing estates, etc.)	$\sigma_z = \sigma_{e(f)5}$	End of extrusion acceleration
<i>Non-critical</i> (e.g. under open land)	$\sigma_z = \sigma_f$	Ultimate stress-deformation yield—this could be apportioned in the same way as above, but there would be little merit in doing so

l_s is the length of the shield and its tail.
 a is the outer radius of the shield.

b is the thickness of any overcutting bead or equivalent device fitted to the shield.

Face loss, V_f . Ground losses at the face proper are a multiple of the area of the face πa^2 (ignoring the small contribution of any bead) and the soil intrusion distance per unit length of advance k if soil intrusion is assumed to take place uniformly over the whole face area. In practice, because of drag at the cutting end of the shield and particularly at the hood, a clay soil will tend to intrude more readily at the centre than at the periphery. Field measurements (section 2.11) using inclinometer access tubes intercepted at the tunnel face and also measurements taken in a shaft towards an approaching tunnel face confirm such a doming effect (Attewell, 1978a; and see Figures 2.40b, 2.41b). A factor of 50 per cent could reasonably be applied to take this doming into account but, to generalize, another factor k_1 , where $0 < k_1 < 1$, could be used so that

$$V_f = \pi a^2 k k_1. \quad (2.1)$$

The factor k may be expressed in terms of the average rate of soil movement at the face, $dm/dt = m'$, and the average rate of tunnel advance $dl/dt = l'$, so that

$$k = \frac{m'}{l'}. \quad (2.2)$$

Thus,

$$V_f = \pi a^2 k_1 \frac{m'}{l'} \quad (2.3)$$

or, as a percentage of the tunnel carcass volume per unit distance of advance (face area),

$$\% V_f = 100 k_1. \quad (2.4)$$

Equation (2.3) does not allow for the fact that when tunnel advance ceases the basic rate of clay inward movement should strictly remain the same. Cording *et al.* (1976) suggested, from the numerical modelling of Ghaboussi and Ranken (1975), that V_f may be approximately related to a parameter V_a , where V_a is the multiple of πa^2 and the soil intrusion m , independent of length of tunnel advance:

$$V_f = \frac{2V_a}{a} \quad \text{for } a \leq 2m \quad (2.5)$$

and

$$\% V_f = \frac{200m}{a}. \quad (2.6)$$

As before, allowing for any intrusive doming of the clay soil,

$$\% V_f = \frac{100\pi a^2 m}{\pi a^2} \times \frac{2}{a} = \frac{200k_1 m}{a}. \quad (2.7)$$

Cording *et al.* (1976) claim that equation (2.7) is applicable to most soils, including granular soils and stiff-to-hard clays.

The example, quoted in Attewell (1978b), of a 4.25 m diameter tunnel at an axis depth of 13.375 m in a silty alluvial clay, may be used to test these equations. Inclinometer measurements showed that face take began 3 days (6.71 m) before the tunnel face intersected a vertical inclinometer tube and increased to 3.17 mm at 0.7 m below tunnel axis level when the face was 1 day (1.83 m) away. Obviously the soil maximum inward displacement at axis level when exposed by excavation would exceed this figure of 3.17 mm. The $\% V_f$ value calculated from equation (2.4) was $0.06 k_1$. From equation (2.7), and extrapolating the measured movement to give a maximum displacement m of 4.6 mm, the estimated $\% V_f$ is $0.43 k_1$, or about 0.2 if k_1 is approximately 0.5.

Radial loss, V_b , over a shield. The construction detail of the shield tends to control the total volume of ground lost. A particular source of loss comprises a bead, or similar device, welded on to the leading edge of the hood and shield in order to overcut the ground, reduce friction during shield advance, and allow the shield to be steered more easily.

There are three usual cases: no bead ($V_b = 0$); the bead spans the upper 180° of hood and shield (Attewell and Farmer, 1974a, b); and the bead covers the full circumference (360°) of hood and shield (Attewell and Farmer, 1973; Attewell *et al.*, 1975).

For purposes of analysis assume a 360° bead. The area of shield and tail extrados over which radial deformation may take place is

$$A_s = 2\pi l_s(a + b) \approx 2\pi l_s a, \quad \text{since } b \ll a. \quad (2.8)$$

In terms of shield advance, the soil adjacent to the shield has the following time t_s in which to deform inwards:

$$t_s = \frac{l_s}{l'}. \quad (2.9)$$

During this time the soil movement m is

$$m = t_s m'. \quad (2.10)$$

Thus, the potential volume of soil moving radially into the excavation over the length of the shield is

$$V_b = A_s m = 2\pi l_s^2 a \frac{m'}{l'}. \quad (2.11)$$

Expressed per unit advance,

$$V_b = A_s m / l_s = 2\pi l_s a \frac{m'}{l'}. \quad (2.12)$$

Since the value of $m (= l_s m' / l')$ must be less than or equal to b , the latter applying when the bead has been completely closed by intrusion of the relaxed soil, another parameter, k_2 , is used:

$$V_b = 2\pi l_s a k_2 \frac{m'}{l'}, \quad (2.13)$$

where $0 < k_2 \leq l$.

Expressed as a percentage of the tunnel face area:

$$\% V_b = 200 l_s \frac{k_2 m'}{a l'}. \quad (2.14)$$

This last equation has been examined by Attewell (1978a) in the light of measurements taken during construction of a London Transport tunnel (Attewell and Farmer, 1974b). The following parameters applied: l_s (shield and tailskin) = 3.348 m, a = 2.073 m, $l' = 0.134$ m/h, $m' = 0.0055$ mm/min. As noted earlier, this quoted value of m' was measured both *in situ* by means of a ring magnet system installed just above the tunnel crown in a borehole, whereby the magnet was able to move with the deforming London Clay and its position was located continuously by an audible probe activated by the magnetic field, and also by the laboratory soil extrusion method described in Attewell and Boden (1971). For this particular shield the bead covered only the upper 180° of the shield hood and so, from equation (2.14),

$$\% V_b = 100 l_s \frac{k_2 m'}{a l'} = 0.40 \quad \text{for } k_2 = 1.$$

However, in Attewell and Farmer (1974b) it was shown that the bead of thickness 6.5 mm was closed by the clay because the potential intrusive deformation m of the clay over the shield and tail length was 8.244 mm ($= l_s m' / l'$). Thus, by proportion,

$$k_2 = \frac{6.5}{8.24} = 0.79 \quad \text{and} \quad \% V_b = 0.40 \times 0.79 = 0.31.$$

For this example, expressed as a direct volume per unit advance,

$$V_b = \frac{0.31 \times \pi a^2}{100} = 0.042 \text{ m}^3/\text{m}.$$

Other losses over the shield, V_p and V_y . There are usually other, generally unquantifiable, losses at the shield that are attributable to the mechanics of shield driving.

First, a shield may tend to dive off-grade at the front end (promoted by the rotational influence of a protruding hood), or it may tend to settle as a whole in a very soft clay (see, for example, Shiraishi, 1968; Muir Wood, 1970). In order to counteract this tendency the shield must be driven with a 'look-up' attitude (an upward pitch). This resulting ploughing action creates a hole of elliptical cross-section, with the major axis vertical, and so results in a further and possibly substantial volume loss V_p .

Second, it must be expected that the shield, unstiffened by any diametral bracing, will squat towards the tail as a result of a relaxed overburden pressure exceeding a relaxed horizontal pressure if the inward deformation of the soil takes it on to the shield tail. This process will be enhanced if there is soft or remoulded clay in the tunnel sidewalls, or if the soil is granular and contains many voids, because then the ground is insufficiently stiff to mobilize passive resistance to horizontal outward deflection of the tail. On the other hand, a shield that has to manoeuvre round a tight curve may become ovaloid at the tail, with its major axis vertical. However, during curve negotiation, or even along straight lengths of tunnel, there may be a lateral twisting, or yawing, at the sides of the shield, with the elliptical cut surface this time having a major axis horizontal. The net result of these ellipticities is another source of loss V_y .

Hansmire and Cording (1972), measuring on the Washington DC Metro, found that V_y was much less than V_p . On the same tunnel Butler and Hampton (1975) noted that grade changes of 1 per cent could generate as much as 0.34 m³/m of lost ground (V_p). This latter figure was a substantial 28 per cent of the observed total surface settlement volume, but of course it is usually impractical to quantify V_y and V_p . For V_p , Cording *et al.* (1976) suggest

$$V_p = \frac{\pi a l_s}{2} \times (\text{excess pitch}). \quad (2.15)$$

'Excess pitch' is defined as p/l_s , where p is the difference in elevation between the front and rear of the shield and tail *minus* the design grade of the tunnel. Thus,

$$\% V_p = 50 \frac{p}{a} \quad (2.16)$$

expressed in terms of the tunnel volume per unit advance.

Ground loss after lining erection, V_u . If a bolted segmental lining is to be used, it will be erected within the protection of a tailskin, a circular extension welded to the rear of the shield and having the same external diameter. The length of the tail will be such as to accommodate rather more than one ring of lining segments (one ring in the UK occupying 0.61 m of tunnel lining length), the leading edge of the penultimately erected ring resting on the rear of the tail and so providing some measure of stability against the shield diving at the front end. When sufficient forward excavation of the soil has been accomplished

ahead of the shield under the protection of a hood, the rams push the shield forward off the newly erected lining ring leaving a length of ground unsupported behind the lining until such time as the annulus is filled by grout, pea gravel (or an equivalent substitute[†]), or a mixture of the two. If the ground is strong enough to stand up unsupported without collapsing, the tunnelling contractor will usually delay contact grouting operations until the end of a shift or the beginning of the next in order to increase his productivity. Three or four erected lining rings may thus remain ungrouted, so allowing more radial ground loss—and surface settlement—to occur than if a single ring had been erected and grouted. When tunnelling beneath buildings it may be necessary for the contract documents to specify a ‘build-one-ring, grout-one-ring’ tunnelling regime in order to limit the ground movements, and hence eliminate or greatly reduce building and/or adjacent pipe damage. In writing such a specification the project designer will have balanced the extra cost of the works against the potential savings from damage and consequential claims.

The simplest method of estimating these losses is to assume that the soil has contacted the extrados of the tail before the shield is shoved forward. Then, in the manner of equation (2.13) with $k_2 = 1$ and l_u being the unsupported ungrouted tunnel length behind the tail,

$$V_u = 2\pi l_u a \frac{m'}{l} \quad (2.17)$$

or

$$\%V_u = 200 \frac{l_u m'}{a l} \quad (2.18)$$

Taking the example quoted earlier of the London Transport tunnel (Attewell and Farmer, 1974a,b), l_u was approximately 1.2 m (two precast concrete segmental rings ungrouted) and so, inserting values into equation (2.18) above,

$$\%V_u = 200 \times \frac{1200}{2073} \times \frac{0.0055 \times 60}{134} = 0.28.$$

Obviously this type of estimation applies only to a reasonably firm clay soil (say $c_u \gtrsim 50 \text{ kN/m}^2$).

Ground loss after grouting, V_g . Radial losses continue after grouting while the grout bleeds and sets, and until such time as the stiffness of the lining and grout match that of the ground. A bolted segmental lining undergoes some ring bending as the segments articulate at the longitudinal joints, and this can be reduced somewhat by ‘rolling’ the key segment at the crown (eliminating the

[†]In the UK, this is typically ‘Lytag’, which comprises spheres of sintered pulverized fuel ash. It is manufactured by Pozzolanic Lytag Ltd of Hemel Hempstead, Hertfordshire, and also serves as a concrete aggregate.

continuity of the longitudinal joints) to give a compositely stiffer ring. Even in soils such as the London Clay for which K_0 has been shown to exceed unity at tunnel depths the lining invariably ‘squats’; outward horizontal deflection of the lining compresses the ground at springline, so helping to equalize the radial pressure on, and reduce the bending moments in, the lining.

Other than by measurements *in situ*, using magnetic settlement monitors installed above the crown before tunnelling and both settlement and horizontal movement monitors at tunnel axis level to determine volumetric strain, there is no satisfactory method of estimating V_g as m' decreases. Measurements by Attewell and Farmer (1974a) in the stiff London Clay indicated that approximately 30 per cent of the total settlement occurred after the lining was grouted, but some of this percentage must be attributed to consolidation effects, which are considered in section 2.7 below. This problem of estimating V_g is further addressed via the Example 2.1 calculation in section 2.1.3.

2.1.2 Granular soil

These soils usually possess some cohesion perhaps through the presence of a little clay, some suction pressure dampness, and sometimes from iron oxide cementation. Damp sands are usually excavated with ease and maintain upright faces. Without any cohesion they would slump into the face of the shield at a slope angle controlled by the interparticle friction, thereby generating very large $\%V_f$ values, and the slumping would persist with shield advance (see, for example, the analysis of Széchy, 1970). For a slump-slope angle of α degrees to the (horizontal) invert of the shield a simple analysis would suggest $V_f = \pi a^2 (2a \cos \alpha)/2 = \pi a^3 \cos \alpha$ and $\%V_f = 100 a \cos \alpha$. Before relaxation, an average medium-to-dense dry soil in its confined condition would probably have an effective friction angle of 35°, and when relaxed and saturated its slope angle would be about 25°. Particular friction angles would be assessed from the ground investigation standard penetration test results (Peck *et al.*, 1953), and from Hough (1957)—see also Lambe and Whitman (1969, Table 11.2, p. 149).

If there is a bead on the shield there will be continuous slumping of the soil on to the shield and tail extrados. V_b will then be equal to $\pi(2ab + b^2) = 2\pi ab$ for a 360° bead and notionally half that figure for a 180° bead. The respective values of $\%V_b$ are approximately $200b/a$ and $100b/a$.

In a similar manner the postshield loss V_u would be approximately $\pi(a^2 - a_1^2)$, where a_1 is the external radius of the lining, and any bead thickness is ignored. $\%V_u$ is approximately $100(1 - (a_1/a)^2)$. During tunnelling for the

[†]In the London Transport tunnel described by Attewell and Farmer (1974a) measurements of soil movement suggested a slight inward lateral movement and an accompanying upward vertical movement above the crown after contact-grout set.

Washington DC Metro in the USA an expansion apparatus was designed partially to enlarge the lining during the shoveling in order to minimize these particular losses. Deep settlement monitors registered slight upward displacements of the ground, but it is thought unlikely that this particular facility will mitigate ground settlements and settlement distributions to any real degree. An alternative system of contact grouting over the lining when it was in the tail of the shield was developed, also for the Washington DC Metro (F2a section). After erection of a ring of steel liner plates inside the tail of a modified Robbins shield, the void between the lining and inside surface of the tailskin was packed with 100 mm diameter tubes of dense foam plastic that were held in place by the action of a thrust ring. A sand–flyash–cement grout was then pumped into the void, and it set to the consistency of a loose silty-clayey sand. As the shield shoved forward the volume of lost ground per unit distance advance was, ideally, restricted to the cross-sectional area of the tailskin.

As in the case of cohesive soils, there is currently no satisfactory method of predicting any further losses that occur over the grouted lengths of tunnel.

2.1.3 Total volume loss

Clearly, the total volume loss V_t at the tunnel will be compounded from the individual losses in the case of bolted and grouted segmental linings:

$$V_t = V_f + V_b + \underbrace{V_p + V_y}_{\text{over the shield}} + \underbrace{V_u + V_g}_{\text{behind the shield}} \quad (2.19)$$

In metric units, the volume loss values are expressed as cubic metres per metre tunnel advance. The following example shows rather more clearly how losses at the tunnel may be estimated by calculation, given information on soil relaxation rates.

Example 2.1 Analysis of ground losses in a clay soil

The following example analysis relates to a tunnel in north-east England where the face passed through both laminated clay and stony clay. Graphical information on intrusion is given in Figure 2.4a.

Tunnel depth to axis level, $z_0 = 7.5$ m.

Tunnel external diameter, $2R = 2.024$ m (hand excavation within a shield; free air).

Shield outside diameter, $2a = 2001.4$ mm.

Bead on shield (360°), thickness (b) = 10 mm; length = 230 mm.

Length of shield = 1926 mm. Length of tail = 930 mm.

Length of shield and tail = 2856 mm.

Length of shield and tail minus bead length, $l_s = 2626$ mm.

Rate of tunnel advance, $l' = 0.182$ m/h (on working days)

$l' = 0.113$ m/h (overall).

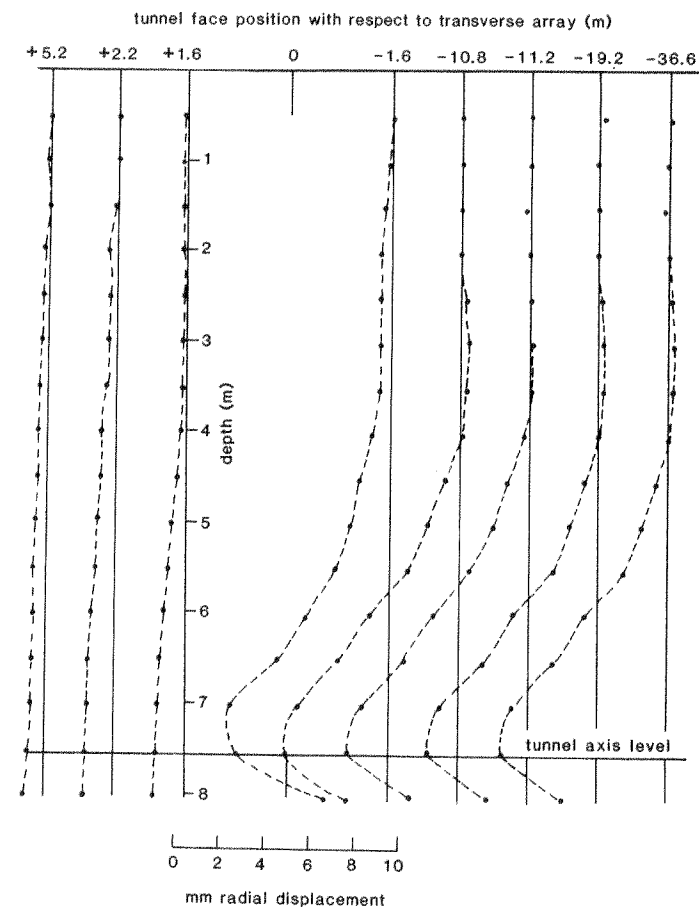


Figure 2.4(a) Radial ground deflection towards an approaching and passing tunnel face as monitored by inclinometer in borehole 4 of Figure 2.39. This borehole is slightly offset from the tunnel sidewall and so does not experience the maximum radial inward movement of the ground.

Rate of soil intrusion, $m' = 0.221$ mm/h (laminated clay).

$m' = 0.0134$ mm/h (stony clay).

1. Using the overall rate of tunnel advance (laminated clay)

Face take

$$V_f = \frac{\pi}{4} (2001.4)^2 k_1 \frac{0.221}{113} \text{ for laminated clay}$$

(see equation (2.3))

$= 0.00308 \text{ m}^3/\text{m}$ for k_1 assumed to be 50 per cent.

Shield/tail radial take

$$V_b = \pi \times 2626 (2001.4 + 20) k_2 \frac{0.221}{113}$$

(see equation (2.13))

$$= 0.03261 k_2 m^3/m.$$

(Check for $k_2, m' = 0.221 \text{ mm/h}$. Therefore, bead thickness, $b (= 10 \text{ mm})$, will be covered by soil intrusion, m , in $10/0.221 = 45.2489 \text{ h}$. Since tunnel advance rate $l' = 0.113 \text{ m/h}$, length before bead closure $= 45.2489 \times 0.113 \text{ m} = 5.1131 \text{ m}$. This length exceeds l_s , and so $k_2 = 1$.)

Loss after lining erection

$$V_u = \pi \times 1800 (2001.4 + 20) \frac{0.221}{113}$$

(see equation (2.17))

$$= 0.02236 m^3/m.$$

(This allows for three ungrouted concrete segmental rings, each ring width 0.61 m , but with the forward ring just resting over the end of the shield tail in order to assist shield stability.)

The measured maximum settlement was 7.86 mm . After plotting the transverse distribution of settlement as measured at the several stations (see Figure 2.39) the area under the settlement curve was calculated by adding 1 mm squares on a graph paper underlay. This area was 0.0774 m^2 . An error curve was then fitted to the measured curve (Figure 2.4b) using the fact that $y = i = 3.9 \text{ m}$, where $w = 0.606 w_{\max}$. Thus, given that $V_s = \sqrt{2\pi} \times i \times w_{\max}$, then $V_s = 0.0768 \text{ m}^3/\text{m}$. The difference between the two areas is less than 1 per cent.

Ignoring V_p and V_g , since in the former case there was no evidence of the shield having to be driven with a 'look-up' attitude in the stiff clay soil to counteract any tendency to dive, and in the latter case there was no evidence of any cutting or shield ellipticity, then rewriting equation (2.19),

$$V_t = V_s = V_t + V_b + V_u + V_g,$$

it is possible to determine the relative contributions of the individual losses to the total loss:

Face take,

$$V_f = 4\% V_s,$$

Shield take,

$$V_b = 42.44\% V_s,$$

Postshield pregrout take,

$$V_u = 29.10\% V_s,$$

Postgrout take,

$$V_g = 24.45\% V_s (= 0.0188 \text{ m}^3/\text{m}) \text{ by difference.}$$

Inward ground movement radially over shield and tail

$$= l_s \frac{m'}{l'} = 5.136 \text{ mm.}$$

Inward ground movement radially over ungrouted rings

$$= l_u \frac{m'}{l'} = 3.250 \text{ mm.}$$

Inward ground movement at the face

$$= \frac{V_f}{2\pi a} = 0.490 \text{ mm} \text{ (using equation (2.5)).}$$

Radial movements of the clay soil around the tunnel were measured by deep settlement ring probes (crown) and inclinometers (axis) (for the latter, see Figure 2.4a) and produced an average value for radial displacement (m) of 12.3 mm . Thus, summing the two radial movements above ($5.136 \text{ mm} + 3.520 \text{ mm}$) and subtracting from 12.3 mm gives the radial inward movement that can be presumed to have taken place over the grouted length of tunnel. Thus, ground movement on to the grout is 3.64 mm (approximately). This represents 29.6 per cent of the total average movement and, for an average 44 mm thickness of contact grout, represents a grout compression of about 8.27 per cent over the setting period. The inward ground movement at the face proper, estimated above at about 0.5 mm , is very small, but is confirmed by inclinometer tube deflections at face level when intercepted by the face (Attewell and Farmer, 1973).

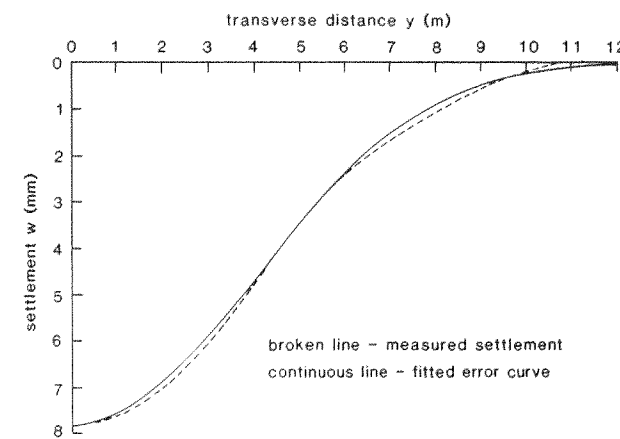


Figure 2.4(b) Settlement distribution in Example 2.1.

2. Using the weekday rate of tunnel advance (laminated clay)

Face take

$$V_f = 0.00191 \text{ m}^3/\text{m} = 2.49\% V_v$$

Shield plus tail take

$$V_s = 0.02025 \text{ m}^3/\text{m} = 26.35\% V_v$$

Postshield pregrout take

$$V_u = 0.01388 \text{ m}^3/\text{m} = 18.06\% V_v$$

Ground movement on to the grout

$\approx 12.3 - (3.189 + 2.186) \approx 6.92 \text{ mm} = 56 \text{ per cent}$ of the total average movement and represents a grout compression of about 16 per cent.

3. Assessment for weekends (laminated clay)

During stoppage periods only face take and shield/tail take continue, since all the rings are grouted up and it is convenient to assume that grout movement has ceased.

At the start of the weekend the 10 mm thick bead will be fully open 230 mm from the front of the shield but will have closed to a gap of only $(b - l_s(m'/l')) = (10 - 2626 \times (0.221/182)) = 6.811 \text{ mm}$ at the end of the shield tail. With the measured clay soil intrusion rate of 0.221 mm/h, the 10 mm annular gap will close completely over a period of $10/0.221 = 45.25 \text{ h}$, which covers the weekend break.

Shield/tail take over the weekend is therefore

$$V_{se} = \pi \times 2626 \times 2021.4 \times \left(\frac{0.010 + 0.006811}{2} \right) = 0.14008 \text{ m}^3.$$

Face take over the weekend is

$$V_{fe} = \frac{\pi}{4} (2001.4)^2 k_1 \times 0.221 \times 48 = 0.01669 \text{ m}^3 \quad \text{for } k_1 = 0.5.$$

Thus, total take over a 48-hour weekend is $V_{se} + V_{fe} = 0.15677 \text{ m}^3$.

4. A more realistic model uses the real (working days) rate of advance plus the calculated weekend losses, although the actual weekend losses may be slightly lower than those calculated because the face would be partly boxed up during the stand period. The boxing would comprise waling boards and battens thrust against the face through the action of the shield jacks (see the four face jacks on the shield in Figure 1.1).

Face take over week

$$= V_f + V_{fe} = 0.00191 + \frac{0.01669}{7 \times 24 \times 0.113} \\ = 0.00279 \text{ m}^3/\text{m} = 3.63\% V_v$$

(Note that the weekend loss must be expressed per unit advance distance. This distance is the overall advance rate (0.113 m/hour) multiplied by the number of hours (7×24) in a week.)

Shield/tail take over week

$$= V_s + V_{se} = 0.02025 + \frac{0.01669}{7 \times 24 \times 0.113} \\ = 0.02112 \text{ m}^3/\text{m} = 27.50\% V_v$$

Postshield pregrout take over week

$$= V_u = 0.01388 \text{ m}^3/\text{m} \text{ (as in 2 above)} \\ = 18.06\% V_v$$

Postgrout take

$$V_g = 0.03904 \text{ m}^3/\text{m} \text{ (by difference)} \\ = 50.81\% V_v$$

Assessing the ground movement radially on to the contact grout (m_g) by proportion:

$$m_g = 12.3 \left(\frac{V_g}{V_g + V_s + V_{se} + V_u} \right) = 12.3 \left(\frac{0.03904}{0.03904 + 0.02113 + 0.01388} \right) \\ = 6.48 \text{ mm.}$$

Thus, by this more realistic calculation the grout is compressed 6.48 mm radially and by 14.73 per cent of its (assumed) original thickness of 44 mm.

Similar calculations could be performed for the other (stony) clay through which the tunnel has passed.

Some rather obvious comments on design stem from these analyses.

Use a shield having as low a length-to-diameter ratio as possible.

If a long shield must be used, then try to design it for articulation so that steering is eased and ovality problems arising from driving round curves are reduced.

Design for a tight diametral build of lining within a tailskin of just sufficient length. Consider using an improved tail seal and place the contact grout as the shield is shoved forward. There must be suitable provision for preventing any build-up of hardened grout on the shield/tail extrados.

Plan the deployment of labour, the soils excavation and support erection as a systems problem so that the only constraints on a high rate of advance are unexpected ground conditions, which themselves can be reduced by good prior ground investigation.

2.1.4 Mechanics of soil deformation

The application of soil mechanics principles to the deformation of soil around an advancing tunnel is a topic too lengthy to be covered in this book and, at present, insufficiently developed for all but the most conceptually simple geometries and homogeneous soils having established predictable behaviours. Atkinson and Mair (1981) have examined the problem in terms of critical-state soil mechanics, but primarily from the standpoint of the magnitude of internal support needed in the tunnel to achieve stability and avoid collapse, and the use of dimensionless stability numbers (three parameters T_c , T_y and T_s analogous to bearing capacity factors N_c , N_y , N_q).

Atkinson and Mair consider two general soil types in terms of their past loading history. Overconsolidated soils that are not in a collapse state at the tunnel deform, under excavation relaxation conditions, with increasing shear stress towards but inside the ultimate failure-state boundary surface. They can be analysed as for elastic deformation, Hooke's law applying to the stress-strain relations. Effective moduli E' , v' define any drained behaviour and 'total' moduli E_u , v_u define undrained behaviour. The ultimate deformation state of a normally consolidated soil maps out the critical-state boundary surface for which the stress-strain relations need to be formulated via some elasto-plastic law.

The (directional) permeability of the soil and the rate of tunnel advance (more specifically, the rate at which a sealed lining is installed) together determine the degree of allowable soil drainage. The rate of change of total stress due to excavation could be fast compared to the rate of excess pore-pressure reduction via a drainage boundary or boundaries. At the limit, the rate of the former relative to the latter could be such as to virtually inhibit drainage, in which case there would be no volumetric strain, and so no consolidation during actual excavation and construction, but there would be undrained shear strain. The state of radial and tangential total stress for elastic conditions and a circular excavation can be estimated from the equations originally formulated by Kirsch (1898)—see also Savin (1961).

Those elements of soil which are relaxed by excavation, but are not excavated, and which consequently dilate, undergo changes in pore pressure which are usually conducive to consolidation. This is the situation that applies around the tunnel as the shield advances. Even if the total stresses, comprising radial, tangential and centre line axis stresses, remain constant behind the face of the shield and before contact grout offers resistance, changes in pore pressure cause changes in effective stress which in turn lead to strains, which

are due to consolidation and occur without changes in external loading. Consolidation is related to radial drainage, the seepage itself creating additional stress that must be supported.

2.2 Reduction of ground loss

In addition to the build-one-ring, grout-one-ring construction method, the ground losses at the tunnel can be reduced by adopting one or more of the following practices.

Smooth shield and tail extrados. Increasing, unquantifiable losses may occur if grout seeps behind the tail and shield, sticks to the rough metal surface, and sets. A build-up of set grout in this manner may cause weak soil around the shield to be disturbed and 'ploughed' as the shield is advanced. This problem occurred on a Tyneside (UK) sewerage scheme contract when tunnelling under compressed air in a soft, silty alluvial clay (details of the work are described in Attewell (1978b) and Attewell *et al.* (1978)). As a result of this experience a specially-prepared Teflon-coated shield and tail extrados was

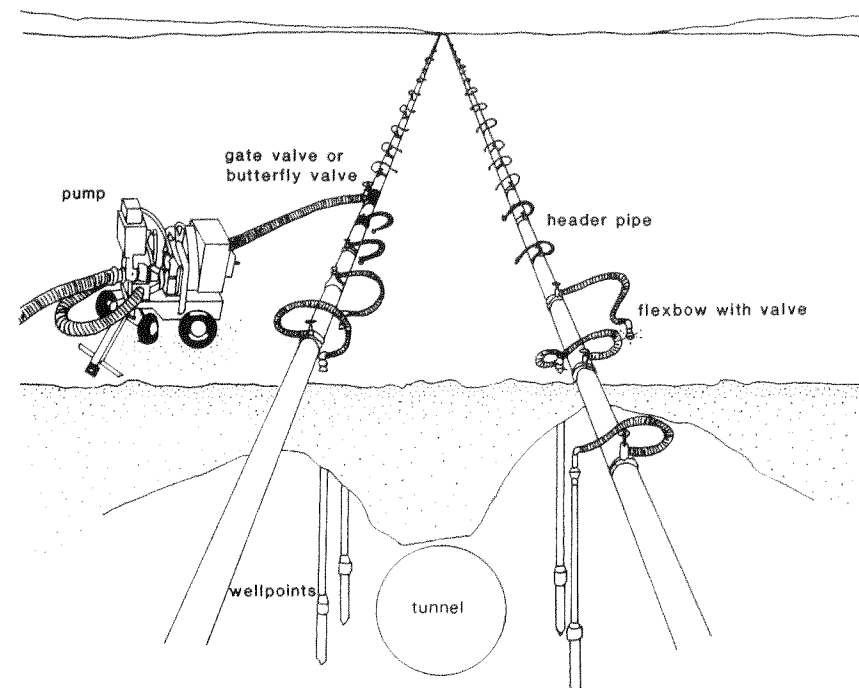


Figure 2.5 A wellpoint dewatering system.

specified by the same water authority for a later urban tunnelling contract (see Attewell, 1981, for details of this contract), the shield being manufactured by Wade and Hobson of South Yorkshire, England.

Wellpoint dewatering. For shallow tunnels in dominantly granular soils, individual wells, generally 40 mm or 50 mm diameter, are sunk to tunnel invert level, secured to the end of riser pipes, and washed into the soil at close centres using high-pressure jetted water (see Figure 2.5). These wells are set to one side of, or both sides of, the proposed tunnel and connected via a suction header pipe to a centrifugal pump fitted with an air exhauster system capable of handling large quantities of air. Pumping depresses the groundwater table via a series of overlapping cones of depression and allows excavation to take place in sensibly dry working conditions. If the groundwater table is required to be lowered by more than about 7 m, a tube well system can be used. This consists of a perforated well liner surrounded by a suitable sand filter, with an electro-submersible pump at the bottom of the hole. Suitable filter design to reduce loss of fines from the surrounding soil is important, otherwise attributable settlement might be induced.

Drawdown itself could lead to differential settlements at the foundations of adjacent property. In the ancient centres of some cities (Amsterdam, for example, where the groundwater table may be only one or two metres below ground surface), the possibility of negative skin friction effects and pile drawdown, together with the rotting of timber piles when exposed to the atmosphere, must be considered. One method of partially overcoming the problem is to drill recharge holes between the tunnel and the property and to circulate the abstracted water through them. The foundation support capacity of the water to the sides of the tunnel is thereby maintained by means of a steepened drawdown surface.

If the tunnel is too deep for complete dewatering to be achieved economically, one option is to lower the water table partially and to tunnel under the reduced head with a tolerable internal compressed-air pressure or with a slurry/earth balance shield.

Neglecting the effects of well overlaps, assuming soil homogeneity and permeability isotropy, the standard Theim equation can be used to establish water quantities requiring to be pumped in order to achieve the requisite drawdown. Letting H be the height of the water table above the base of the soil stratum to be dewatered, h the height from the base of the stratum to the point of maximum drawdown at the well, b the thickness of the aquifer, r_0 the radius of the drawdown depression, r_w the radius of the well, k the ground permeability (assumed to be isotropic), and Q the flowrate in units of volume per unit time from the well, then the radial water flow in a confined aquifer must be

$$Q_c = 2\pi k b (H - h) / 2.30 \log(r_0/r_w) \quad (2.20)$$

and, for an unconfined aquifer,

$$Q_u = \pi k (H^2 - h^2) / 2.30 \log(r_0 - r_w) \quad (2.21)$$

in order to achieve the required drawdown ($H - h$) at the well. Reference should be made to standard textbooks for further reading on the theory of this subject, but it is preferable to seek practical advice from specialist groundwater-lowering contractors since the ideal ground conditions required to satisfy the theory will rarely pertain in practice.

Grout injection. This again is a subject on which a specialist contractor's advice must be sought, and reference may also be made to the numerous papers, technical articles and books on the topic. Some grouts act dominantly as 'water stops' to reduce the porosity (and permeability) of the soil before the use of, or as a substitute for, compressed air, the stabilized ground being excavated without too much difficulty. Other grouts greatly enhance the compressive strength of the ground, causing it to require more excavation effort. Some grouts may be used to densify loose non-cohesive soils and others may be used to fill known voids—for example, around building foundations and pipes that may have settled. Sometimes, as an alternative to the use of slurry walls for isolating tunnels from adjacent properties, it may be necessary to grout soil beneath a building in order to provide added, 'underpinned' support before tunnelling. Grouting can be from the ground surface ahead of the tunnel, or, more expensively, from a pilot tunnel or from (and ahead of) the main tunnel. Compaction grouting has been used with some success in tunnelling where large (say, greater than 12 mm) structural settlements have been anticipated in built-up areas. The aim is, after each shove of the shield, to place a low-slump cement through holes drilled from ground surface and thereby replace the volume of ground lost around the tunnel during its advance. At suitable pressures the grout tends to densify the soils surrounding the grout bulb, heaving the overlying soils and pushing down on to the tunnel lining. The cost of this operation and the possible difficulties of access for drilling have to be balanced against the projected savings in building reinstatement costs.

The types of injection grouts range from particulate (usually) cementitious grouts through silicate grouts to organic polymer grouts, the choice being determined by cost and by the particle size of the soil into which the injection is to be made. In the case of the cheaper particulate grouts, the maximum size d_p of particle capable of passing in suspension through the minimum-pore cross-section of a soil will have a diameter in the region of $0.15d_0$, where d_0 is the diameter of the (assumed) spherical soil particles. In practice, the maximum diameter d_p of injection particle may be taken as $0.1d_0$, where d_0 is equated to the D_{10} soil grain size in a mass of irregular-sized particles. D_{10} is the size below which 10 per cent of the particles are finer. Ordinary portland cements normally contain particles up to 100 μm in size, and this restricts the use of

these cement grouts to medium sands and coarser. High-early-strength cements having a maximum grain size of 20 µm could be used to grout all sands with a permeability as low as 10^{-4} m/s. Prediction of groutability from *in-situ* permeability tests or vice versa may be made on the basis of the Hazen formula

$$k(\text{cm/s}) = D_{10}^{-2}(\text{mm}^2).$$

Freezing. This temporary ground-improvement option is suitable for a wide range of water-bearing soil types, including mixed ground where grouting may be inapplicable or where compressed-air pressures would be too high. Freezing is normally done from the ground surface ahead of the tunnel face. Basically the choice lies between relatively slow freezing, commonly using an indirect circulatory brine system, and a direct-injection fast freeze down to about -25°C using liquid nitrogen. The former is usually cheaper, but requires adequate site space on which to house the bulkier freeze plant. Such space is not always available in city centres. Liquid-nitrogen running costs are usually higher, but the system demands less space. All freezing systems disrupt traffic flows because when (as is often the case) a tunnel follows the line of a road, that road must be closed during the freezing and tunnelling operations. During tunnelling under property it may not be economically possible to freeze at all. Liquid nitrogen is of greatest use as a standby facility when local water ingresses might occur unexpectedly. The ground can then be quickly frozen, the tunnel can proceed rapidly through the bad area, and the ground then left to thaw out. A major disadvantage of freezing is that it is very difficult to control and estimate the position of the ice front, with the possibility of affecting buried pipes and creating ground heave beneath building foundations. Services can, however, be isolated from the effects of freezing by excavating the surrounding soil. Furthermore, the frozen ground creates unpleasant environmental conditions in which the tunnellers must work, and there can be a danger if the freeze tubes are broken inadvertently when intercepted at the tunnel face. Excavation will usually be by hand-held pneumatic spades and jigger picks, but explosives may sometimes be needed. The overall effectiveness of a freezing operation will be reduced if water is actually flowing in more permeable soils that are to be frozen, since some heat is generated by the motion.

Compressed air. The introduction of an air pressure above atmospheric pressure into a tunnel behind an airlock, while technically attractive and much used, is physiologically undesirable. There are stringent controls on the use of compressed air (in the UK via the use of the 'Blackpool Tables'[†]) and

[†]Construction Industry Research and Information Association (1973). *A Medical Code of Practice for Work in Compressed Air*. CIRIA Report 44. London.

prescribed requirements for medical supervision when gauge pressures exceed one atmosphere.

Compressed air acts in three ways:

By balancing the external head of water (the compressed air going into solution with the groundwater over a diffuse zone) and resisting its intrusion into the tunnel.

By providing a direct reaction to the field forces attempting to propel the soil particles themselves into the tunnel.

By drying out a 'skin' of soil at the tunnel face and, by so increasing its effective strength, enabling it more easily to resist the passive pressures in the ground.

Compressed air is used only when the effects of groundwater would otherwise prevent the tunnel being advanced. Because of its low soil permeability, a high head of water in a clay is unlikely to create tunnelling problems. Within a glacial till any granular inclusions may contain water at artesian or sub-artesian pressures and could severely affect tunnel progress. If the site investigation evidence is not reasonably conclusive about the need or otherwise for compressed air in a tunnel, then it is prudent to make provision for it in a bill of quantities at a (1983) installation cost of circa £25 000 for a facility up to 1 bar gauge pressure and a 20 per cent increase in cost above that. Installation of a compressed-air facility at a later stage after tunnelling has begun would cause progress to be disrupted and would be more expensive.

Tunnellers have used compressed air for more than a century in order to control water intrusions from silty/sandy/gravelly soils. Air and water permeability in such soils depends very much upon the volume of fine material present in the deposit. If there is a very low silt content the water may be controlled only at the expense of unacceptably high air losses. Furthermore, compressed air depends for its effectiveness upon continuity of the deposit to be locally dewatered. If water is contained in isolated pockets or lenses of silt or sand within a dominantly clay soil stratum, for example in tills, at artesian or sub-artesian pressures, then the pocket becomes uniformly pressurized because the water cannot be driven back, and simply seeps into the tunnel. On the other hand, there may be continuity of such lenses beyond the local tunnelling area. Compressed air may then drive back the water over quite large distances, seeking out loss paths through, for example, foundations and any voids between building services and the soil in urban areas.

Experience is needed to judge the size of plant necessary to accommodate air losses. The adopted pressure (in kN/m², equal to 9.81 times the water head in metres) will usually be chosen to balance at tunnel axis level. However, the most sensible criterion for specifying compressed air pressure is that the pressure should be low enough to permit a water seepage of insufficient magnitude at the face to delay progress. These seepages may, however, cause some groundwater lowering and induce early consolidation settlement (see

section 2.8) to be added to ground-loss settlement. Thus, decisions as to the compressed-air balance pressure should also be based on a review of possible consequential settlements and the effect of those settlements upon in-ground (Chapter 3) and surface (Chapter 4) structures.

In all cases the thickness of cover above the tunnel crown should be checked to make sure that there is no possibility of excessive ground heave from tunnel air pressure. Cover stability obviously demands special attention during subaqueous tunnelling.

Enclosed shields. Of the two principal types of enclosed shield adopted for weak water-bearing ground, one is termed 'active' and the other 'passive'. In soft clay soil or non-cohesive running ground tunnelled below the water table without the use of compressed air for temporary support, or some other form of ground improvement, a passive shield may act as a bulkhead to seal off the face but with provision for retractable hydraulic breasting doors the opening of which will allow a controlled inward movement of the ground as the shield is thrust forward. A small-diameter shield of this enclosed type is shown in Figure 2.6.

Although the rate of advance depends on the total area of opening, the thrust for advance must match the intrusion rate, otherwise grossly excessive ground losses may occur. In very mobile ground problems could arise at the

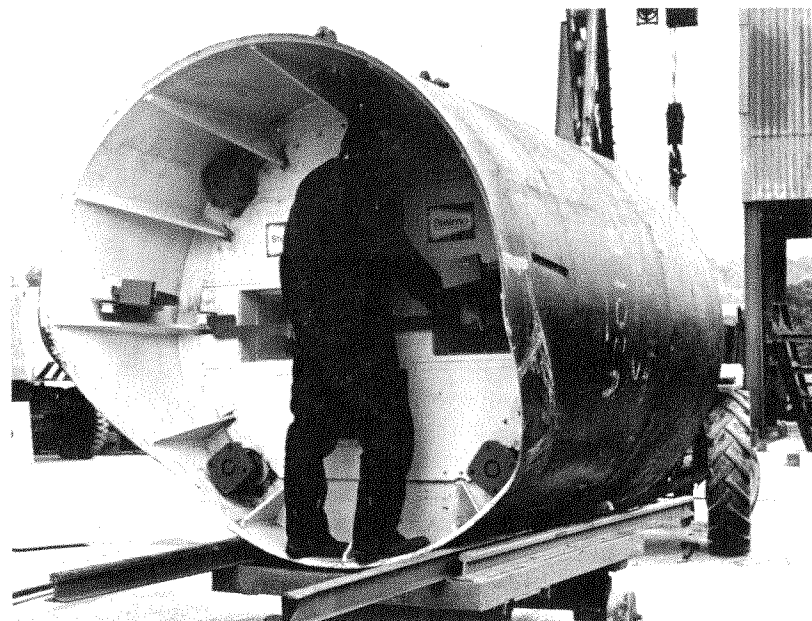


Figure 2.6 Small-diameter, fully welded shield with closed front for working in loose sand conditions. Photograph courtesy Stelmo Ltd.

seal between the rear of the shield and the lining, but the system has a major advantage in that the tunnelling crew is not exposed to the disadvantages of compressed-air working and decompressions.

Large shields comprise several compartments, each having its own door through which a miner can dig out the soil. Such shields may also incorporate vacuum ejectors for dewatering immediately ahead of the shield, and this system can be used in conjunction with deep-well dewatering from ground surface.

An enclosed shield of this type is heavy, and the additional steel at the front end pulls the centre of gravity of the shield forward. In very weak ground the shield may then tend to dive more readily off-grade, particularly if tunnelling down an incline. An upward pitch will then be necessary to counteract the dive, so producing overcut volume losses V_p . On the other hand, the additional forward weight of the shield could be offset somewhat because a shield hood might not then be needed.

Breasting doors may be designed to cover only the upper half of a tunnel face, the shield not being compartmentalized. Cording *et al.* (1976) have described Washington DC Metro F2a-L Route shields having six doors across the upper half of the shield (see Figure 2.7). The doors were hinged to the shield circumference and were used at the discretion of the shield driver during shield shoves in order to admit soil into the heading. However, they were not particularly effective in controlling the ravelling-to-running sand and gravel encountered in the upper half of the heading throughout most of the L Route.

This passive system has been largely superseded by the more recent bentonite-shield, slurry-shield and earth-pressure balance tunnelling systems in which the face is again sealed but in which ground intrusion is resisted on the

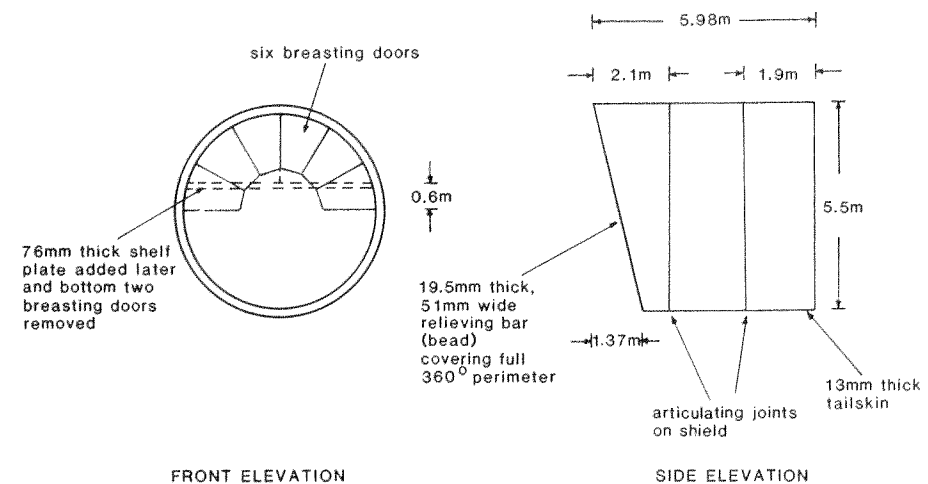


Figure 2.7 Washington DC Metro L Route shield (after Cording *et al.*, 1976).

face side of the shield by the injection of a pressurized bentonite–water slurry or by a pressurized slurry of the soil itself. The bentonite-shield system was invented in Britain but has been exploited in Germany (Wayss and Freytag Hydroshield system) and, more particularly, as slurry-shield tunnelling in Japan and by the Japanese in other countries. Particular features of the system include the design of the rotating cruciform arms to mobilize the soil and slurry it up at the face, the design of the sealing at the tail of the shield, and the mechanical design for spoil removal at the face of the shield. The handling of boulders created severe problems for the British experimental bentonite shields. Recent Japanese shields, examples of which were used on 1984 sewer tunnel contracts on the south bank of the River Tyne in northern England and in Oldham, Lancashire (Iseki Poly-Tech Inc. 'Crunchingmole') are claimed to have a facility for crushing boulders of size up to 250 mm diameter. They are operated remotely from ground surface. An example of one such shield is shown in Figure 2.8.

There is currently little measurement evidence to confirm the likely effect that these latter shields permit very low ground losses. They will be increasingly adopted for large-diameter, relatively shallow tunnels in weak water-bearing ground where compressed-air tunnelling (with accompanying physiological and pressure-balancing problems) would otherwise be specified. They will also offer particular attractions for urban tunnelling where small-diameter man-entry- and non-man-entry- size sewers must be built.

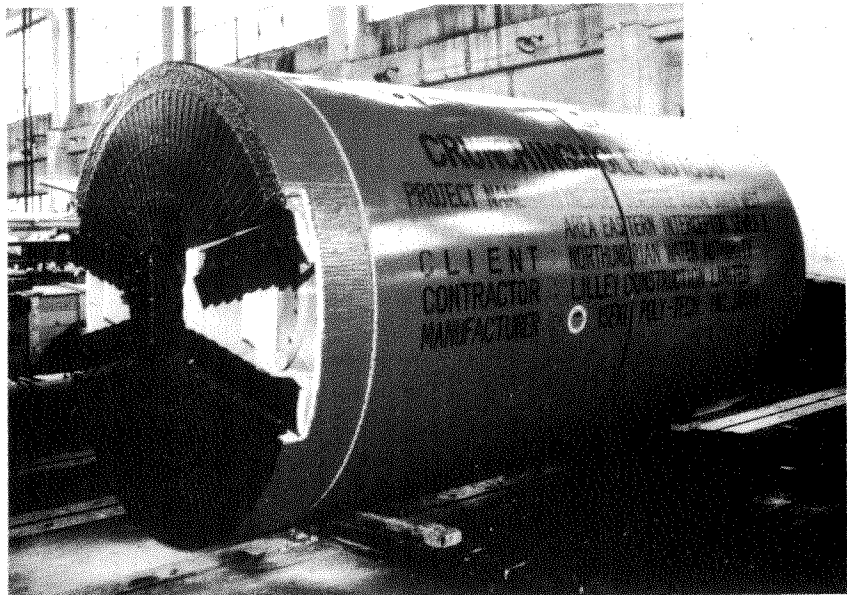


Figure 2.8 Slurry shield. Photograph courtesy Iseki Poly-Tech Inc.

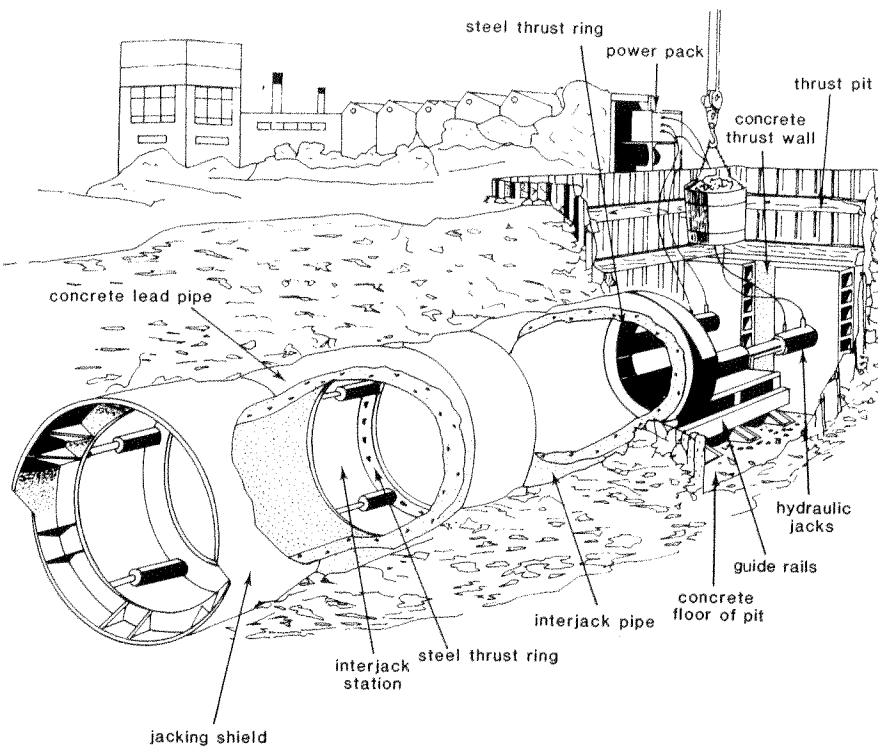


Figure 2.9 Pipe jacking system for concrete pipes.

Pipe-jacking. This is a method of installing (usually circular) pipes of about 900 mm diameter and above by driving a line of them through the ground by hydraulic rams from a prepared jacking pit (Craig, 1983). The minimum practicable size for man-entry during construction is 900 mm. Excavation is carried out, usually by hand, at the forward shield end of the pipe as the pipeline is thrust from the jacking pit. After a full pipelength is pushed into newly excavated ground a further pipe is put in the pit and the process repeated.

A lubricant, such as bentonite, is sometimes used on the outside of the pipe to reduce ground/pipe friction, which absorbs a large proportion of the jacking force. For greater pipe-jack distances, intermediate jacking stations can be used to reduce the jacking force at the pit (see Figure 2.9), which usually varies from about 1500 kN to 4000 kN. Problems related to maintaining line and level have been much reduced in recent years, and pipe-jacking may be performed around curves. If there is careful control on excavation and minimal overbreak at the face, then the radial ground losses should be less with this form of construction than with 'Mini Tunnelling'[†] where three-segment

[†]Mini Tunnel is the trade mark of William F. Rees Ltd.

lining rings are erected conventionally within the protection of a shield tail, and injected pea gravel or Lytag behind the lining is not usually grouted up before the tunnel is completed.

Pipe-jacking was introduced into the UK in the late 1950s and is gathering momentum as a tunnelling technique. Slurry systems are now also being used with jacked pipes which can have diameters below 900 mm. However, the system currently most common involves hand excavation under the protection of a shield. The advantages of pipe-jacking, which provides a reinforced precast lining from 900 mm diameter incorporating flexible joints, are claimed to be strength, watertightness, fewer joints, reduced ground settlements, and elimination of secondary lining. Jacking lengths are usually restricted to about 400 m, unless the ground is homogeneous and has good self-support characteristics. *Tunnel jacking* is a similar construction technique, but related to larger-diameter excavations. Smaller-diameter pipes (non-man-entry) are usually installed by thrust bore and auger methods.

In the recently introduced Uni-Tunnel system (Richardson and Scruby, 1981) rubber bladders are inserted between the pipes. Pipe progress is achieved by inflating the bladders sequentially so that every third pipe is driven forward simultaneously. The frictional resistance of the two following pipes acts against the ground in reaction to the thrust, and so contrasts with the conventional pipe-jacking system where frictional resistance increases with drive length. With this system, in order for the full frictional resistance to be mobilized by the two thrust pipes of each set of three, it is specially important that the excavated diameter be the same as the pipe external diameter. Radial ground losses can thus be very much reduced.

Some difficult decisions often have to be made as to whether the cost of protective measures for adjacent properties should be borne by the project promoter, in the expectation that problems will arise. If the perception of the likelihood of problems developing is uncertain, then the promoter may decide instead that it is more cost-effective to plan for the temporary relocation of occupants, the reinstatement of buildings, compensation for loss of business, and so on. Costs in this area, as indeed in engineering and life in general, depend on a personal, experienced view of the degree of risk involved in the operation.

2.3 Transmission of ground losses to ground surface

This subject is discussed in Attewell (1978a, pp. 855–867), reference to which is recommended. Details of measurement case histories are given for single tunnels, for adjacent parallel tunnels, and for superadjacent parallel tunnels. The following conclusions may be drawn:

- (i) For most single tunnels in *firm-to-stiff clay soils* the volume V_s of the settlement depression created at ground surface is approximately equal to

the volume V_t of ground lost at the tunnel. In practice, the time lapse between creation of the loss source and its contribution to ground-surface settlement may be small.

(ii) For single tunnels in *granular non-cohesive soil*, dilation V_d may occur through arching above the tunnel crown if $z_0 \geq 3R$ (Hansmire, 1975). This arching absorbs some of the ground loss and reduces the surface settlement volume below that predicted from any ground-loss estimates. Soil above the arch and up to ground surface must then be supported as a surcharge to the sides of the tunnel. In a loose compressible soil the surface settlement trough may thereby be widened as a result of such compression V_c . If the tunnel is of large diameter and/or near ground surface the arch may break through to the surface, subsequent losses at the tunnel becoming volumetric settlement losses. Although the general equation is $V_s = V_t - V_d + V_c$, V_d and V_c could be ignored for any estimate of V_s , remembering that in dense sands and gravels, the dilation V_d could reduce V_s and in loose disturbed sands some compression could develop above and to the sides of the tunnel to increase V_s . If large displacements are permitted to develop at the tunnel face and crown, then in granular soils a funnel-type upward transmission movement, creating a narrow but deep surface settlement trough, can occur.

(iii) The greatest concentration of vertical movement occurs at the tunnel crown, and there have been measurements, usually by adopting deeply-emplaced magnetic settlement rings, to quantify it. Clearly, the intensity of vertical movement should decrease upwards from the crown to ground surface simply as a function of the increasing transverse spread of the disturbance. By adjusting the crown movement for this spread and then comparing the adjusted movement with the settlement actually measured, conclusions can be drawn as to whether the soil between tunnel crown and ground surface has compressed in volume or has dilated. This matter is discussed in Attewell (1978a, pp. 894–900, with particular reference to Table 6, on pp. 898–9 of that paper). It would be unwise in practice to offer any specific recommendations, since the behaviour of the ground depends also on the tunnelling and lining method.

(iv) It must usually be assumed that, as the ground movement is transferred from the tunnel source to the ground surface, the transverse settlement distribution as a function of depth ($z_0 - z$) takes normal probability form. The transverse trough width increases and settlement w decreases as $z_0 - z$ tends to z_0 (at ground surface). For buried pipelines and building foundations, the settlement trough parameters are those appropriate to depth z , where z is finite below ground level and is zero at ground surface, with the standard probability equations describing the form of ground movement distribution (equations (2.22) to (2.27)) and with an i -parameter being entered for depth z .

(v) For the style of vertical movement suggested in (iv) above to occur, the ground movement vectors would be directed towards the tunnel, although some temporary ground-surface heave may develop ahead of a conventional hand shield when it is jacked forward. Observations from compressed-air shield-driven tunnels in weakly cohesive soils confirm the compressions to the sides of the tunnel at axis level as noted above. Slurry/earth-pressure balance shields may also push the ground temporarily and locally away from the shield. Upward movements above the crown have also been reported by Attewell and Farmer (1974b) for free-air tunnelling in stiff overconsolidated London Clay and for compressed-air tunnelling in a soft silty clay at Stockton in north-east England (Hurrell, 1985).

(vi) Settlements caused by adjacent tunnels are discussed in Attewell (1978a, pp. 863–865). The most detailed measurement evidence is from Cording and Hansmire (1975) on the driving of Washington DC Metro twin tunnels in *medium dense silty sand and gravel, interbedded with sandy silty clays*. Settlement due to a second, later, but close tunnel produces a composite settlement trough which is asymmetrical with respect to shape and location above the two tunnels. The Washington measurements showed the additional asymmetrical settlement over the second tunnel to have been caused by additional deflection of the lining of the first tunnel, by compression of the abutment between the tunnels, and by compression of the previously-dilated region over the crown of the first tunnel. Thus, the volume component of the surface settlement trough attributable to the second tunnel exceeded the volume lost at that tunnel, the difference being termed the interference volume. The sequence of recompression of dilated non-cohesive soil in the arch over a first tunnel, further vertical squat of the primary support system, lateral outward deflection of the support system and further compression of intervening pillar soil depends on the stiffness of both the ground and the tunnel support system. If the first tunnel support system is very stiff, then the interference volume will be small. The final composite settlement trough is created by the superimposition of the two tunnel individual troughs and the summation of the settlement vectors. In many cases the final settlement trough width outside the centre lines of the two tunnels will be the same as a symmetrical half-width of trough above a single tunnel.

In the case of twin tunnels driven at the same level in clay soil there will be little or no dilation of the ground above the crown of the first tunnel and thus no recompression when the second tunnel is driven. The second tunnel may, in fact, dilate ground that had previously compressed above the first tunnel. There will be vertical compression at the sides of both tunnels and some lateral interference compression at both sides of the abutment between the tunnels. With clay soils, therefore, any final settlement trough asymme-

try should be less than that associated with granular soils. An example of settlement trough superposition in clay soil is given in Attewell (1978a pp. 866, 867).

In assessing the effects of interaction between tunnels and, for example, at tunnel junctions, it will be realized that subsequent construction takes place in soil that may well have deformed down to its residual strength as a result of earlier disturbance. Later soil deformations and contributions to total settlement may therefore be greater.

2.4 Ground deformation and strain equations

The primary notation to be used in the ground deformation equations is listed below for convenience, but a comprehensive symbol list is included at the beginning of the book.

x, y, z are the cartesian coordinates of any point in the ground deformation field. Theoretically, $x = y = 0$ vertically above the tunnel face on the tunnel centre line. Positive (+) x is ahead of the tunnel on the centre line, and horizontal. $\pm y$ is horizontal at right angles to x . Positive (+) z is vertically downwards. This coordinate system is shown in Figure 2.2.

u, v, w are the ground displacements in the x, y, z directions, respectively. u and v are always towards the origin of the cartesian coordinate system. w (settlement) is always positive downwards.

$\epsilon_x, \epsilon_y, \epsilon_z$ are the ground strains in the x, y, z directions, respectively. These strains can change from tensile (positive) to compressive (negative) depending upon position in the deformation field. Tensile ground strains are more likely to have a serious effect upon the brittle foundation of a building or upon a brittle pipe than are compressive ground strains.

γ_{xy} is the ground shear strain in a horizontal plane.

z_0 is the depth of the effective source of ground loss (taken as approximating to the tunnel axis).

R is the excavated radius of a tunnel with circular cross-section.

K_R is an empirically-determined constant.

n is the power of $z_0 - z$ to which i_x, i_y, i are proportional.

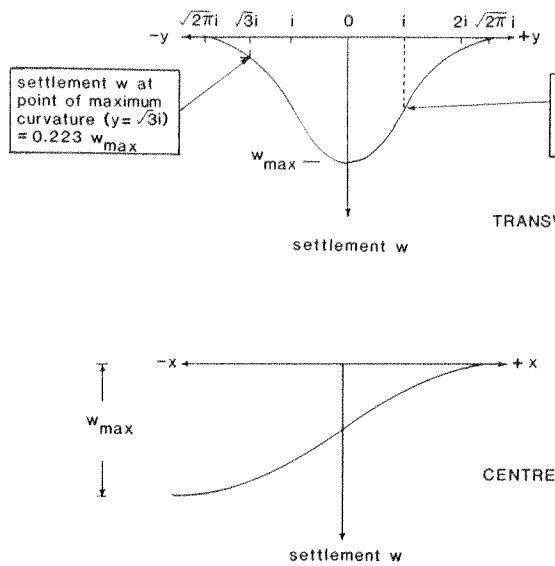


Figure 2.10(a) Normal probability transverse and cumulative probability centre line settlement profiles (see Figure 2.2 for full impression of settlement trough).

V_s is the volume of the settlement trough per unit distance of tunnel advance, the settlement being attributable to ground losses and not incorporating any longer-term consolidation movement.

i is a parameter defining the form and span of the settlement trough, on the assumption that the semi-transverse (y -axis) settlement profile can be described by a normal probability equation (Schmidt, 1969; Peck, 1969; Attewell, 1978a). On the transverse settlement profile (Figure 2.10), i_y is half the distance between the points of inflection (greatest slope) either side the tunnel centre line. On the centre line profile (Figure 2.10), i_x is the distance from the point of inflection to the 15.9 per cent (of maximum) settlement point, and twice the distance from the point of inflection to the 30.9 per cent settlement point. For the numerical examples discussed in the book, i_x is taken to be equal to i_y and written simply as i . Case history evidence on i_x and i_y is discussed in section 2.7.

x_i is the initial or tunnel start point ($y = 0$).

x_f is the face or final tunnel position ($y = 0$).

$$G(\alpha) = \frac{1}{\sqrt{2\pi}} \int_{-\infty}^{\infty} \exp\left[-\frac{\beta^2}{2}\right] d\beta$$

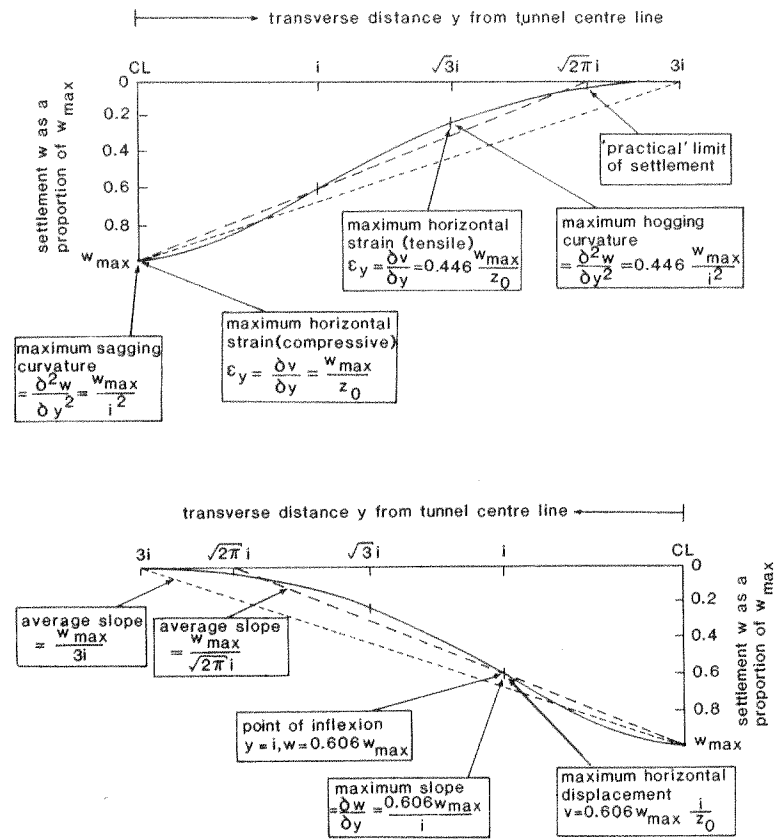


Figure 2.10(b) Transverse surface settlement trough, detail based on a normal probability curve fit to the trough profile (refer to Attewell and Woodman, 1982, for equation derivation).

and may be determined from, for example, a standard probability table such as Table 2.2. Note particularly that $G(0)$ (e.g. $x - x_i = 0$ directly above the tunnel face) gives a value of 1/2 and $G(\infty)$ (e.g. $x - x_i \rightarrow \infty$ for substantial distances of tunnel advance from the face start position) gives a value of 1.

The equations are based on the assumption that the transverse ground settlement profile (yz -plane) is of normal probability, or Gaussian, form. Empirical evidence suggests that this is generally valid for many soils and substantially insensitive to the method of tunnelling, but not to the quality of workmanship in dominantly granular soils. Experienced judgement, however, must be applied to the application of the subsequent ground-movement equations to particular cases. Attempts have been made to match measured profiles with alternative mathematical expressions, but there seems now to be

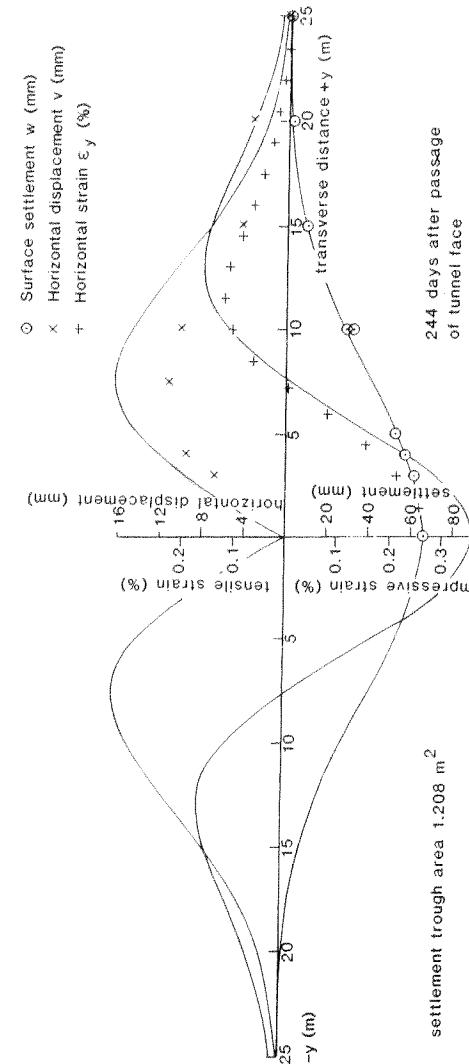
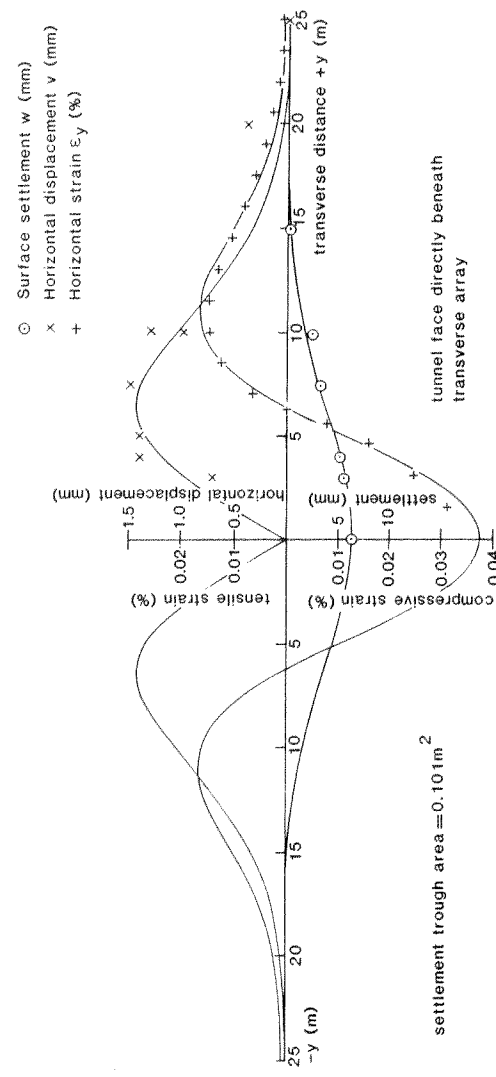
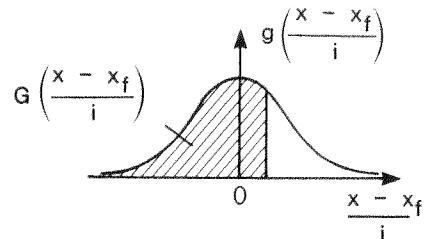


Figure 2.10(c) Illustrating the essential elements of transverse (y -axis) settlement (w), horizontal displacement (v) and horizontal strain (ϵ_y) distribution. These curves should be read in association with the information given in Figures 2.10(a) and 2.10(b). The *settlement curves* represent best-fit normal probability functions to actual measurement data. The displacement and strain curves are derived from the best-fit normal probability settlement curve and are not best fits to the measurement data. Information was derived from a tunnel of 2.45 m external diameter driven under compressed-air pressure at an axis depth of 13.375 m in silty alluvial clay (Sizer, 1976; Attewell *et al.*, 1978). These two graphs are the first and last members of a suite which demonstrates the effects of time and the removal of compressed air upon the ground movements.

Table 2.2 Numerical integration of the normal probability curve.Table of $G[(x - x_i)/i]$

$(x - x_i)/i$	0	1	2	3	4	5	6	7	8	9
0.0	.500	.504	.508	.512	.516	.520	.524	.528	.532	.536
0.1	.540	.544	.548	.552	.556	.560	.564	.567	.571	.575
0.2	.579	.583	.587	.591	.595	.599	.603	.606	.610	.614
0.3	.618	.622	.626	.629	.633	.637	.641	.644	.648	.652
0.4	.655	.659	.663	.666	.670	.674	.677	.681	.684	.688
0.5	.691	.695	.698	.702	.705	.709	.712	.716	.719	.722
0.6	.726	.729	.732	.736	.739	.742	.745	.749	.752	.755
0.7	.758	.761	.764	.767	.770	.773	.776	.779	.782	.785
0.8	.788	.791	.794	.797	.800	.802	.805	.808	.811	.813
0.9	.816	.819	.821	.824	.826	.829	.831	.834	.836	.839
1.0	.841	.844	.846	.848	.851	.853	.855	.858	.860	.862
1.1	.864	.867	.869	.871	.873	.875	.877	.879	.881	.883
1.2	.885	.887	.889	.891	.893	.894	.896	.898	.900	.901
1.3	.903	.905	.907	.908	.910	.911	.913	.915	.916	.918
1.4	.919	.921	.922	.924	.925	.926	.928	.929	.931	.932
1.5	.933	.934	.936	.937	.938	.939	.941	.942	.943	.944
1.6	.945	.946	.947	.948	.949	.951	.952	.953	.954	.954
1.7	.955	.956	.957	.958	.959	.960	.961	.962	.962	.963
1.8	.964	.965	.966	.966	.967	.968	.969	.969	.970	.971
1.9	.971	.972	.973	.973	.974	.974	.975	.976	.976	.977
2.0	.977	.978	.978	.979	.979	.980	.980	.981	.981	.982
2.1	.982	.983	.983	.983	.984	.984	.985	.985	.985	.986
2.2	.986	.986	.987	.987	.987	.988	.988	.988	.989	.989
2.3	.989	.990	.990	.990	.990	.991	.991	.991	.991	.992
2.4	.992	.992	.992	.992	.993	.993	.993	.993	.993	.994
2.5	.994	.994	.994	.994	.994	.995	.995	.995	.995	.995
2.6	.995	.995	.996	.996	.996	.996	.996	.996	.996	.996
2.7	.997	.997	.997	.997	.997	.997	.997	.997	.997	.997
2.8	.997	.998	.998	.998	.998	.998	.998	.998	.998	.998
2.9	.998	.998	.998	.998	.998	.998	.998	.999	.999	.999
3.0	.999	.999	.999	.999	.999	.999	.999	.999	.999	.999



a general consensus of opinion that a normal probability curve match is more appropriate and convenient for estimation purposes. Its application to tunnelling-induced ground settlement is discussed in Schmidt (1969), Attewell (1978a), and Attewell and Woodman (1982). Some of the more important elements of this curve (which has been reproduced in several papers by different authors) are shown in Figure 2.10. These features relate to the surface

of a settlement trough but, of course, the real problems, considered in Chapters 3 and 4, concern the response of buried pipelines and building foundations within the trough. It is indicated subsequently that the response of in-ground structures to ground movement may not be especially sensitive to the form of ground settlement profile.

The transverse settlement trough represents a terminal state of ground deformation induced by ground losses alone or by ground losses plus longer-term consolidation type movements (see section 2.8). However, ground movements—settlements and their derivatives—are also projected ahead of the tunnel face. These forward movements, although a temporary wave of disturbance as the tunnel face advances, also have an effect on buildings and buried pipes, which are twisted and subjected to torsion in three dimensions.

If the state of ground-surface deformation ahead of and to the sides of a tunnel is to be fully estimated, then the form of the settlement profile in an xz -plane, parallel to the tunnel centre line, must also be specified. A logical extension of the earlier assumption of normal probability form for the transverse (yz) settlement is that the tunnel centre line (xz) profile should be of cumulative probability form (see Figure 2.10). This assumption has been reasonably validated by examination of several field study reports (see Attewell and Woodman, 1982). Preliminary analysis assumes that the origin of the cartesian coordinate system, vertically above the tunnel face, coincides with the point of 50 per cent of maximum settlement. Although case history evidence from tunnels in cohesive soils suggests that in many cases only 30 per cent to 40 per cent w_{\max} will have developed vertically above the tunnel face, this is really only academic, since all points at ground surface ahead of and within the boundaries of the transverse settlement trough will at some time realize their ultimate maximum movements for the translating tunnel source of ground loss.

If the above assumptions as to the form of the *ground-loss* settlement trough apply, if it is assumed that deformations occur without volume change, and if the deformation at the tunnel is approximated as a linearly translating point source of loss then the displacements and strains for any field point with coordinates x , y , and z are

$$w = \frac{V_s}{\sqrt{2\pi i}} \exp\left[-\frac{y^2}{2i^2}\right] \left\{ G\left(\frac{x-x_i}{i}\right) - G\left(\frac{x-x_f}{i}\right) \right\}, \quad (2.22)$$

$$v = \frac{-n}{z_0 - z} yw, \quad (2.23)$$

$$u = \frac{nV_s}{2\pi(z_0 - z)} \exp\left[-\frac{y^2}{2i^2}\right] \left\{ \exp\left[-\frac{(x-x_i)^2}{2i^2}\right] - \exp\left[-\frac{(x-x_f)^2}{2i^2}\right] \right\}, \quad (2.24)$$

$$\begin{aligned} \varepsilon_z &= \frac{-nV_s}{\sqrt{2\pi}i(z_0-z)} \exp\left[\frac{-y^2}{2i^2}\right] \left\{ \frac{-1}{\sqrt{2\pi}} \right\} \left(\frac{x-x_i}{i} \right) \\ &\quad \times \exp\left[\frac{-(x-x_i)^2}{2i^2}\right] - \left(\frac{x-x_f}{i} \right) \exp\left[\frac{-(x-x_f)^2}{2i^2}\right] \} \\ &\quad + \left(\frac{y^2}{i^2} - 1 \right) \left[G\left(\frac{x-x_i}{i}\right) - G\left(\frac{x-x_f}{i}\right) \right], \end{aligned} \quad (2.25)$$

$$\varepsilon_y = \frac{n}{z_0-z} w \left(\frac{y^2}{i^2} - 1 \right), \quad (2.26)$$

$$\begin{aligned} \varepsilon_x &= \frac{-nV_s}{2\pi i(z_0-z)} \exp\left[\frac{-y^2}{2i^2}\right] \left\{ \left(\frac{x-x_i}{i} \right) \exp\left[\frac{-(x-x_i)^2}{2i^2}\right] \right. \\ &\quad \left. - \left(\frac{x-x_f}{i} \right) \exp\left[\frac{-(x-x_f)^2}{2i^2}\right] \right\}. \end{aligned} \quad (2.27)$$

As noted earlier, reference to Table 2.2 is required for the resolution of the functions $G(x-x_i/i)$ and $G(x-x_f/i)$. For a tunnel face that has advanced sufficiently (say, two to three tunnel depths, $3z_0$) to allow the transverse (yz -plane) ground-loss settlement profile to develop fully, the function $G(x-x_i/i)$ can be re-expressed in the above equations as unity. It remains to determine possible input values for the other non-geometric parameters.

2.4.1 Practical estimation of volume-loss parameter, V_v , and the surface settlement volume, V_s

The contributory sources of ground loss have been identified in section 2.1. For ground-movement estimation purposes expert advice should be sought, but the following ranges of values could be appropriate for guidance in different soils.

In cohesive soils it is usual to expect a ground loss of between about 0.5 per cent and 2.5 per cent of the tunnel face excavated area, depending upon the stiffness of the soil and the speed (Attewell 1978a, p. 849, and section 2.1) at which the initial support is installed. Estimation may, however, be more satisfactorily attempted on the basis of an overload factor where the driving pressure for ground loss is the multiple of tunnel depth-to-axis (z_0) and soil unit weight (γ), and this is resisted by the undrained shear strength (c_u) of the soil at the tunnel face. If a building imposes a distributed surface surcharge pressure q , then this pressure should be added to the γz_0 term. Internal support (σ_i), usually in the form of compressed air but increasingly, as noted in section 2.2, with the use of newer technology, closed shields in the form of pressurized slurry, obviously resists ground loss at the tunnel.

Figure 2.11a was originally presented in Attewell and Yeates (1984) and

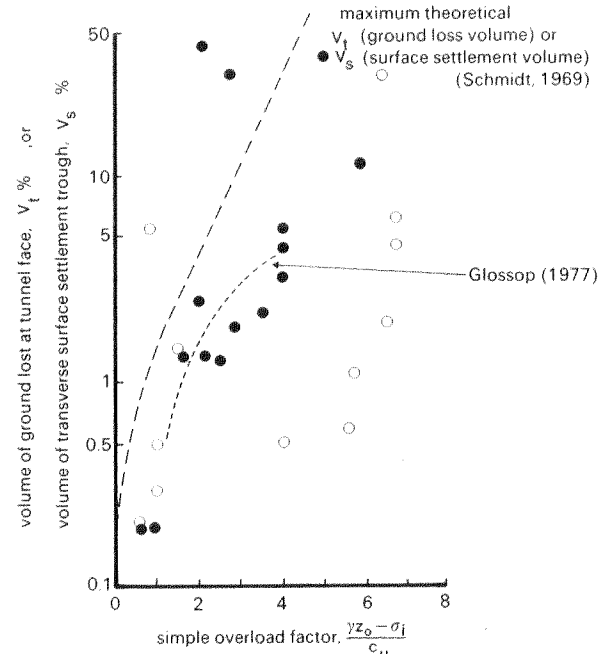


Figure 2.11 (a) Estimation of ground losses and surface settlement volumes from the overload factor for tunnels in cohesive soils. Open circles are Schmidt's (1969) data from shield-driven tunnels. Solid circles are as presented in Attewell and Yeates (1984).

indicates quite a considerable spread of the volume loss data as a function of the overload factor. Glossop has suggested the expression

$$V_s\% = 1.33 \times (\text{simple overload factor}) - 1.4 \quad (2.28)$$

for $1.5 \leq \text{OFS} \leq 4$, which is reasonably representative for tunnelling in most clay soils. More recently the curves in Figure 2.11b have been used for design purposes. If the plotted data are thought to be sound, the unbroken line serves as an upper bound for ground loss in 75 per cent of the cases. It seems reasonable to adopt the level of 75 per cent probability for design where there is such an obvious measure of uncertainty, and it is thought unreasonable always to assume a 'worst case' for design purposes. The positions of pipe joints transverse to a tunnel are assessed, for example, on the basis of 75 per cent probability. It should also be noted in Figure 2.11b that the broken lines denoting twice and half the chosen 75 per cent design curve contain 50 per cent of the data points.

Some concern might be expressed at the high ground losses (30 per cent and 40 per cent) associated with mini-tunnelling. These two results are from soft alluvial soil and can be explained by the delay in contact grouting and high consequential radial intrusions. (Mini-tunnel three-segment rings have their

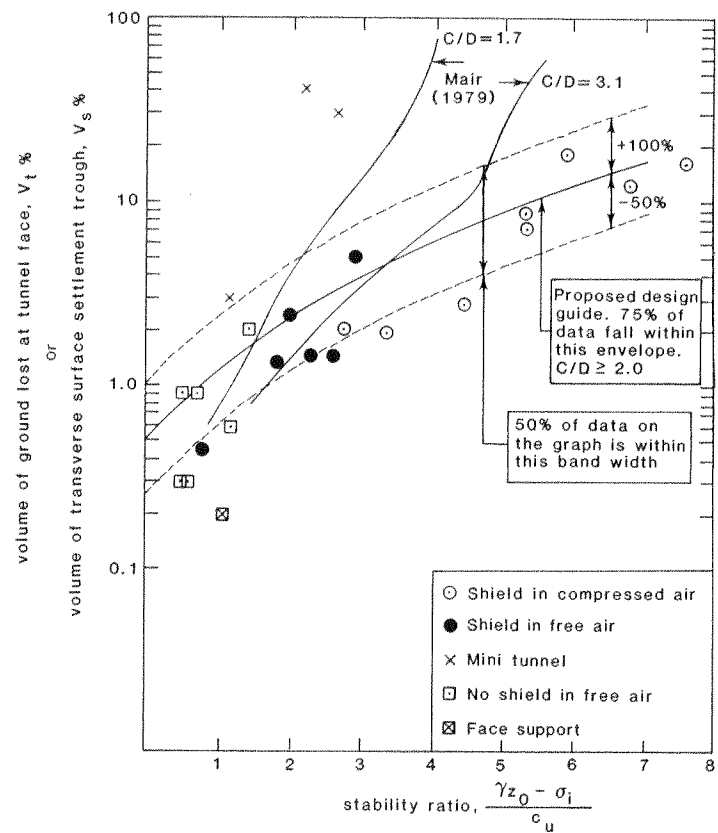


Figure 2.11(b) Ground losses related to stability ratio (partly after Leach, 1985, and with additions). The curves after Mair (1979) relate to two centrifuge model tests. Symbol C is the cover (depth to tunnel soffit).

annular voids filled with pea gravel or Lytag on erection, but the infill is usually grouted up only when the tunnel is completed.) Thus although the excavation may be generally stable, the method is somewhat unsatisfactory for controlling ground movements. Fortunately, because of the relatively small face area of such mini-tunnels, the absolute volume loss may be tolerable in all but the most critical of urban conditions.

Attewell (1978a), pp. 868–878 contains quite a detailed discussion on, and further literature reference to, the subject of stability ratio or simple overload factor. For values of $(\gamma z_0 + q - \sigma_i)/c_u$ less than unity there should be little or no ground movement at the face, and so negligible attributable surface settlement. For stability ratios between 1 and 2, the deformations are regarded as being elastic and cause only very small surface movements. Ratios from 2 to about 4 cause elasto-plastic movements, and between 4 and 6 the movements are deemed to be plastic. Above a ratio of about 6 (6.28 according to Broms and

Bennetmark, 1967) shear failure will be mobilized in a clay soil from the tunnel up to ground surface, and so this should be regarded as the limiting overload factor for face stability.

The importance of speed in the erection of initial support has been noted, and in critical urban areas the adoption of a build-one-ring, grout-one-ring construction regime is often advocated. However, the benefits to be derived from this procedure may in part be lost by the inevitable slowing of advance and the greater time offered for movement inwards at the face proper.

Based on the case studies summarized by Peck (1969) and Schmidt (1974), Mitchell (1983, p. 99) defines the volume loss as

$$V_t = \frac{c_u}{E_u} \exp \left[\frac{\gamma z_0 - \sigma_i}{2c_u} \right] \quad (2.29)$$

where E_u , the undrained deformation modulus, is generally about 200 to 700 times c_u for soft soils. Mitchell suggests that for very sensitive soils or for poor construction control (for example, excavating ahead of the shield, and poor jacking techniques at the shield) the ground loss estimate should be increased by a factor of about 3.

There is now a considerable corpus of data available on ground losses and surface settlements in *stiff fissured clays* tunnelled with or without a shield. V_t (and V_s) for these materials is normally between 1 and 2 per cent. *Glacial tills* often contain silt/sand/gravel lenses with water at artesian or sub-artesian pressures, and so although the clay soil itself may be stiff the presence of the lenses may dictate the adoption of compressed-air temporary support measures. During shield-tunnelling of such deposits in free air, the volume losses would probably be 2–2.5 per cent, but with compressed-air support they could be reduced to 1–1.5 per cent. Recent *silty clays*, having undrained shear strengths probably in the range 10–40 kN/m², and shield-tunnelled under compressed-air pressure (an example being Attewell *et al.*, 1978) would tend to incur ground losses in the range 2–10 per cent.

When tunnelling in *granular soils* above a water table a V_t range of 2–5 per cent is appropriate, but of course the losses in these soils, compared with the losses in cohesive soils, are more dependent on operator experience and skill. If compressed air is used to control the stability of a granular soil tunnelled below the water table, then a V_t range of between 2 and 10 per cent will apply. In both cases, a 5 per cent trial value could be adopted for preliminary calculations, but it is preferable to base any selection of trial values on site investigation standard penetration test (SPT) evidence. In structurally sensitive urban areas it is particularly important that the potential ground loss, even in loose non-cohesive soil, can be reduced by adopting a build-one-ring, grout-one-ring construction regime in a segmentally-lined tunnel.

Man-filled ground must be tunnelled in certain areas, and estimation of ground loss in such cases is made difficult by the usually quite variable

composition and compaction of the fill. Ground losses of about 17 per cent have been estimated for a recent household/industrial waste fill in the north of England (Dobson *et al.*, 1979). For guidance purposes, a lower value of about 8 per cent should probably be used for an old fill comprising natural ground material, a value of 10–12 per cent for an old, established industrial fill, and a figure of 15 per cent for a recent loose industrial or household waste fill. Good ground investigation is obviously required in order to establish a working value.

More complex expressions for the vertical pressure which drives the ground loss at the tunnel may be found in Széchy (1973). These expressions, attributable to different authors, accommodate $c\phi$ soils, surface surcharge pressures, and arching relevant particularly to frictional soils.

These practical values of volume loss are usually adopted directly as surface settlement volumes and used in equation (2.39a) in order to estimate maximum surface settlement. The values are related to medium-sized (say 3 m to 3.5 m diameter) tunnels and should be increased somewhat for smaller-diameter tunnels (less than 1.5 m). It should also be noted that the movement data used to estimate future settlements and ground losses are biased, since those tunnels chosen for monitoring are expected to generate significantly large ground movements and are often in areas that are not built up (otherwise measurements would be hampered). Small or immeasurable movements never appear in the general data set. Ground movements in urban areas may thus be subject to a degree of overestimation.

2.4.2 Settlement trough dimension parameter, i

Attempts have been made to estimate this parameter empirically from case history evidence of settlement trough measurements in different types of ground. Whereas the ground loss depends upon the shear strength of the soil at tunnel level, the settlement trough dimensions will be related more closely to the soil strength nearer to ground surface. The equation that has been used, $i = RK_R(z_0 - z/2R)^n$, has been discussed by Attewell and Woodman (1982) in the context of a stochastic model and has been shown to be unsatisfactory. It is to be expected that i should depend to some degree on the excavated diameter d , and indeed for ground-surface settlement Peck (1969) proposes the approximation

$$i = 0.2(d + z_0). \quad (2.30)$$

On the other hand, O'Reilly and New (1982) have been unable to detect any such dependence in their survey of UK tunnel settlements. It is probably advisable (certainly in the case of cohesive clay soils) to assume that both K_R and n tend to unity, which suggests that i approximates to half the tunnel axis depth (in practice a range of between 0.4 times and 0.7 times the tunnel depth as observed for stiff clays and for soft silty clays, respectively). Alternatively,

O'Reilly and New have suggested, from case history reviews, that the following relations apply for UK tunnels for which adequate ground settlement records are available:

$$i = 0.43(z_0 - z) + 1.1 \text{ m for cohesive soils } (3 \leq z_0 \leq 34), \quad (2.31a)$$

$$i = 0.28(z_0 - z) - 0.1 \text{ m for granular soils } (6 \leq z_0 \leq 10). \quad (2.31b)$$

More recently Leach (1985) has analysed data from 23 tunnels constructed by different methods (no-shield, shield in free air, mini-tunnel, shield in compressed air) and has produced the following relations:

$$i = 0.57 + 0.45(z_0 - z) \pm 1.01 \text{ m} \quad (2.32a)$$

for those sites where consolidation effects are deemed to have been insignificant;

$$i = 0.64 + 0.48(z_0 - z) \pm 0.91 \text{ m} \quad (2.32b)$$

for those sites where consolidation effects are deemed to have been significant.

These relations, and particularly equation (2.31b) for granular soils, are not dissimilar to those derived by Atkinson and Potts (1976) from their laboratory model experiments. Reference may also be made to the graphs in Attewell (1978a) pp. 884, 885, which confirm that narrower (lower i -value) surface settlement troughs tend to be associated with granular soils, where running and ravelling may be concentrated at the tunnel crown and over the tail void of the shield.

Rather than accepting reported values of i (almost invariably i_0) for the development of the above empirical relations, it is preferable to plot the logarithm of the original recorded settlements ($\log w$) against the square (y^2) of the transverse distance and draw a regression line through the points. Maximum settlement (w_{\max}) can then be defined by the intercept of the regression line with the axis $y^2 = 0$, and the value of i by the fact that i^2 is the value of y^2 where $w/w_{\max} = 0.606$.

It is noted that under the normal probability profile assumptions, the width of the fully-developed transverse settlement trough is infinite, but in practice can be taken as $2\sqrt{2\pi} i$ (i.e. $5i$). The forward trough extends a practical distance of $\sqrt{2\pi} i$ (i.e. $2.5i$) ahead of the tunnel face if the latter is located directly beneath the 50 per cent maximum surface-settlement point (which will not usually be the case). The full form of the ground-loss settlement distribution is shown graphically in Figure 2.14.

Example 2.2 Settlement calculation

Consider a case history example (Attewell and Farmer, 1973) used in Attewell and Woodman (1982).

Tunnel axis depth, $z_0 - z = 7.5$ m

Settlement trough width parameter, $i = 3.9$ m.

Maximum surface settlement, w_{\max} (at $y = 0$) = 7.86 mm.

Ground-loss volume, $V_t = 0.077 \text{ m}^3/\text{m}$ (see equation (2.22),
with $w = w_{\max}$ and $y = 0$).

Let the tunnel face be well-advanced from the start point.

Then $(x - x_i) \rightarrow \infty$ and $G(x - x_i/i) = 1$.

Take a point on ground surface having coordinates $(x - x_t) = 4$ m, $y = 1.5$ m.

Then $G(x - x_t/i) = G(1.020) = 0.846$ (from Table 2.2).

It follows from equation (2.22) that the ground settlement at the specified point is 1.13 mm.

Calculation on equations (2.23) and (2.24) produces values of -2.23 mm for v and -0.90 mm for u . (The negative signs denote displacements horizontally inwards towards the centre of the trough.) A check summation of the three displacements having regard to sign confirms the no-volume-change assumption underlying the analysis.

Further calculation produces ground strain values of $-110 \mu\epsilon$ (compressive), $-130 \mu\epsilon$ (compressive) and $+240 \mu\epsilon$ (tensile) for ε_z , ε_y and ε_x , respectively. These values sum to zero and so satisfy the no-volume-change assumption.

2.5 Design-curve graphs

With respect to buildings and in-ground structures, information on ground-surface settlement and strain is only part of the requirement. The horizontal u , v ground displacements impose direct strains on a foundation or buried pipe, the upper bound structural strains being equated to ε_x , ε_y by neglecting ground-structure differential stiffness and assuming no ground material shearing. Building foundations, however, settle differentially and incur angular distortions, the magnitudes of which depend on the position of the foundation in the settlement trough (see Attewell, 1978a). Strains associated with angular distortions are additive to the direct lateral distortional strains. It should also be realized that a foundation is subjected to a wave of torsion before the advance of the tunnel face removes the effects of the forward settlement trough. Similarly, buried pipes within a ground settlement trough experience direct strain, bending strain (related to ground curvature) and torsion. These matters are discussed in Attewell and Woodman (1982), but they are probably more easily accommodated by use of design-curve graphs. There is also more detailed discussion later in the book.

The use of equations implies a degree of precision in estimation that in fact does not exist. The approximate character of the assessment is probably better reflected by expressing the equations graphically in such a way that a foundation or buried pipe analysis can be conducted more easily and perhaps more rapidly.

Figures 2.12–2.17 were originally constructed by desk computer and graph plotter from adaptations of equations (2.22) to (2.27). The coordinates for the

TUNNELS : GROUND DISPLACEMENTS AND STRAINS

X-DISPLACEMENT PLOTTED AS PERCENTAGE OF MAXIMUM ◆
SCALED IN TERMS OF INFLEXION DISTANCE (i)

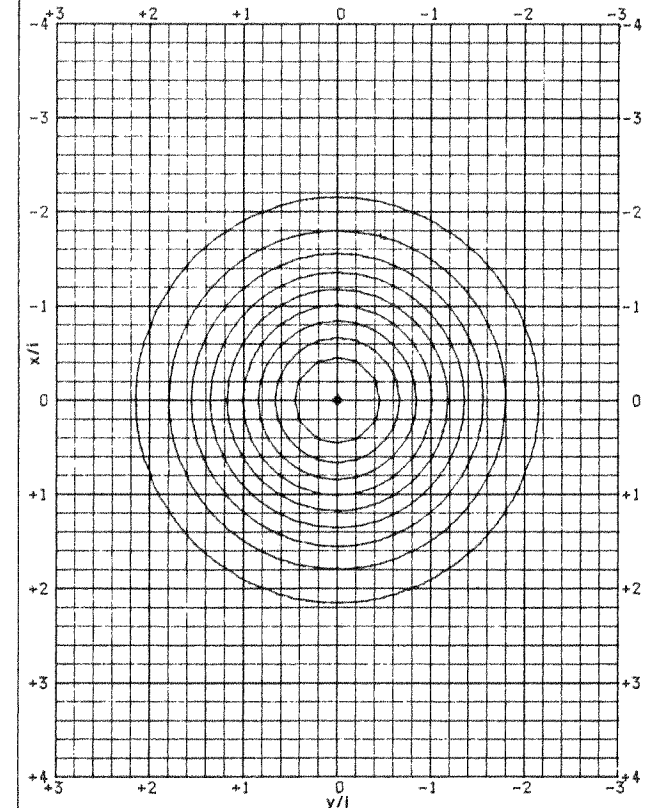


Figure 2.12 10% incremental ground displacement (u) curves, x -axis.

curves are scaled as x/i (ordinate: down the graph) and y/i (abscissa: across the graph), and the positive z -axis is directed downwards into the plane of the paper. On the graphs, the tunnel face is theoretically positioned at the origin. The curves assume that the tunnel is of infinite length (in practice, the distance of advance must be large compared to $(z_0 - z)$) and that the increments of horizontal ground displacement are radial (always towards the current tunnel face origin). Each curve on a particular graph represents 10 per cent of the parameter absolute maximum, each maximum being marked by a small infilled parallelogram.

The curves show a number of interesting features. For example, the settlement, or z -displacement (w), curves (Figure 2.14) profile the settlement

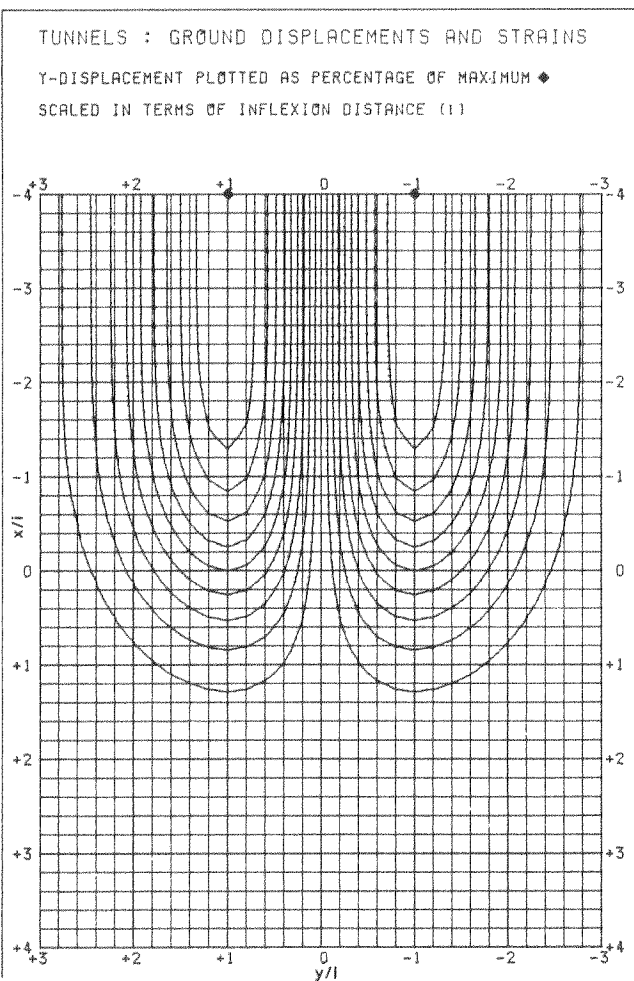


Figure 2.13 10% incremental ground displacement (v) curves, y -axis.

distribution about the source ($x/i = y/i = 0$) and show that the transverse ground-loss settlement profile becomes almost fully developed when the tunnel face has advanced about $2i$ beyond the profile section. Figure 2.15 shows that the tensile (positive) ϵ_x regime ahead of the tunnel face is a mirror image of the compressive (negative) ϵ_x behind the face. Figure 2.16 shows that the transverse ϵ_y has a compressive maximum above the tunnel centre line which decreases to zero with increasing y to a tensile ϵ_y maximum that is between 40 per cent and 50 per cent (theoretically 44.6 per cent) of the absolute maximum. The relatively complex pattern of ϵ_z (Figure 2.17) can be interpreted by remembering that $\epsilon_z = -(\epsilon_x + \epsilon_y)$ according to the underlying

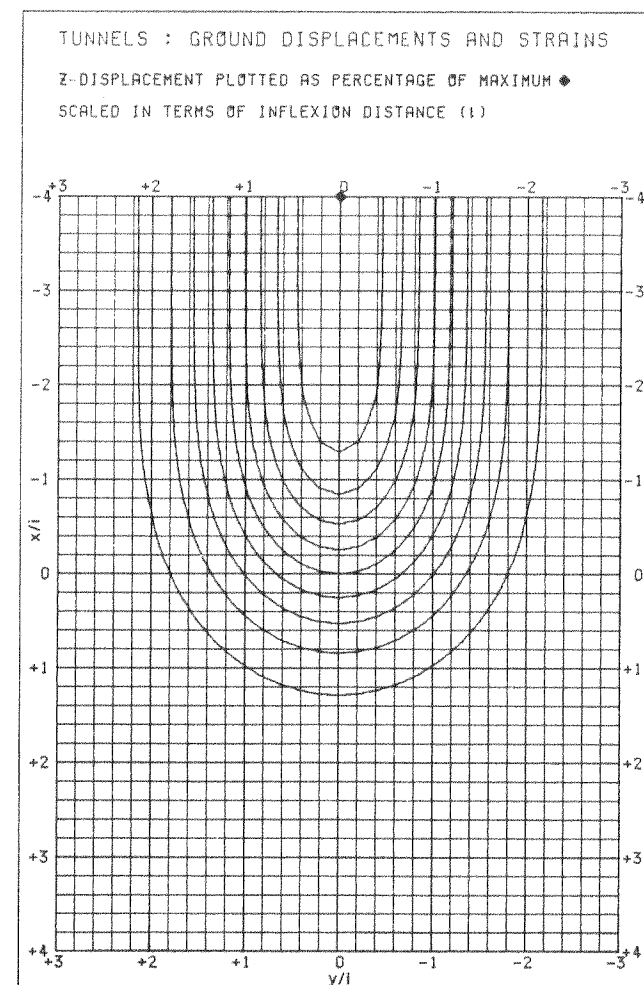


Figure 2.14 10% incremental ground displacement (w) curves, z -axis.

assumption of no volume change in the soil. There is a tensile maximum on the tunnel centre line and behind the face; it decays with radial distance to zero strain and thence to compression. However, vertical strain distribution is of marginal practical importance in the present work, and is not considered further.

Only six graphs are necessary. Although this number may be inadequate for some practical purposes, there are simple relations and equivalences between parameters which allow the use of these graphs to be extended. For greater completeness, the i subscript (x or y) is given, although in most cases an unsubscripted i -parameter ($i_x = i_y = i$) must be used. Reference should be made

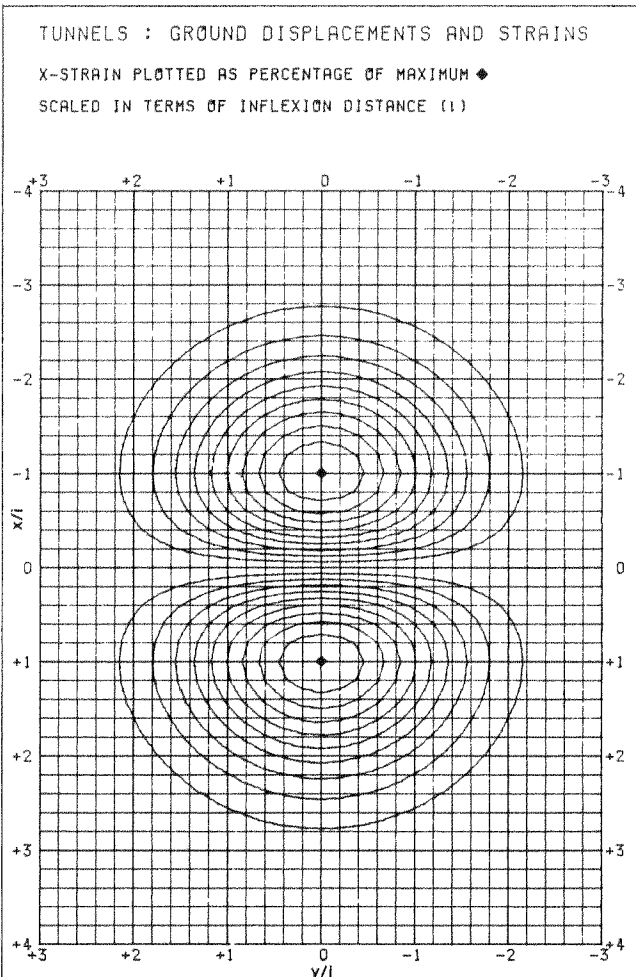


Figure 2.15 10% incremental ground strain (ε_x) curves, x-axis.

to section 2.7 for further discussion on this point.

$$\gamma_{xy} \text{ graph} \equiv \varepsilon_y \text{ graph rotated about the } z\text{-axis through } \pi/2. \quad (2.33)$$

$$\text{xz-plane gradient } \frac{\partial w}{\partial x} = \frac{z_0 - z}{ni_x^2} u \sim u. \quad (2.34)$$

$$\text{yz-plane gradient } \frac{\partial w}{\partial y} = \frac{z_0 - z}{ni_y^2} v \sim v. \quad (2.35)$$

$$\frac{\partial^2 w}{\partial x^2} = \frac{z_0 - z}{ni_x^2} \varepsilon_x \sim \varepsilon_x, \quad \frac{\partial^2 w}{\partial y^2} = \frac{z_0 - z}{ni_y^2} \varepsilon_y \sim \varepsilon_y,$$

$$\frac{\partial^2 w}{\partial x \partial y} = \frac{z_0 - z}{n} \cdot \frac{\gamma_{xy}}{i_x^2 + i_y^2} \sim \gamma_{xy}. \quad (2.36)$$

(These second derivatives of w are approximations to the components of curvature of the settled surface, given small displacement and gradient, and to the components of bending strain referred to the initial pre-settlement horizontal plane, under conditions of small strain and small gradient.)

Sufficient parameters have probably now been covered for building foundations, but not for buried pipes. In particular, horizontal pipes also need

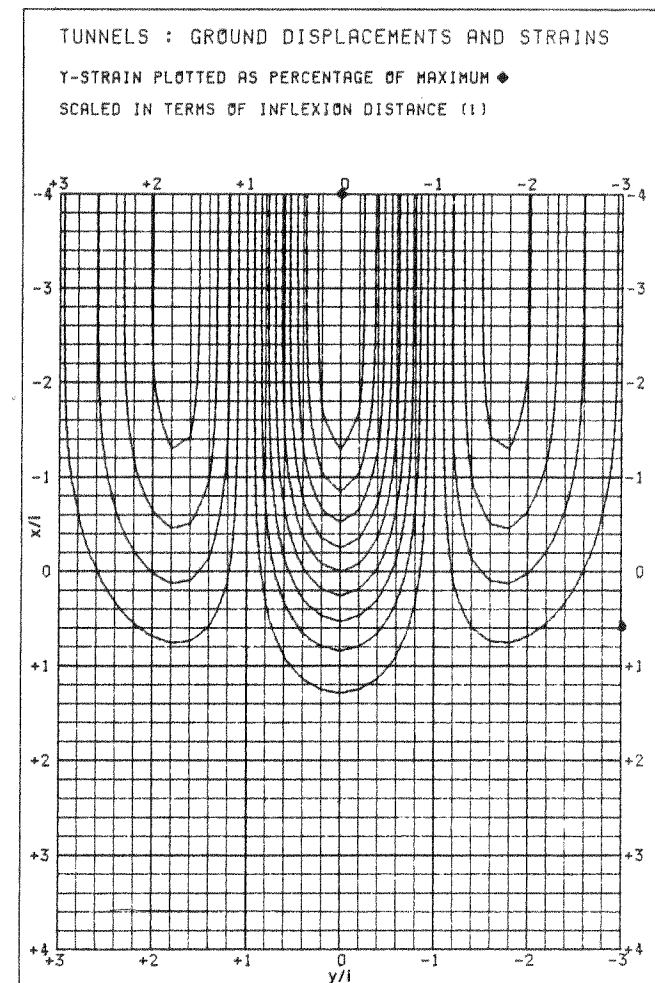


Figure 2.16 10% incremental ground strain (ε_y) curves, y-axis.

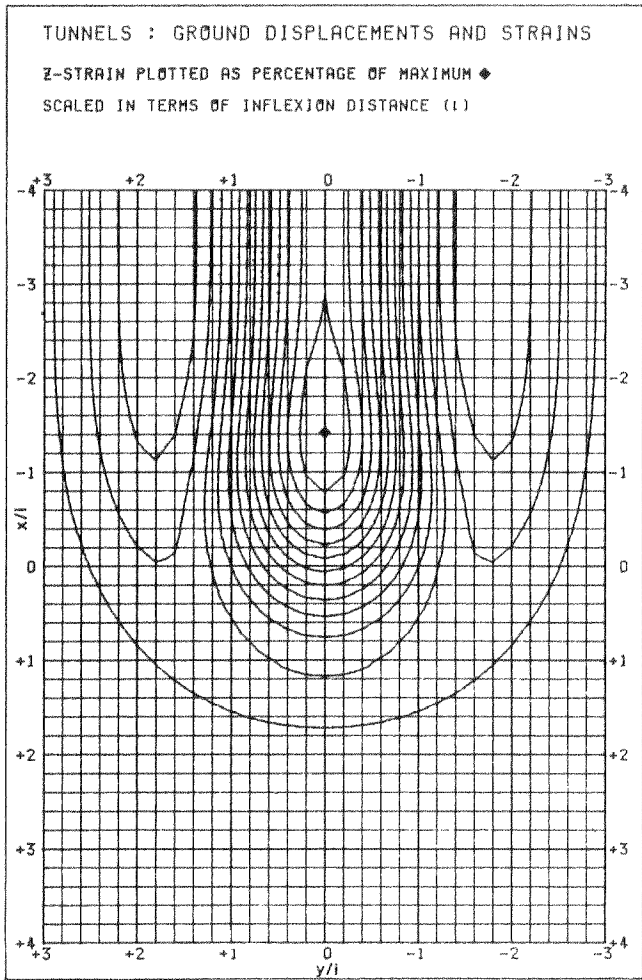


Figure 2.17 10% incremental ground strain (ε_z) curves, z -axis.

the following:

$$\frac{\partial u}{\partial y} = \frac{i_x^2 \gamma_{xy}}{i_x^2 + i_y^2} \sim \gamma_{xy}, \quad \frac{\partial v}{\partial x} = \frac{i_y^2 \gamma_{xy}}{i_x^2 + i_y^2} \sim \gamma_{xy}. \quad (2.37)$$

$$\begin{aligned} \frac{\partial^2 u}{\partial x^2} &= \left(\frac{x^2}{i_x^2} - 1 \right) u, & \frac{\partial^2 u}{\partial y^2} &= \left(\frac{y^2}{i_y^2} - 1 \right) u, & \frac{\partial^2 u}{\partial x \partial y} &= -\frac{y}{i_y^2} \varepsilon_x; \\ \frac{\partial^2 v}{\partial x^2} &= -\frac{y}{i_x^2} \varepsilon_x, & \frac{\partial^2 v}{\partial y^2} &= \left(\frac{y^2}{i_y^2} - 3 \right) v, & \frac{\partial^2 v}{\partial x \partial y} &= \left(\frac{y^2}{i_y^2} - 1 \right) \frac{u}{i_x^2}, \end{aligned} \quad (2.38)$$

It is noted in Reeves *et al.* (1983) that there is an argument for graphically displaying gradient magnitude $\sqrt{(\partial w/\partial x)^2 + (\partial w/\partial y)^2}$ and principal lateral strains/bending strains of the horizontal plane, but these curves depend on the ratio i_x/i_y , unlike contours for the above parameters.

Provided that values are available for the essential input parameters, the percentages of the reference values for each displacement and strain parameter are then assessed by interpolation between curves on the graphs. Numerical values for the displacement and strain parameters are calculated by defining the reference displacements and strains corresponding to absolute maxima defined as follows:

$$w_{\max} = \frac{1}{\sqrt{2\pi}} \frac{V_s}{i_y} \text{ at } (-\infty, 0). \quad (2.39)$$

This is an important and well-used equation, expressed in the form

$$V_s = 2.5 i_y w_{\max} \quad (2.39a)$$

which allows maximum settlement w_{\max} to be estimated from an input value of V_s (itself usually estimated from the type of practical information given in section 2.4.1) and an input value of i_y (estimated from the information given in section 2.4.2). The volume of ground displaced by settlement at the surface (V_s) expressed per unit length of tunnel advance (usually in units of $\text{m}^3/\text{m} = \text{m}^2$) is obtained by integration of the area under the error curve assumed to define the form of the transverse settlement trough. Equation (2.39a) is derived mathematically in Attewell and Farmer (1974a), Appendix 1, pp. 379, 380.

$$v_{\max} = -w_{\max} \frac{n i_y}{z_0 - z} \exp \left[-\frac{1}{2} \right] \text{ at } (-\infty, 1), \quad (2.40)$$

$$u_{\max} = -w_{\max} \frac{1}{\sqrt{2\pi}} \frac{n i_x}{z_0 - z} \text{ at } (0, 0), \quad (2.41)$$

$$\varepsilon_{z\max} = w_{\max} \frac{n}{z_0 - z} \left[\frac{\exp(-1)}{\sqrt{\pi}} + \frac{1 + \text{erf}(1)}{2} \right] \text{ at } (-\sqrt{2}, 0), \quad (2.42)$$

$$\varepsilon_{y\max} = -w_{\max} \frac{n}{z_0 - z} \text{ at } (-\infty, 0), \quad (2.43)$$

$$\varepsilon_{x\max} = w_{\max} \frac{n}{z_0 - z} \frac{\exp(-\frac{1}{2})}{\sqrt{2\pi}} \text{ at } (1, 0), \quad (2.44)$$

$$\gamma_{xy\max} = \varepsilon_{x\max} \frac{i_x^2 + i_y^2}{i_x i_y} \text{ at } (0, 1). \quad (2.45)$$

(Note that 'erf' in equation (2.42) denotes 'error function'.)

Input parameters $i_x, i_y, z_0 - z$ are often specified in metres and V_s in cubic metres per metre. In that case the reference displacements expressed in millimetres are

$$\begin{aligned} w_{\max} &= 399 \frac{V_s}{i_y}, & v_{\max} &= -0.607 w_{\max} \frac{i_y}{z_0 - z}; \\ u_{\max} &= -0.399 w_{\max} \frac{i_x}{z_0 - z}. \end{aligned} \quad (2.46)$$

Similarly, if w_{\max} is in millimetres, then the reference strains in microstrains are

$$\begin{aligned} \varepsilon_{z\max} &= 1.129 \varepsilon_{y\max}; & \varepsilon_{y\max} &= -1000 w_{\max} \frac{n}{z_0 - z}; \\ \varepsilon_{x\max} &= 0.242 \varepsilon_{y\max}; & \gamma_{xy\max} &= \varepsilon_{x\max} \frac{i_x^2 + i_y^2}{i_x i_y}. \end{aligned} \quad (2.47)$$

2.6 Ground movements and structures—use of design curves for preliminary assessment

Two matters must be emphasized initially. First, the ground-structure interaction is one of ground shear against the (assumed) stiffer contact surface of the foundation or buried pipe structure combined with an induced bending, the latter being simple or torsional. It is the ground displacements, not the strains, that are important, although, as stated earlier, the calculated ground strains provide upper-bound values for the structural strains and so are used here. Second, assumed limiting levels of structural deformation must be known, and these are specified in terms of the type of structure at risk (Attewell, 1978a; Norgrove *et al.*, 1979). Although criteria suggested by Burland and Wroth (1975), and based on Skempton and Macdonald (1956) and others (see section 4.13 below), have been proposed for tunnelling-induced ground deformation, caution is required. Self-weight settlements and deformations are long-term developments, and much of their potential effect can be accommodated during the actual construction. Tunnelling-induced movements are imposed on a structure very quickly, and so the self-weight damage criteria will have no in-built conservatism with respect to dynamic movements.

2.6.1 Application of design curves—use of overlays

When a structure at risk has been identified, its foundation (in the case of a building) should be dimensionally-scaled on a transparent overlay and then

superimposed on each of the design-curve graphs in turn. The distribution of the 10 per cent design curves on the area of the structure is then noted and interpreted with respect to an adopted (usually empirical) damage criterion.

If the tunnel passes beneath a heavily built-up area it is recommended that the relevant portion of the national or state survey plan be photographed with national grid or other orientation feature marked. The scale of the plan is then noted and a further calculation performed to scale its dimensions by the factor i_s for further printing. Finally, a design-curve overlay transparency can be prepared from the print. Suppose that the scale of the survey plan is 1:S. The design-curve graphs, as originally drawn to scale by the microcomputer, reproduce a linear dimension scaled to i_s in units of $g = 25$ mm linear measure. If p is a dimension of a building measured (say in mm) on the plan, then the corresponding required length of the building on the photographic print overlay transparency is gpS/i_s . It is noted that this procedure is valid only for foundations in the same horizontal plane.

Example 2.3 Building foundation assessment

A sewer tunnel, having an excavated radius 1.105 m, is to be driven in a mainly granular soil at an axis depth of 10.5 m. The ground loss is estimated to be 5 per

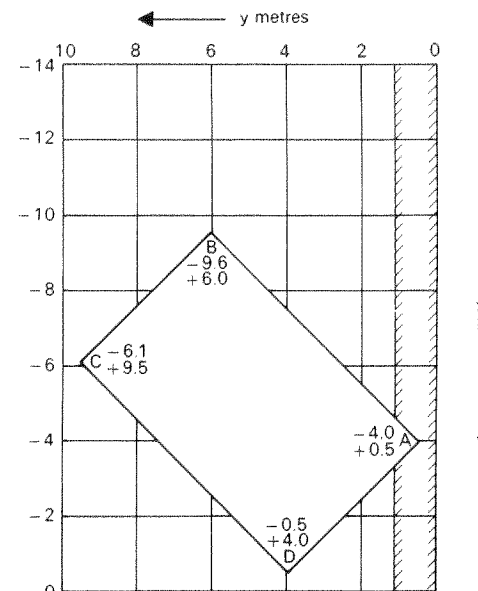


Figure 2.18 Plan location of building with respect to tunnel.

cent (i.e. $0.192\text{m}^3/\text{m}$) and it is assumed that this loss is fully transferred to ground surface as settlement. A building, having a raft foundation of rectangular area at a mean depth of 0.5 m, is located with respect to the tunnel centre line as shown in Figure 2.18. Prediction of the effects on the building might proceed as follows: $z_0 - z = 10.5\text{ m} - 0.5\text{ m} = 10\text{ m}$.

Let $i = 0.28(z_0 - z) - 0.1\text{ m}$ (after O'Reilly and New (1982)).

Thus $i = 2.7\text{ m}$. Let the n parameter be unity.

(Although the above equation is derived from UK tunnelling case histories, a check against a batch of international case histories suggests that it might be more generally relevant.)

The scaled coordinates of the foundation are:

$x(\text{m})$	x/i	$y(\text{m})$	y/i
-4.0	-1.481	+0.5	+0.185
-9.6	-3.555	+6.0	+2.222
-6.1	-2.259	+0.5	+3.518
-0.5	-0.185	+4.0	+1.481

The scaled foundation is redrawn in Figure 2.19 for superimposition on the design-curve graphs.

Lateral distortion and tensile failure. As the tunnel face advances, most of the foundation will eventually be subjected to virtually the whole deformation field on one side of the tunnel centre line. Tensile effects are most forcefully impressed on the foundation in two main regions:

$x > 0, y^2 < i_y^2$ and $x < 0, y^2 > i_y^2$. However, if $i_x = i_y$, wherever $\varepsilon_x \geq \varepsilon_y$ the more tensile principal strain in the horizontal plane is less than the overall maximum tensile $\varepsilon_y, \varepsilon_{ytmax} = -0.466\varepsilon_{y, \text{max}}$. The region ahead of the tunnel face $x > 0, y^2 < i_y^2$, is thus less dangerous than the region of permanent deformation $x < 0, y^2 > i_y^2$ transverse to the tunnel centre line. In this present example, $\varepsilon_{ytmax} \approx 0.127$ per cent.

A factor of some importance is the area of the foundation that is required to sustain a large tensile-strain field. Superimposing Figure 2.19 on Figure 2.16 shows that high permanent tensile strains would be experienced over a large area of the foundation, centred approximately on an x -axis just to the tunnel side of corner B . From Figure 2.13, -90 per cent $v_{\text{max}} = 0.0065\text{ m}$ displacement occurs over a horizontal distance of about 4.86 m, suggesting horizontal (y) distortion (see Figure 4.37) of approximately 0.096 per cent. At a superficial damage threshold of 0.05 per cent tensile strain the foundation would be vulnerable, even if a certain amount of interfacial slippage is allowed for.

Mid-planar bending. This can be analysed in a similar manner to horizontal strain. However, whereas in the case of horizontal strain it is the tensile directional component that is important, in a brittle material foundation, with bending the positive (convex up) and negative (concave up) components are of equal concern. Noting again the equivalence between ground curvature and

direct horizontal strain curves, and superimposing Figure 2.19 overlay on Figure 2.16, it is seen that the more negative principal bending strain at corner A exceeds 80 per cent $(\partial^2 w / \partial y^2)_{\text{max}} = 80$ per cent $(w_{\text{max}} / i^2) \approx 0.00389\text{ m}^{-1}$, and will eventually exceed 90 per cent $(\partial^2 w / \partial y^2)_{\text{max}}$ as the tunnel face advances a short distance further. This bending strain is clearly much more significant than the smaller, but near maximum and stabilized, positive principal bending strain already present at corner B .

If i_x is taken equal to i_y , the maximum ground slope, similar to the maximum horizontal displacement, is bounded absolutely in any region by the values

$$\left(\frac{\partial w}{\partial x} \right)_{\text{max}} = \frac{z_0 - z}{ni_x^2} u_{\text{max}} \approx 0.42 \text{ per cent and}$$

$$\left(\frac{\partial w}{\partial y} \right)_{\text{max}} = \frac{z_0 - z}{ni_x^2} v_{\text{max}} \approx 0.64 \text{ per cent.}$$

As with tensile failure, the average value may be more significant. From

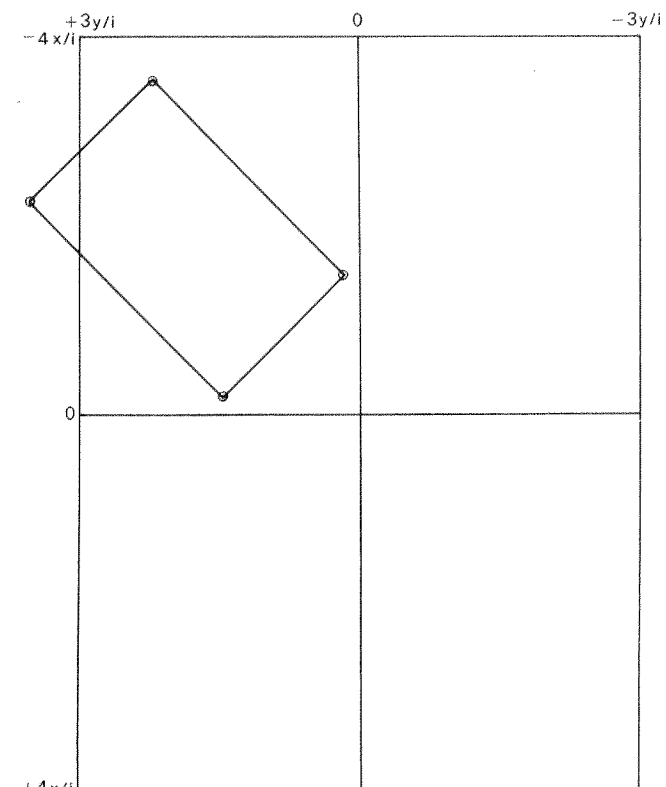


Figure 2.19 Overlay incorporating building plan dimensions scaled to i .

Figure 2.14 approximately 80 per cent w_{\max} (0.0277 m) is developed over a distance of about 5 m, giving a y -direction angular distortion (see Figure 4.36) of approximately 0.454 per cent (1 in 220). Threshold values of angular distortion depend upon the actual construction of the building (Attewell, 1978a; Norgrove *et al.*, 1979; see also Table 4.5). However, this predicted ground slope is sufficiently severe to create some concern for a building where the foundation is likely to follow the slope profile.

Example 2.4 Buried pipeline assessment

The general assessment of induced longitudinal pipe strain generally follows the above lines, predicted bending strains being additive to direct axial strains (the latter are the only strains experienced by the pipe neutral axis). For superimposition on the design-curve graphs the pipe can usually be represented by a line, since its diameter scaled to i is small. As earlier, it is assumed that the pipe deforms conformably with the predicted ground deformation that would be experienced without the presence of the pipe; the design curves effectively represent upper-bound predictions of pipe deformation. Any slippage at or near the pipe-soil interface implies that the actual direct and bending strains in the pipe may well be substantially less than those calculated on the basis of no interfacial slippage. Furthermore, the concept of an 'interface' may in many cases be invalid, since old cast iron pipes (for which assessments are likely to be made) may be severely corroded on the outside and so may have mechanical properties, over the zone of corrosion, intermediate between those of the uncorroded pipe material and those of the pipe bedding. Depending upon the type of pipe joint and its age, there may be a facility for rotation and direct translation at the joints which absorbs some of the potential strain in the pipe material.

For the example calculation, locked joints and an upper-bound strain condition have been conservatively assumed. Consider a 2 ft (0.61 m) diameter pipeline buried at a depth of 1.5 m and lying parallel to—but 3.13 m from—the centre line of a tunnel, axis depth 13.5 m. The ground volume loss at the tunnel is estimated at 2.5 per cent or $0.103 \text{ m}^3/\text{m}$, and the i -value is 6.26 m. It is assumed that n is close to unity.

An overlay incorporating a line distant $y/i = 3.13/6.26 = 0.5$ from and parallel to the tunnel centre line ($y/i = 0$) may be prepared (Figure 2.20) but this is really unnecessary since for this simple structural configuration all the information can be readily drawn by direct inspection of the design-curve graphs. From Figure 2.15 the maximum tensile strain along the line of the pipe $|y/i| = 0.5$ is 85 per cent $\varepsilon_{x\max}$, approximately $100 \mu\epsilon$. Maximum vertical and horizontal axial bending strains occur at the same point, since

$$\frac{\partial^2 w}{\partial x^2} \sim \varepsilon_x \quad \text{and} \quad \frac{\partial^2 v}{\partial x^2} = -\left(\frac{y}{i^2}\right)\varepsilon_x$$

Consequently, maximum vertical axial bending is 85 per cent $(\partial^2 w / \partial x^2)_{\max} = 32 \mu\epsilon/\text{m}$, and maximum horizontal axial bending is approximately $9 \mu\epsilon/\text{m}$. The maximum resultant bending strain is approximately

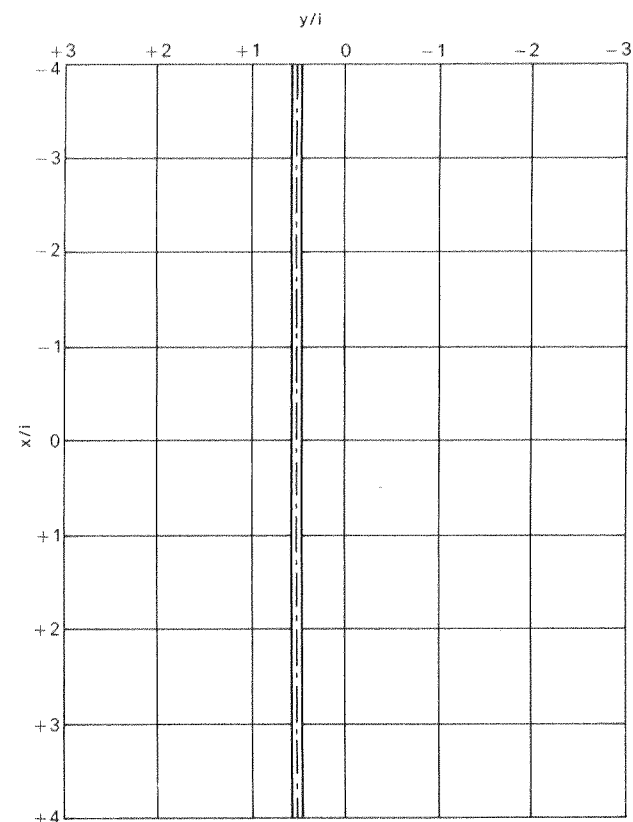


Figure 2.20 Example of pipeline lying parallel to the tunnel centre line.

$\sqrt{32^2 + 9^2} \approx 33 \mu\epsilon/\text{m}$. Thus, assuming constant shear in a pipe of radius r , the maximum axial tensile strain is approximately $\varepsilon_x + r \partial^2 w / \partial x^2 \approx 120 \mu\epsilon$.

Analyses of the above type would be applied to old pipes of traditional brittle material construction (cast iron or clay). Take, for example, an old pit-cast grey iron pipe of pre-BS 78 vintage, corroded on the outside, and unable to translate or rotate at the joints. Subject to all the assumptions discussed earlier, all of the potential strain calculated above would be experienced by the pipe material. With an allowable pipe stress of one-quarter the material ultimate tensile strength, an allowable strain of $400 \mu\epsilon$ would probably be applicable. It follows that the estimated upper-bound axial strain in the example pipe is less than one-third of its allowable strain. Had the estimated strains been much closer to the allowable strain, a criterion of failure based on the biaxial state of strain would have been applied, using the fact that for all

pipe orientations the mean transverse strain is everywhere equal, but of opposite sign, to the axial strain under the assumption of no volume change. Two failure criteria could most conveniently be used: the Tresca maximum shear stress theory and the Huber–Hencky–von Mises distortional energy criterion. Examples of the application of these theories are not given in this book, but reference may be made to standard textbooks on material mechanics.

2.6.2 Pipes aligned obliquely to the direction of tunnel advance

Many of the major problems with underground services occur in urban areas when tunnel alignments and buried water and gas distribution mains are parallel to main roads, as in the example considered above. However, if a horizontal buried pipe is at an angle θ to the tunnel advance direction (x -axis), defined by direction cosines[†] $l, m, 0$, the following expressions apply for point values and mean values over a straight-line segment of length L between points 1 and 2:

$$\text{point axial strain} = \varepsilon_x l^2 + \gamma_{xy} l m + \varepsilon_y m^2 \quad (2.48)$$

$$\text{mean axial strain} = [(u_2 - u_1)l + (v_2 - v_1)m]/L \quad (2.49)$$

$$\text{point vertical axial bending} = \frac{\partial^2 w}{\partial x^2} l^2 + 2 \frac{\partial^2 w}{\partial x \partial y} l m + \frac{\partial^2 w}{\partial y^2} m^2 \quad (2.50)$$

mean vertical axial bending

$$= \left[\left\{ \left(\frac{\partial w}{\partial x} \right)_2 - \left(\frac{\partial w}{\partial x} \right)_1 \right\} l + \left\{ \left(\frac{\partial w}{\partial y} \right)_2 - \left(\frac{\partial w}{\partial y} \right)_1 \right\} m \right] / L \quad (2.51)$$

point horizontal axial bending

$$= \frac{\partial^2 v}{\partial x^2} l^3 + \left(2 \frac{\partial^2 v}{\partial x \partial y} - \frac{\partial^2 u}{\partial x^2} \right) l^2 m - \left(2 \frac{\partial^2 u}{\partial x \partial y} - \frac{\partial^2 v}{\partial y^2} \right) l m^2 - \frac{\partial^2 u}{\partial y^2} m^3 \quad (2.52)$$

mean horizontal axial bending

$$= [(\varepsilon_{y2} - \varepsilon_{y1} - \varepsilon_{x2} + \varepsilon_{x1}) \sin 2\theta + (\gamma_{xy2} - \gamma_{xy1}) \cos 2\theta] / 2L. \quad (2.53)$$

It is worth emphasizing that this section in general, and the above equations in particular, represent in effect upperbound solutions which assume that even a brittle pipe will follow the contours of the settlement trough. For specific solution of problems of buried pipes the reader's attention is directed to Chapter 3.

[†] $l = \cos \theta; m = \cos(90 - \theta) = \sin \theta$.

2.7 Relations between i_y and i_x

It has been assumed throughout the development of the ground movement equations in section 2.4 that the tunnel centre line settlement development profile may be described by a cumulative probability function based on the same statistical mean (w_{\max}) and standard deviation (i) parameters as define the transverse normal probability settlement profile. In particular, it is assumed that $i_y = i_x$.

The easiest way of checking the reasonableness of this assumed and rather convenient equality is to compare a 'theoretical' cumulative probability centre line (xz -plane) settlement curve based on the i_y parameter with the actual 'best fit' recorded curve which defines i_x , the latter curve having been translated along the tunnel advance axis so that the 50 per cent maximum settlement (w_{\max}) points on both curves match. Table 2.3 and Figure 2.21 demonstrate how this is done. This x -axis translation will usually be necessary because the

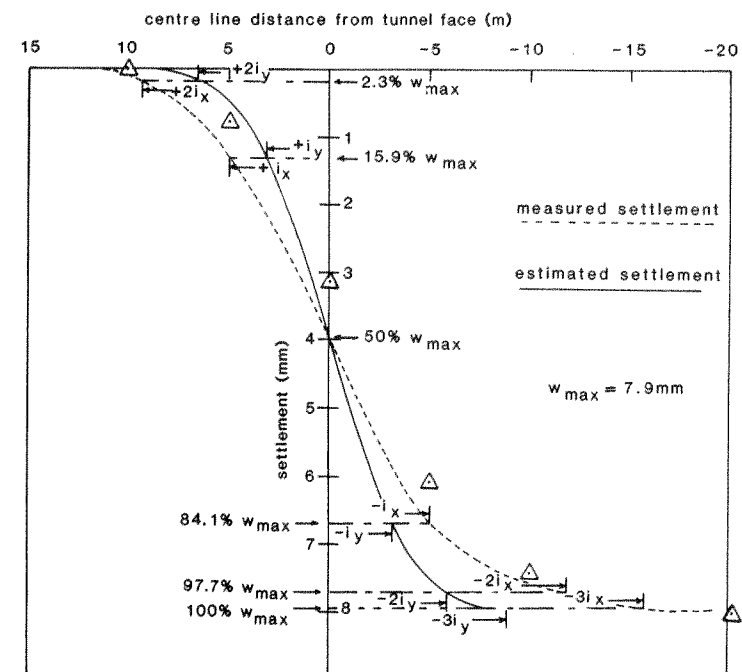


Figure 2.21 Centre line settlement distribution measured above a tunnel in stony/laminated clay at Hebburn, north-east England (Glossop, 1978), together with a distribution generated by the transverse settlement parameter i_y . The actual measurement points are marked by the triangular symbol and the measured curve has been translated forward by 1.3 m to set the 50% w_{\max} point above the tunnel face.

Table 2.3 Percentage of maximum settlement as a function of position on the tunnel centre line settlement curve as expressed ideally in terms of the transverse settlement parameter i_y .

(Note: It is assumed that 50% w_{\max} will have developed directly over the tunnel face on this centre line settlement profile; + x distances are ahead of the face position and - x distances are behind the face position.)

Location on centre line settlement profile	Approximate theoretical percentage of maximum settlement assuming that a cumulative probability function applies
+ $3i_y$	0% w_{\max}
+ $2i_y$	2.3% w_{\max}
+ i_y	15.9% w_{\max}
0	50% w_{\max}
- i_y	84.1% w_{\max}
- $2i_y$	97.7% w_{\max}
- $3i_y$	100% w_{\max}

value of the ratio w/w_{\max} at ground surface above the tunnel face is in almost all cases less than 50 per cent. For firm-to-stiff clays the range seems to be 30–50 per cent (Attewell and Woodman, 1982).

Obvious discrepancies between the two curves develop at low settlements and towards the maximum measured settlement. For such settlement development curves in general, these discrepancies can be quantified in terms of

$$i_y : \frac{+(3i_x)}{3}; \quad i_y : \frac{+(2i_x)}{2}; \quad i_y : +i_x; \quad i_y : -i_x; \quad i_y : \frac{-(2i_x)}{2}; \quad i_y : \frac{-(3i_x)}{2}.$$

The above relations between i_y and i_x are plotted in Figures 2.22–2.27 for the 14 tunnel case histories listed in Table 2.4 and carefully examined for this purpose. Original detailed measurements were available from most of these case histories.

Examination of measured centre line settlement development profiles indicated that the centre line settlement field almost always exceeds the length ($6i_y$ metres) of the cumulative probability curve generated from the transverse settlement trough i_y parameter. This is also shown by the plots on Figures 2.22–2.27, which lie generally above the equality line. These data points are also seen to lie closer to the estimated line ahead of (+ x) the face than they are behind (- x) the face, where the incremental settlements are much attenuated. However, the symmetry of the estimated ($i_x = i_y$) centre line settlement curves about the tunnel face position could only be satisfied if the

Table 2.4 Tunnel locations for centre line settlement estimations

Case history number on graphs (Figs. 2.22–2.27)	Tunnel location	Type of ground	Reference
1.	Belfast, N. Ireland	Soft silt with overlying fill	Glossop <i>et al.</i> (1979)
2.	Ouseburn, Newcastle upon Tyne, England	Recent fill (rubble, household waste and ash) in a soft clay matrix	Spencer (1978), Dobson <i>et al.</i> (1979)
3.	Howdon, Newcastle upon Tyne, England	Boulder clay	Glossop (1978)
4.	Willington Quay, Newcastle upon Tyne, England	Silty organic alluvial clay	Sizer (1976), Attewell <i>et al.</i> (1978)
5.	Hebburn, Newcastle upon Tyne, England	Stony laminated clay	Attewell and Farmer (1973)
6.	Green Park, London, England	London Clay	Attewell and Farmer (1974b)
7.	Grimsby B2, England	Soft alluvial clay (Marine 'warp')	Glossop (1980)
8.	Grimsby BI, England	as 7	as 7
9.	Grimsby C, England	as 7	as 7
10.	Thunder Bay South, Canada	Silt	Morton and Dodds (1979)
11.	Heathrow, London, England	Upper ground section of London Clay with 3.6 m of clay cover to tunnel under wet gravel	Wood and Gibb (1971), Smythe-Osborne (1971)
12.	Norton, Cleveland, N.E. England	Sandy, silty clay	Hurrell (1984a)
13.	San Francisco, USA	Slightly cemented dense silty fine sand dewatered by deep wells	Peck (1969)
14.	Washington DC, USA	Medium dense silty sand and gravel, interbedded with sandy silty clays	Hansmire (1975)

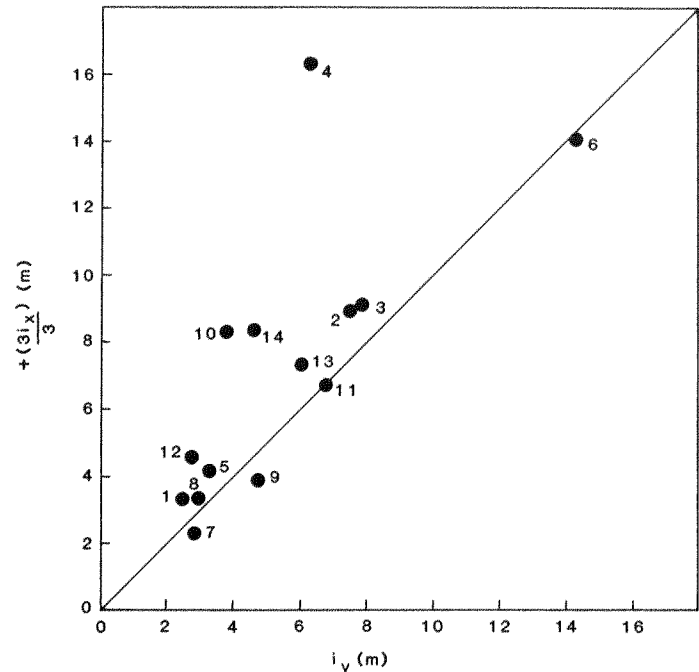


Figure 2.22 Quality of fit between estimated and measured tunnel centre line settlement curves just at the onset of settlement.

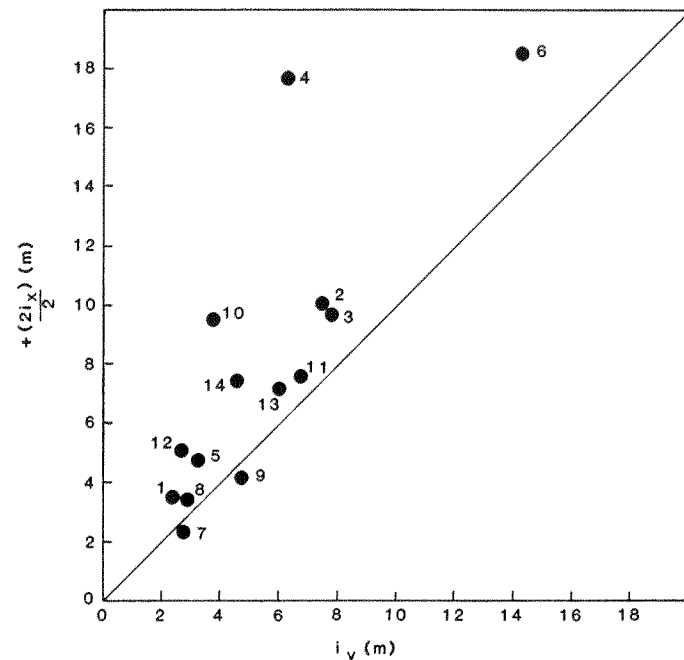


Figure 2.23 Quality of fit between estimated and measured tunnel centre line settlement curves at the point where the settlement is 2.3% maximum.

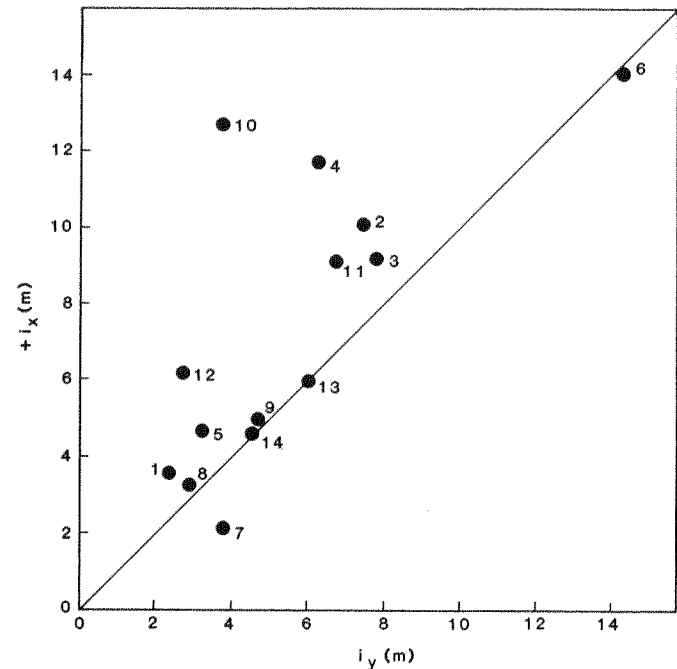


Figure 2.24 Quality of fit between estimated and measured tunnel centre line settlement curves at the point where the settlement is 15.9% maximum.

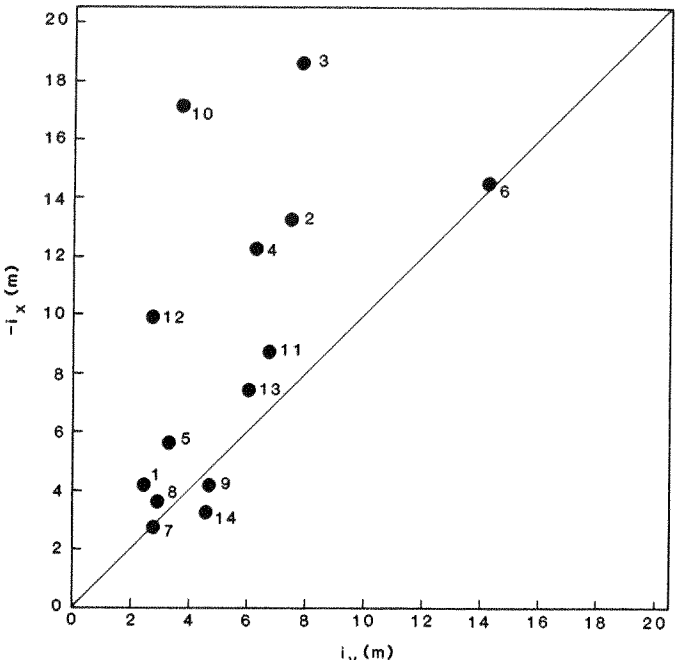


Figure 2.25 Quality of fit between estimated and measured tunnel centre line settlement curves at the point where the settlement is 84.1% maximum.

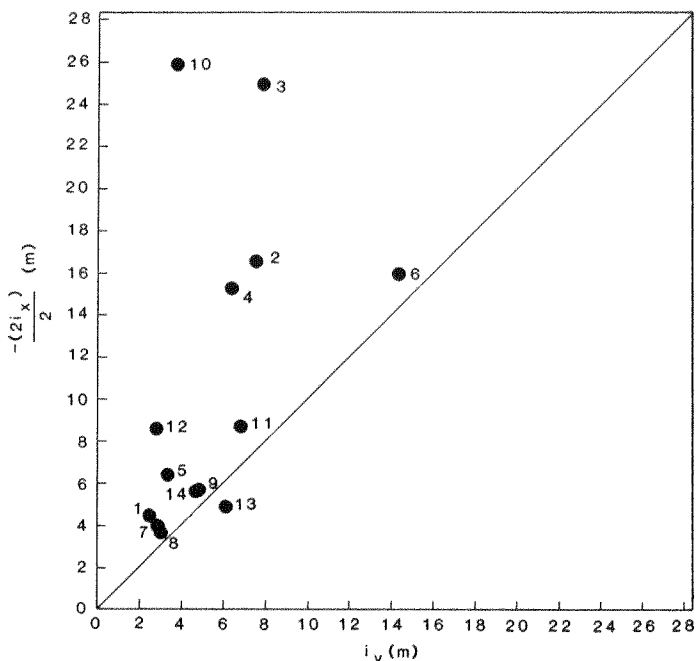


Figure 2.26 Quality of fit between estimated and measured tunnel centre line settlement curves at the point where the settlement is 97.7% maximum.

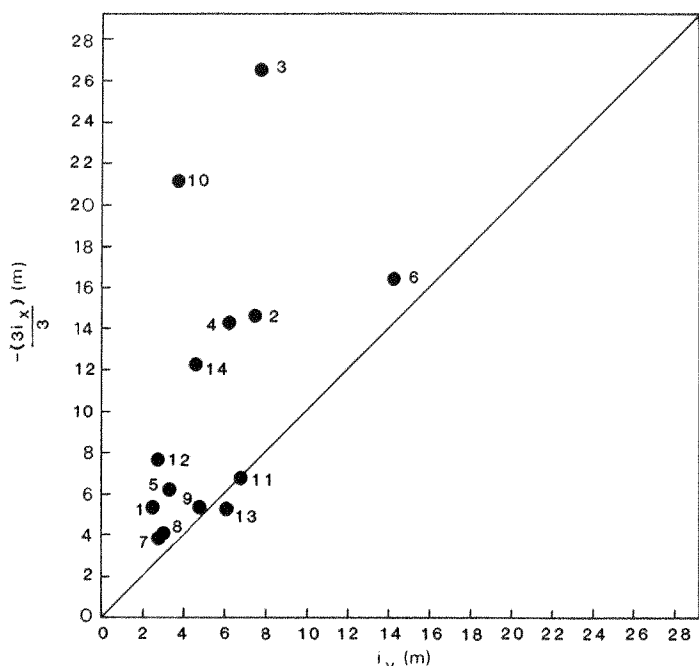


Figure 2.27 Quality of fit between estimated and measured tunnel centre line settlement curves at the point where the settlement has maximized.

tunnel actually behaved as the point source of linearly translating ground loss specified by Attewell and Woodman (1982) for their analyses and incorporated in equations (2.22) to (2.27). While it may be reasonable to idealize a tunnel face proper as a point source of loss for settlements ahead of the face, the continuing settlements above a lined tunnel owe their origins more to distributed radial losses at the tunnel, these losses being progressively inhibited and delayed as contact grout sets behind a segmental lining and the lining ring stiffness is fully mobilized. Because consolidation effects in clay soils, discussed in section 2.8, should be additive to ground loss settlements, the differences between measured and estimated centre line settlement curves behind the face could be expected to be less than actually indicated by the points on Figures 2.22–2.27.

The practical implications of the curve mismatches are not as serious as might at first be suspected. Since all points in the vicinity of the translating tunnel face experience the same wave of x -axis ground movement and strain, the preliminary translation in x on the graphs may be ignored in any practical appraisal. Ahead of the tunnel face the ground around buried pipes and building foundations lying along the centre line is strained such that they experience their worst longitudinal (x -axis) tensions and superimposed bending tensions. In this area where the curve mismatches are usually not large, any structural analysis based on i_y and an x -coordinate cumulative probability curve is reasonable. Behind the face, where the mismatches are greater, the cumulative probability centre line curve based on i_y estimates early postshield settlements and rates of settlement that are greater than those measured. Accordingly, the estimated (and temporary for any given element of ground) radii of curvature parallel to the tunnel centre line are usually greater than those actually measured, and any structural damage assessment based on the equation (2.22) generating the settlement curve, or the curve itself, would tend to be conservative.

It is concluded that the adoption of parameter $i = i_y = i_x$ for the estimation of settlement and its derivatives parallel to a tunnel line is generally valid for most practical design problems.

2.8 Time-dependent settlement

Having estimated ground losses at the tunnel (sections 2.1 and 2.3.1), for clay soils perhaps on the basis of an overload factor (see equation (2.28) and Figure 2.11), and then having decided on the degree to which those losses are transferred to form a settlement volume, there is still a need to predict additional consolidation[†] effects. Although consolidation actually begins at the excavation stage and with settlement trough formation, it is its superpo-

[†]The term ‘consolidation’ relates strictly to clay soils. Any long-term settlement effects in granular soils should be referred to as ‘compression’.

sition on the shorter-term transverse settlement profile formed immediately after passage of the tunnel face that requires investigation. Deepening and (in many cases) widening of a ground-loss settlement trough can obviously change the response of a building or in-ground structure over the longer term of consolidation. It is emphasized that the effects of consolidation must be added to those of ground loss in order to predict any terminal settlement magnitude and distribution.

Two of the mechanisms promoting consolidation of the ground above a tunnel have been noted earlier. There is the phenomenon of direct gravitational drainage, under transient drawdown conditions, into the excavated void. Drainage may continue until the tunnel is sealed (lined, caulked and contact-grouted), although the sealing will rarely be absolute. Even very slight seepages can have a significant ground-volume reduction effect in view of the originally small volumes of porewater in clay soils. There is also the reduction of porewater-pressure effect in the soil around the tunnel. Soil dilates into the tunnel void until restrained by the lining and so encourages porewater migration towards the disturbed ground. In a similar manner stiff fissured clays may be locally sheared, weakened and diluted, any opening up of existing fractures creating a zone of higher permeability around the tunnel.

Autoritative guidance on this important subject is currently limited, since case history evidence is sparse. Some general comments may, however, be helpful for design purposes.

2.8.1 Total maximum settlement estimation from simple overload factor

Hurrell (1983, personal communication) has examined several case histories and, for cohesive soils below the water table, has tentatively suggested an empirical relation for the total (ground loss plus longer-term consolidation) maximum settlement $w_{\max t}$ (mm) above the tunnel centre line:

$$w_{\max t} = (2w_{\max})A \cdot \text{OFS} \quad (2.54)$$

where w_{\max} is the maximum ground loss settlement (mm), A is a consolidation settlement coefficient to be determined, and OFS is the simple overload factor

$$\frac{\sigma_{z_0}(+q) - \sigma_i}{c_u} = \frac{\gamma z_0 (+q) - \sigma_i}{c_u}$$

The coefficient A is evaluated in Table 2.5 for the cases shown in Figures 2.28–2.32.

Figure 2.33 suggests that the lower the ground-loss settlement (that is, the stiffer the ground), the higher, proportionately, is the consolidation settlement contribution to the total settlement. The form of the relation between A and w_{\max} can be used, albeit approximately, to predict the total maximum

Table 2.5 Some settlement case history data for the evaluation of the A coefficient.

Belfast (Glossop and Farmer, 1977)	Grimsby Array B1 (Glossop, 1980)	Grimsby Array C (Glossop, 1980)	Willington Quay (Attewell <i>et al.</i> , 1978)
$w_{\max} = 17 \text{ mm}$ OFS = 3.64 $w_{\max t} = 40 \text{ mm}$ From eqn (2.54) $A = 0.32$	$w_{\max} = 36 \text{ mm}$ OFS = 3.95 $w_{\max t} = 70 \text{ mm}$ From eqn (2.54) $A = 0.25$	$w_{\max} = 55 \text{ mm}$ OFS = 5.62 $w_{\max t} = 103 \text{ mm}$ From eqn (2.54) $A = 0.17$	$w_{\max} = 25 \text{ mm}$ OFS = 5.9 $w_{\max t} = 85 \text{ mm}$ From eqn (2.54) $A = 0.29$

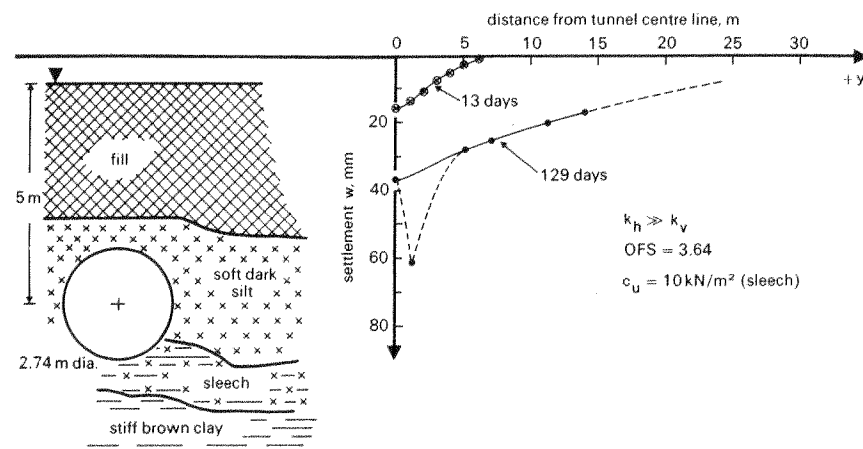


Figure 2.28 Transverse surface settlement distribution: Belfast, King George VI playing fields (after Glossop and Farmer, 1977, 1979).

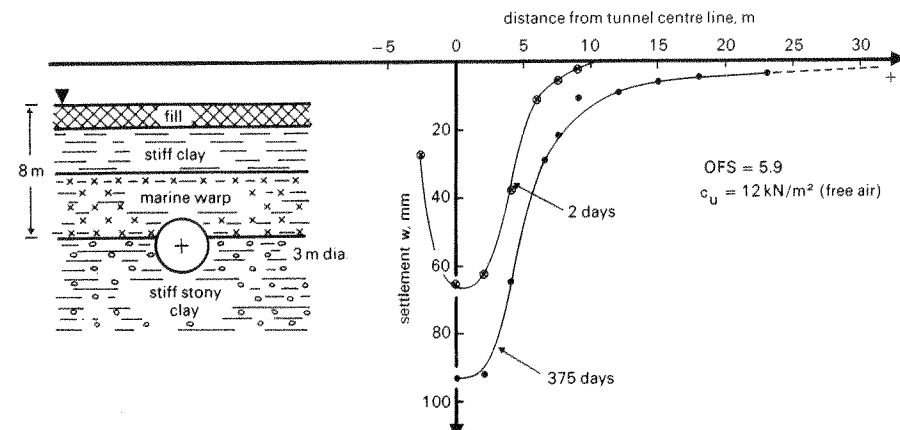


Figure 2.29 Transverse surface settlement distribution: Grimsby Array A (after Glossop, 1980; Glossop and O'Reilly, 1982).

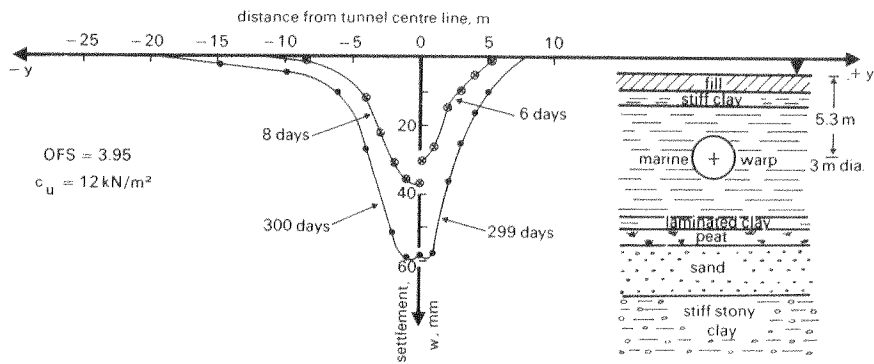


Figure 2.30 Transverse surface settlement distributions: Grimsby Array B1 (after Glossop, 1980; Glossop and O'Reilly, 1982).

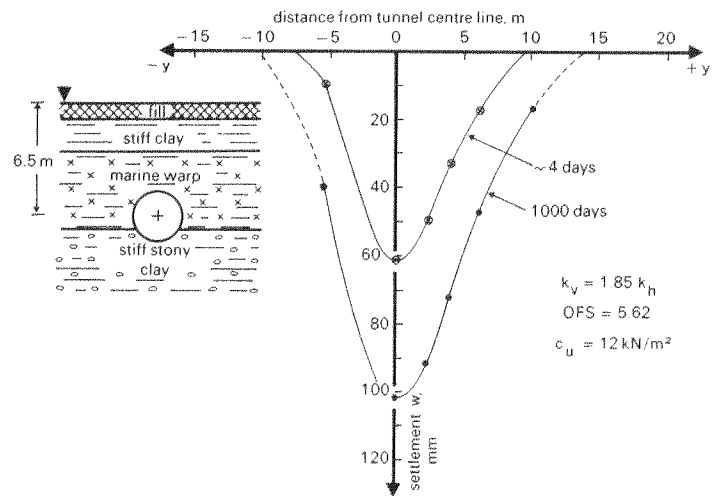


Figure 2.31 Transverse settlement distributions: Grimsby Array C (after Glossop, 1980; Glossop and O'Reilly, 1982).

settlement, w_{\max} , for other case histories. This can be done by reading off the A value appropriate to a measured ground-loss settlement and then inserting it in equation (2.54) or by incorporating the $A-w_{\max}$ relation directly into equation (2.55):

$$w_{\max} = 0.78 \text{ OFS } (w_{\max} - 0.01 w_{\max}^2) \quad \text{for } 6 \text{ mm} \leq w_{\max} \leq 63 \text{ mm.} \quad (2.55)$$

It is likely that this equation will be modified when more consolidation settlement data become available. Its application to some other case histories is shown in Table 2.6.

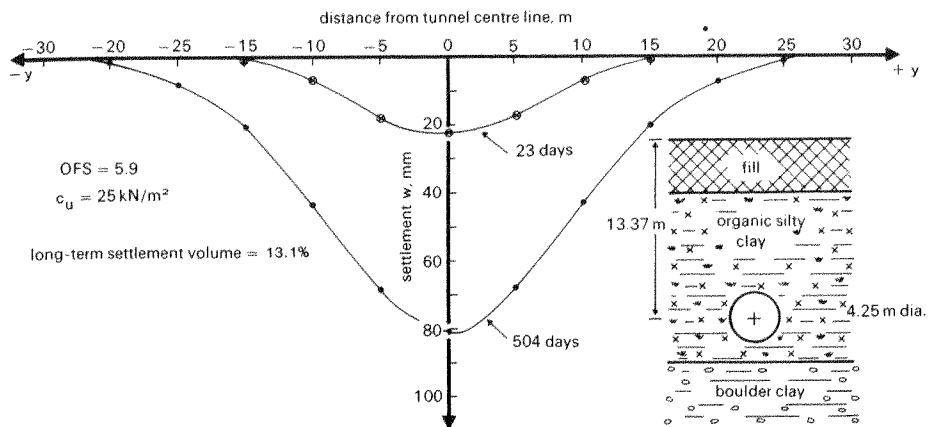


Figure 2.32 Transverse surface settlement distributions: Willington Quay (after Glossop, 1978).

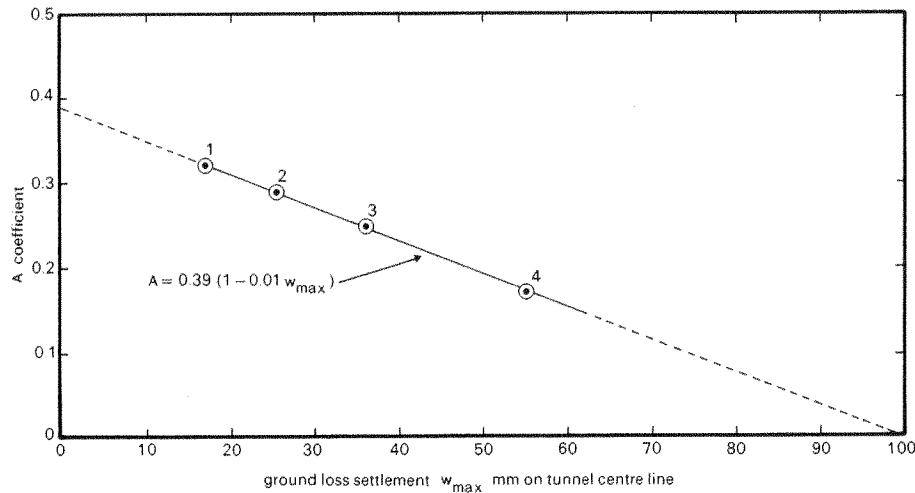


Figure 2.33 Variation of consolidation coefficient A with short-term ground loss settlement. For data points, see Figures 2.28–2.32 inclusive. 1, Belfast, OFS = 3.64; 2, Willington Quay, OFS = 5.9; 3, Grimsby B, OFS = 3.95; 4, Grimsby C, OFS = 5.62.

2.8.2 Total maximum settlement estimation using a compression index

This method, used by Attewell *et al.* (1978) for analysis on a Northumbrian Water Authority interceptor sewer at Willington Quay, northeast England (see Figure 2.32) requires measurement of the long-term porewater-pressure change by a piezometer installed above the tunnel crown. It takes no account of any possible consolidation below tunnel invert level. Maximum centre line consolidation settlement $w_{\max c}$ is related to piezometric pressure change Δp by

Table 2.6 Comparison of observed and estimated settlements (based on Hurrell, 1984b).

Project	Tunnel diameter (m)	Depth z_0 (m)	OFS	Observed w (m)	Observed w_{\max} (m)	Predicted w_{\max} (m)	w_{\max}^* (m)	Remarks
Willington Quay, Newcastle upon Tyne	4.25	13.375	5.9	25	85	75.4	85	Silty alluvial clay. Compressed air working. (Attewell <i>et al.</i> , 1978)
Grimsby Array B1	3.0	5.3	3.95	36	70	44.8	70	Inorganic high plasticity clay. Compressed air working. (Glossop, 1980)
Grimsby Array C	3.0	6.5	5.62	55	103	66.1	103	
Belfast	2.74	5.0	3.64	17	40	27.4	40	Soft estuarine plastic clay. (Glossop and Farmer, 1977)
Green Park, London	4.15	29.5	2.10	6.17	12	5.5	8.5	Stiff fissured overconsolidated clay. (Attewell and Farmer, 1974a)
Regent's Park, London	4.15	34.0	2.90	5.0	10	5.9	12.6	10.8 Stiff, fissured overconsolidated clay. (Barratt and Tyler, 1975)
Hebburn, Newcastle upon Tyne	2.08	7.5	2.02	7.86	13	6.1	9.0	
Howdon, Newcastle upon Tyne	3.68	14.18	1.50	8.90	11.2	5.4	6.0	9.5 Stony/laminated clay. (Attewell and Farmer, 1973)

*denotes that the prediction is based on short-term response.

the equation

$$\Delta V = \varepsilon_z = \frac{\Delta H}{H} = \frac{\Delta e}{1 + e_0} = \frac{C_c}{1 + e_0} \log\left(\frac{p_0 + \Delta p}{p_0}\right) \quad (2.56)$$

where ΔV is the volumetric strain, which is equal to the vertical strain ε_z for one-dimensional consolidation, ΔH is the change in thickness of soil element having initial total thickness H , Δe is the corresponding change in void ratio from an initial value of e_0 , p_0 is the initial vertical pressure at the tunnel crown before measurable soil consolidation occurs, Δp is the change in ground pressure above the tunnel crown as a result of drawdown and soil consolidation (equivalent to the increase in effective stress); Δp ultimately is equal to $\gamma_w \Delta H$, where γ_w is the unit weight of water; and C_c is the compression index.

Note that the thickness, H , of the consolidating layer must be estimated from settlement measurements in the ground. Effective stress normal to ground surface then increases as a result of drawdown, and ΔH is equivalent to consolidation settlement w_{\max} .

In the case history quoted by Attewell *et al.* (1978), values of 1, 0.3, and 4 m were assigned to e_0 , C_c and H , respectively, for the soft silty alluvial clay. A p_0 value of 205 kN/m² was calculated from the tunnel depth to crown and the soil bulk unit weight. A recorded reduction in piezometric pressure Δp of 22 kN/m² was accompanied by a measured settlement of 25 mm. The calculated settlement based on the above equation was 27 mm.

Estimation of consolidation settlement above future tunnels may be based on knowledge of p_0 from the soil properties measured during the ground investigation and calculation of Δp from possible or allowable seepage rates into and along the tunnel as indicated by measured or by inferred ground permeabilities.

The method presented by Mitchell (1983) assumes consolidation settlement to occur through an entire soil profile from ground surface down to an impermeable stratum below tunnel invert. Mitchell (1983) takes the case of a tunnel, excavated diameter d , positioned with its centre at a distance z_2 above a stiff base layer which serves as a reference horizon. The axis depth of the tunnel is equal to $z_1 + h$, where h is height of the original groundwater table above axis before tunnelling and z_1 is the soil cover above that groundwater table. If γ is the unit weight of the soil, γ' is the submerged unit weight ($= \gamma - \gamma_w$), and $z_3 = h + d + 0.5z_2$, then the maximum consolidation settlement for a normally consolidated soil can be expressed as

$$\Delta H = \frac{hC_c}{1 + e_0} \log\left(1 + \frac{\frac{1}{2}h\gamma_w}{z_1\gamma + \frac{1}{2}h\gamma'}\right) + \frac{z_2C_c}{1 + e_0} \log\left(1 + \frac{h\gamma_w}{z_1\gamma + z_3\gamma'}\right). \quad (2.57)$$

Application of this equation relies on the identification, at the ground investigation stage before tunnelling, of a horizon, below tunnel level, that could be deemed 'impermeable'.

Table 2.7 A guide to values of compression index C_e of saturated soils (Lee *et al.*, 1983, Table 5.1, p. 190)

Soil type	Index properties Liquid limit	Plasticity index	C_e	Source (see Lee <i>et al.</i> for full references)
Normally consolidated estuarine silty clay (undisturbed)	100 +	High	1 to 1.4	Lee <i>et al.</i> (1983)
Marine sediment, B.C., Canada	130	74	2.3	Finn <i>et al.</i> (1971)
Remoulded marine silty clay, Kyushu, Japan	70	43	1.1	Lee <i>et al.</i> (1983)
Deep-water brown marine clay	100 to 200	High	0.5 to 1	Noorany and Gizeski (1970)
Undisturbed organic silty clay, Delaware, USA	84	46	0.95	Schmidt and Gould (1968)
Undisturbed clay, New Orleans, USA	79	26	0.29	Lambe and Whitman (1969)
Stiff mottled clay	69	20	0.20	Lee <i>et al.</i> (1983)
Undisturbed Boston Blue clay	41	20	0.35	Lambe and Whitman (1969)

The Terzaghi and Peck (1967) equation

$$C_e \approx 0.009(L_w - 10\%) \quad (2.58)$$

where L_w is the liquid limit, could be used for a very approximate value of the compression index. Alternatively, Table 2.7 (after Lee *et al.*, 1983) could be used for guidance.

2.8.3 Form of the terminal (ground loss plus consolidation) transverse settlement profile

The complete long-term behaviour of superadjacent structures cannot be assessed without some knowledge of the form of the terminal settlement profile. Maximum settlement is only one element of ground movement composing this profile. Although there is a shortage of measurement evidence, some guidance can be given.

Since it is the soil drainage facility which controls its consolidation, the first approach considers the effect of permeability anisotropy. When the horizontal permeability k_h greatly exceeds the vertical permeability k_v the long-term settlement trough width would seem to increase substantially beyond the short-term ground-loss trough. As an approximation, the terminal transverse settlement curve may be constructed by dropping ordinates, equal in amplitude to the maximum consolidation settlement ($w_{max} - w_{max}$), from all

points on the ground-loss curve and extrapolating laterally beyond the span of the latter. Thus, the terminal trough has a wider span than the ground-loss trough but maintains the same curvatures. In those cases where the soil permeability is more isotropic, the width of the transverse settlement trough will still tend to increase in the longer term but to a much lesser extent because of the dominance of vertical drainage. Since the potential for structural damage is a function of differential settlement it is suggested that for structures or parts of structures within the span of the ground-loss trough, this trough should be considered to be deepened but not widened by consolidation settlement. Thus, in the earlier predictive equations ((2.22) to (2.27) inclusive) for ground-loss settlement (and derivatives) distribution, w_{maxt} would be used instead of w_{max} and i_t would be the same as i , so inevitably increasing the ground curvatures and leading to a likely upper-bound pessimistic assessment of possible damage for structures within the ground loss settlement trough. For structures or parts of structures outside the span of the ground-loss trough, any differential settlements could be treated as being negligibly small.

A second approach to the prediction of consolidation settlement distribution (Hurrell, 1984b) considers the longer-term surface settlements to result from consolidation volume loss in the zone of disturbed ground adjacent to the tunnel springings. These loss sources are located at tunnel axis level and at distances plus and minus one tunnel diameter d from the tunnel centre line. They propagate normal probability-form settlement waves to the surface in a manner similar to that which generated the ground-loss settlement profile. The terminal transverse settlement profile is then the resultant superimposition of the short-term ground-loss settlement profile and the two consolidation settlement profiles, the normal probability form of the latter being defined by the same inflection distance i -parameter determined empirically for the ground-loss profile. This condition is illustrated in Figure 2.34. Quantitatively, the component of maximum consolidation settlement w_{maxc} , at transverse distance $\pm d$, is

$$w_{maxc} = \frac{w_{max}(B - 1)}{2 \exp(-d^2/2i^2)} \quad (2.59)$$

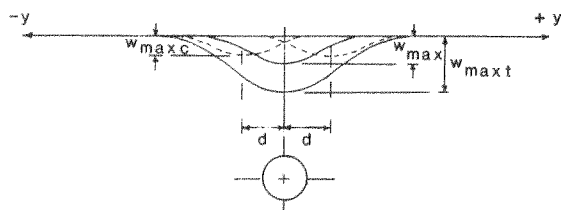


Figure 2.34 Development of long-term surface settlement.

where

$$B = 0.78 \left(1 - \frac{w_{\max}}{100} \right) \text{OFS for } 6 \text{ mm} \leq w_{\max} \leq 63 \text{ mm} \quad (2.60)$$

after equations (2.54) and (2.55).

The long-term surface settlement profile is then defined by

$$w_t = w_{\max} \exp(-y^2/2i^2) + w_{\max c} (\exp C_1 + \exp C_2) \quad (2.61)$$

where

$$C_1 = -(y + d)^2/2i^2 \quad (2.62)$$

and

$$C_2 = -(y - d)^2/2i^2. \quad (2.63)$$

Thus, by this second method, the procedure for terminal transverse settlement profile definition is as follows:

Evaluate the short-term ground-loss trough parameters w_{\max} , i , V_t . Parameter V_t is evaluated from equation (2.19) in section 2.1.3 and/or the information given in section 2.4.1. Parameter i may be evaluated from equations (2.31) or (2.32), or by reference to Norgrove *et al.* (1979) and Attewell and Woodman (1982). Parameter w_{\max} is then evaluated from equation (2.22) in section 2.4 for $y = 0$, $G(\bar{x} - \bar{x}_i/i) = 1$ and $G(\bar{x} - \bar{x}_f/i) = 0$.

Calculate the value of the ultimate centre line surface settlement $w_{\max t}$ from equation (2.55).

From equation (2.59), estimate the maximum component of consolidation settlement, $w_{\max c}$, at $\pm d$ from the tunnel centre line.

Use equation (2.61) above to define the complete long-term surface settlement w_t as a function of transverse distance $\pm y$ from the tunnel centre line.

2.9 Numerical methods

The finite-element method of analysis has direct application to the problem of tunnelling ground movements and the effect of those movements on structures. As shown in sections 2.5 and 2.6, any foundation or buried pipe within the zone of influence of the tunnel excavation will be subjected to a cycle of deformation. Accordingly, any finite-element modelling must take account of the three-dimensional character of the movements. It is not satisfactory to model two-dimensionally on a plane-strain basis solely for the permanent transverse deformation.

Finite-element modelling cannot be considered in any detail in this book. Three-dimensional finite-element programs are available commercially (e.g. PAFEC in the UK) and may purchased or rented by organizations such as

universities for use on suitably powerful mainframe computers. Civil engineering consultants often have their own in-house facility. There are varying degrees of refinement on offer—mesh generation, plasticity, viscoelasticity and so on. It will be realized, however, that these programs are non-specific, and further programming may be needed to apply them to a particular ground engineering problem. For this reason it is often desirable to develop a program for the special problem of tunnelling ground movements and ground-structure interaction. In outlining the application of such a program, some of the problems and some of the methods of avoiding them are mentioned.

The relative dimensions of the structures in the ground create difficulties. A typical tunnel may be 2.5 m excavated diameter at an axis depth of, say, 13.5 m. Pipes likely to be affected by ground movements could be 0.5 m diameter at a depth of 1.5 m, but with a wall thickness of only a few millimetres. In most cases it is impractical to mesh the pipe wall(s) in continuity with, and as part of, the general mesh which also incorporates the tunnel. The same restriction applies to column footings.

Two methods, each with their own particular disadvantages, have been used in an attempt to overcome these problems. First, and in the case of buried pipes, the finite-element mesh in the vicinity of a pipe has been constructed so that a suite of nodal points creates a definable boundary line around the pipe at a distance of between 2.5 and 3 pipe diameters from it. The pipe is then removed from the mesh, the zone vacated by the pipe and surrounding soil remeshed to a scale compatible with that for the rest of the ground, and the program run for the tunnel in a pipe-less (and foundation-less) ground. Note is made of the orthogonal displacements at the nodes forming the above boundary. The limited zone of ground around the pipe is then expanded to a scale suitable for meshing the ground and the thickness of the pipe wall cross-section. The boundary node displacements for this limited zone, as previously determined in the absence of the pipe, are then applied. Output data with respect to total strain is then retrievable for the pipe with respect to position in advance of, or behind, the tunnel face. By noting the relative amplitude of strain, at pipe soffit and pipe invert, along the pipe length, it is then possible to resolve the bending components and direct components of strain which compose the total pipe strain at the different positions along the pipe, although clearly it is the total applied strain that will form the basis of any criticality assessment.

The second method again involves isolating a volume or volumes of ground around a pipe, but this time defining the movements u, v, w at the selected boundary nodes of the finite element mesh by the use of equations (2.24), (2.23), (2.22) in section 2.4. The BASIC computer program for the generation of the design curves in section 2.5 has been used by the present authors for this purpose. These displacements are then entered, as above, into the three-dimensional finite-element program for solution of the pipe strains.

It follows that the two-stage finite-element approach, and/or the analytical-

numerical hybrid approach, can be adopted for the solution of isolated foundation strains.

Modelling the geotechnical properties of the soil in a realistic manner presents problems. Anisotropy can often be handled rather more easily than can inhomogeneity. For the overconsolidated soil that nowhere approximates to a collapse condition at the tunnel, the deformation behaviour may be assumed to be elastic. Estimates of settlement should be based on effective stress parameters E' and v' for drained states of deformation and on total stress parameters E_u and v_u for undrained deformation. Values of v_u just less than—not equal to—0.5 would be adopted. For such numerical analyses, depth-dependent values of E' , v' , E_u , v_u would be required from a rather lengthy and expensive laboratory test program. The resulting values would be likely to show considerable scatter anyway, and there would be some difficulty in selecting representative values for input to the program. If the soil is only very lightly overconsolidated, or if the unsupported portion of the tunnel is close to collapse, the ground will behave plastically. The finite-element program must be able to accommodate such non-linear properties. It will also be realized that whereas soil deformation conditions in the vicinity of the tunnel face approximate quite closely to a state of plane stress undrained, further back down the tunnel near the newly lined section they become more nearly plane-strain and drained. Even further back, where contact grout has fully set and the transverse surface settlement trough has stabilized, the conditions will be those of plane strain and (if the tunnel has been properly sealed) undrained.

2.10 Site investigation for tunnels in soil

The term 'site investigation' incorporates the early desk studies and site walk-over studies, as well as the actual ground investigation. Knowing where to acquire information on ground conditions (including the geology of the area, geomorphology, hydrology and topography), together with the results from earlier ground investigations, is important at the desk-study stage. Sufficient information from the site investigation is needed for the construction work to be designed for maximum efficiency and safety, to enable contractors to submit realistically 'keen' bids for the work, and to allow employers to make sensible estimates of their financial commitments.

A site investigation that is 'inadequate' with respect to the ground conditions that are actually revealed and which adversely affect the contractor's planned rate of progress will incur financial penalties for the project promoter in the UK via Clause 12(1) of the ICE Conditions of Contract (Institution of Civil Engineers 1973, revised January 1979), which relates to the contractor's encountering physical conditions or artificial obstructions that as an experienced contractor he could not reasonably have foreseen, and/or perhaps via Clauses 44 (extension of time for completion), 51 (ordered variations) and 56(1) (increase or decrease of rate).

The following notes should in no way be regarded as a complete guide to site investigation for tunnels in soil! It is assumed that an employer who identifies and seeks to overcome some of the potential problems discussed in this book will engage the services of an experienced geotechnical engineer. For information on the technicalities of site investigation generally, readers are urged to refer to Dumbleton and West (1976a), to the British Standard Code of practice for site investigations (British Standards Institution, 1981), to Weltman and Head (1983) and to Joyce (1982). Site investigation specific to tunnels is covered in Dumbleton and West (1976b) and West *et al.* (1981). Contractual conditions for ground investigation are formulated in the document issued by the Institution of Civil Engineers (1983) and analysed in Cottingham and Akenhead (1984). Contractual and cost benefit aspects of site investigation for tunnels are discussed in Attewell and Norgrove (1984, *a, b, c,*) and in Norgrove and Attewell (1984). Mathematical assessment of risk, decision-taking and decision reliability, often centred on Bayesian probability, have recently been discussed with respect to engineering geology and geotechnical engineering by Einstein and Baecher (1983) and by Whitman (1984), respectively.

Ground investigations are often phased so that, for example, later borehole locations, sampling and testing can be prescribed in the light of knowledge gleaned from earlier boreholes. This step-by-step approach is perhaps more easily implemented through a 'Schedule of Rates'-style term contract for the investigation. Retrieval of geological, geotechnical and groundwater information should continue during the construction phase. As a minimum requirement the exposed face should be mapped with respect to soil type each day, and the positions of any groundwater seepages noted on the sketch. This operation can be performed for smaller contracts by a competent clerk of works who has been instructed in the recognition of different soil types. If contractual claims based on unforeseen ground conditions are expected or have been submitted, it would then be sensible for the face to be mapped each shift and for the employer and contractor jointly to take soil samples. If there is any risk of inundation at the face the in-tunnel investigation would be extended to forward probing, with a cost penalty for production delays, but the need for any such probing should be anticipated when the Specification and Bill of Quantities are being written.

Although tunnelling is contractually and physiologically one of the most risky civil engineering construction operations with respect to ground conditions, special site investigation and test procedures are rarely adopted. Exploratory boreholes are normally put down at the centre of each access shaft location unless artesian pressures are anticipated, in which case the holes are offset from the shaft walls. Further exploratory boreholes are usually put down at 200 m or so intervals between shaft positions, these holes being offset about 1.5 tunnel diameters from the tunnel centre line. Care must be taken to record water strikes in each exploratory hole. The ground investigation

contract documents must provide for drilling to cease as soon as water is encountered in a hole, and for time-related incremental readings of water-level increases to be recorded until a maximum head is achieved. Water levels should also be recorded at the beginning and end of each shift. Normal practice is to install standpipe piezometers in the holes for post-investigation readings of groundwater levels, but it should be remembered that smearing of clay soils at the sides of a borehole can render piezometer readings inaccurate. Great care should therefore be taken in the interpretation of readings for soil permeability. Boreholes not receiving piezometers should be suitably backfilled with an impermeable material and capped with a concrete slab.

There is often an argument for putting down large-diameter man-entry boreholes so that the ground can actually be inspected *in situ* through slots in



Figure 2.35 Ground investigation in Newcastle upon Tyne.

the borehole casing. These holes are expensive, however, and may not be easy to justify. For many tunnelling schemes access shafts are sunk at the beginning of the contract, and this should be encouraged purely for site investigation and geotechnical reasons.

Special problems can arise through lack of space in urban areas. Traffic flows may be disrupted, and locations for boreholes may be severely limited. Figure 2.35 shows a soft-ground percussive rig being operated in one of the narrow main streets of Newcastle upon Tyne, but even then with the hole and its casing passing through a vault beneath the pedestrian pavement—see Figure 2.36. Reinstatement after drilling must pay particular attention to sealing against future water ingress into such basements.

Most common *in situ* tests are pumping-in/out (borehole packers) for soil

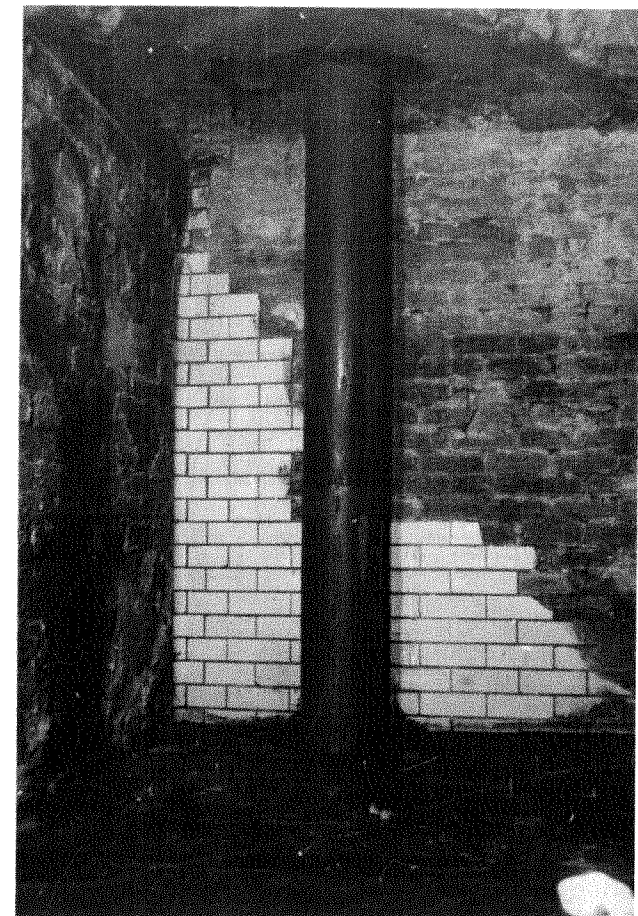


Figure 2.36 Cased hole from the rig shown in Figure 2.35.

permeability assessment, standard penetration (SPT) for granular soils, and perhaps vane tests for cohesive soils. Ground investigation contractors would advise as to whether less common investigations, such as borehole photography/CCTV and pressuremeter tests, are justified. Simple rising-head tests are to be preferred because of their self-cleansing character.

Although the quantity of ground information may be limited, its quality and style of presentation are of major importance in tunnelling. The bid baseline might be expected to rise with reduced information density, as might the likelihood of claims based on unforeseen physical conditions.

The contract documents will include a factual site investigation report and perhaps an engineering report which expands this report. The factual report will contain the borehole logs which identify the soil type pictorially and descriptively. The logs will also identify water strike and rest water levels, type of sample (disturbed or 'undisturbed') and sample depth, nature and depth of any *in situ* test (e.g. SPT, dynamic cone penetration, vane, permeability). Borehole surface levels must be accurately surveyed from benchmarks or temporary benchmarks, and each borehole must be unambiguously identified on the log. Dates and drilling rates must also be recorded on the log. Within the factual report will be a large-scale plan or plans of the tunnel route and adjacent area. A 1:500 scale is often appropriate for the plan. Beneath the plan, often at a 1:100 scale, will be pictorial representations of the borehole logs, mutually aligned with respect to ordnance datum and showing both ground surface and proposed tunnel boundaries. Soil types and any rock head will be marked, as will water strikes and rest water levels. Such information, properly and unambiguously presented, is essential if a contractor is to price the job to the limit of his experience and if the employer is not to incur unnecessary expense in the form of contractual claims for unforeseen ground conditions that had, in fact, been foreseen.

For technically and geologically difficult work in an urban area where buried pipelines and high-value buildings may be at risk, and where some form of ground-improvement measure (perhaps compressed air) will almost certainly be needed, a more visual representation of the character of the ground can be beneficial. One such problem area is described in Norgrove *et al.* (1979). A simple three-dimensional representation of the ground is shown in Figure 2.37. It comprises a 1:500 area plan pasted to a baseboard, the board representing a certain level above ordnance datum. Quadrant dowelling is used to depict the tunnel ground investigation boreholes and also boreholes put down earlier by other clients for other developments. Rod lengths are scaled to the depths of the individual boreholes. The curved surfaces of the rods are coloured according to the different soil descriptions, and the flat surfaces of the rods are used for marking water strikes and rest water levels. Coloured cotton threads can be used to link stratifications between boreholes and so render interpretation a little easier.

The range of possible laboratory tests (grading, index properties, natural

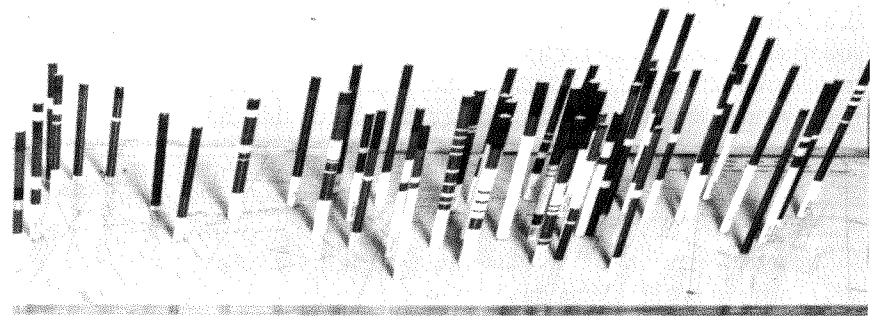


Figure 2.37 Ground investigation borehole model.

moisture content, bulk density, strength, deformation modulus and chemical) on disturbed and 'undisturbed' samples is large, but those most generally used and useful for tunnel design are noted below. Ground investigation samples should be taken at tunnel face level, and between one tunnel diameter above soffit and one tunnel diameter below invert unless comprehensive finite-element analyses are to be performed, in which case the full depth profile to tunnel horizon should be sampled for testing (see section 2.9). Borehole log definition of the character of the soil at and just above face level is clearly important for estimating ground losses, as discussed in sections 2.1, 2.2, 2.3, 2.4.1, 2.4.2 and 2.8. Special attention must be directed to laminated clays in which silt intercalations containing water at sub-artesian or even artesian pressure have been known to create unexpected problems at the tunnel face. Water-bearing lenses in tills can create similar problems, and so the site investigation must aim, for example, to define any compressed-air or other ground-improvement requirements. It is obviously much less easy from borehole investigations to assess the presence of boulders—their spatial density and their possible size—but such information can be quite crucial in the case, for example, of slurry-shield tunnelling. If their presence is not revealed by the ground investigation (or if the contractor is not expressly cautioned about it in the contract documents), this could lead to substantial claims for extra payment. Borehole cores must be properly handled, labelled, logged, and then stored in an accessible place for inspection by the contractors bidding for the tunnelling work.

Granular soils

Grading curves. Careful note should be taken of the form of the particle-size distribution and the percentage of silt-size material. The amount of silt in the soil when assessed in the context of piezometric information from the borehole is an essential indicator of tunnel face stability and the choice of ground improvement measure(s). It should be remembered that there can be a loss of fines during the drilling process, leading sometimes to an underestimate of the silt contents of disturbed samples.

Cohesive soils

Index tests (liquid and plastic limits). From these values the soil should be defined according to the Unified Soil Classification System (see Casagrande, 1948; Terzaghi and Peck, 1967, pp. 39–42; Attewell and Farmer, 1976, pp. 36–42) and its location with respect to the A-line on the plasticity index–liquid limit modified plasticity chart (Terzaghi and Peck, 1967, p. 41) noted.

Natural moisture content. Great care must be taken throughout the sampling and testing procedures to preserve the true moisture content of the soil. When soil is percussively drilled and sampled above the groundwater table addition of water to the hole to assist penetration should not be allowed. Special note should be taken of how closely the natural moisture content approaches the liquid limit. Particularly with respect to tunnelling, it is useful to calculate the liquidity index from the natural moisture content and the Atterberg limits.

Bulk density. This soil property is invariably measured as part of a laboratory testing package, but in practice when used in calculations it is not normally a sensitive parameter. Soil unit weight is required for stability ratio estimation (see section 2.4.1).

Quick (UU) triaxial tests. There may sometimes be a shortage of material for testing of three or four specimens at different cell pressures. Multistage undrained triaxial tests on a single sample can then be used. The results, plotted as a Mohr diagram, give an approximate idea of soil shear strength, but it is not always easy to assess the strength contribution of any friction component. Undrained shear strength compared with the product (multiple) of tunnel depth and soil unit weight (and taking account of any air pressure temporary support at the face) produces a stability ratio from which the magnitudes of ground losses can be estimated (see section 2.4.1 and Figure 2.11). For overconsolidated soils and for those tunnelling conditions where the factor of safety against collapse is quite clearly high, the mechanical state of the soil will remain within the critical state boundary surface, its behaviour will be elastic and path-independent, and the ground movements will depend only on the

initial and final states of the deformed soil. Simple triaxial testing may then be specified. If the soil is only lightly overconsolidated or mechanically could be close to collapse in an excavated, unsupported tunnel, then a high standard of sample acquisition must be specified and consideration given to implementing stress path testing.

All soils

Chemical analyses. Tests of pH, sulphates (Building Research Establishment, 1981a), and occasionally chlorides, in soil and water samples should be made. These tests are necessary for primary lining-concrete specification and perhaps extrados protection in chemical environments that are particularly aggressive. They are also needed for specifying worker protection in the tunnel.

Deformation modulus. The analysis of both pipeline deformation (Chapter 3) and structural foundation deformation (Chapter 4) requires data on foundation stiffness. Therefore, for these particular purposes, but not as a general ground investigation test procedure, laboratory stress-strain curves should be derived from specimens confined at pressures equivalent to overburden pressure at pipeline or foundation depth. It may difficult to select an appropriate modulus from a non-linear curve, and it must also be recognized that a laboratory sample can rarely be ‘representative’ of ground conditions generally. Furthermore, it is likely that a laboratory-derived modulus value will exceed an *in situ* modulus value and, if used in the design calculations could lead to underestimations in the pipeline or foundation deformation calculations.

It is important to note that the desk-study and walk-over phases of the investigation should give attention to the buildings and buried pipelines likely to be affected by ground movements. Operation in the UK of the Public Utilities Street Works Act 1950 (PUSWA) is noted with respect to buried pipelines in section 3.5.1, and the preparation by building surveyors of pretunnelling property schedules is discussed in section 4.14.

2.11 Measurement of ground movements

Measurement programmes serve three primary objectives: (1) to acquire settlement data in anticipation of claims for damage; (2) with some feedback to the resident engineer, and subject to contractual constraints, to suggest changes in construction method and perhaps progress of the works, leading to a reduction in contract costs and compensation claims; and (3) to conduct research into the fundamental causes of, and controls on, deformation and to increase the store of information for improving the quality of future ground-movement estimates.

Some degree of ground movement must be regarded as the unavoidable result of the construction operation in accordance with contract and in the sense of Clause 22(1) (b) (iv) of the ICE Conditions of Contract (Institution of Civil Engineers 1973, revised January 1979). It is tempting to infer that movements, and especially settlements, estimated empirically for the purposes of current project design from earlier case history measurement data, could form the bases from which an 'unavoidable' element could be specified. By implication, movements above those estimated for the particular geological, hydrological and geotechnical conditions pertaining on the current contract would be 'avoidable', and hence the contractor's responsibility on a contractor-client risk-sharing basis. However, problems would ensue from attempting to implement such an approach. It is preferable to use case history experience as a target for restricting ground-loss settlements and consolidation settlements by the adoption of the best possible workmanship in the tunnel, encouraged by a tight specification for the works and keenly overseen by the resident engineer and his staff.

Programme 1 involves precise levelling, by standard surveying methods, of stations secured to the ground surface within the expected zone of influence of the tunnel. For tunnels in urban areas it is not satisfactory simply to hammer studs into a tarmacadam surface and level to the studs. The stiffer membrane represented by a road or pavement construction resists settlement and will not therefore reflect the true soil settlement.

A typical measurement station, cut into a road surface, is shown in Figure 2.38. The 12.7 mm diameter stainless steel rod, cut to half-metre length, domed at the top and machined to a point at the bottom, is driven into the soil after breaking out the road surface. The soil is then excavated carefully by hand before concrete placement around it. The rod clears the top of the concrete by 25 mm and is then concealed by a manhole cover.

Subject to the constraints of space and the presence of adjacent buildings, several stations would normally constitute a transverse array, the likely span of the transverse settlement trough having been calculated previously. A

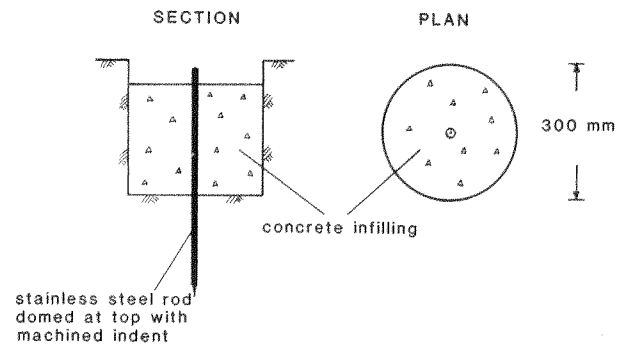


Figure 2.38 A typical surface levelling and banding station.

minimum of five stations, including a centre line station, is required for defining the form of half the settlement trough. There should be further measurement stations on the other side of the tunnel centre line, otherwise symmetrical movement about the centre line will have to be assumed.

Using repeated measurements as a tunnel passes beneath it, a single station on the tunnel centre line will define a settlement development profile. If possible, however, additional centre line stations should be prescribed in order

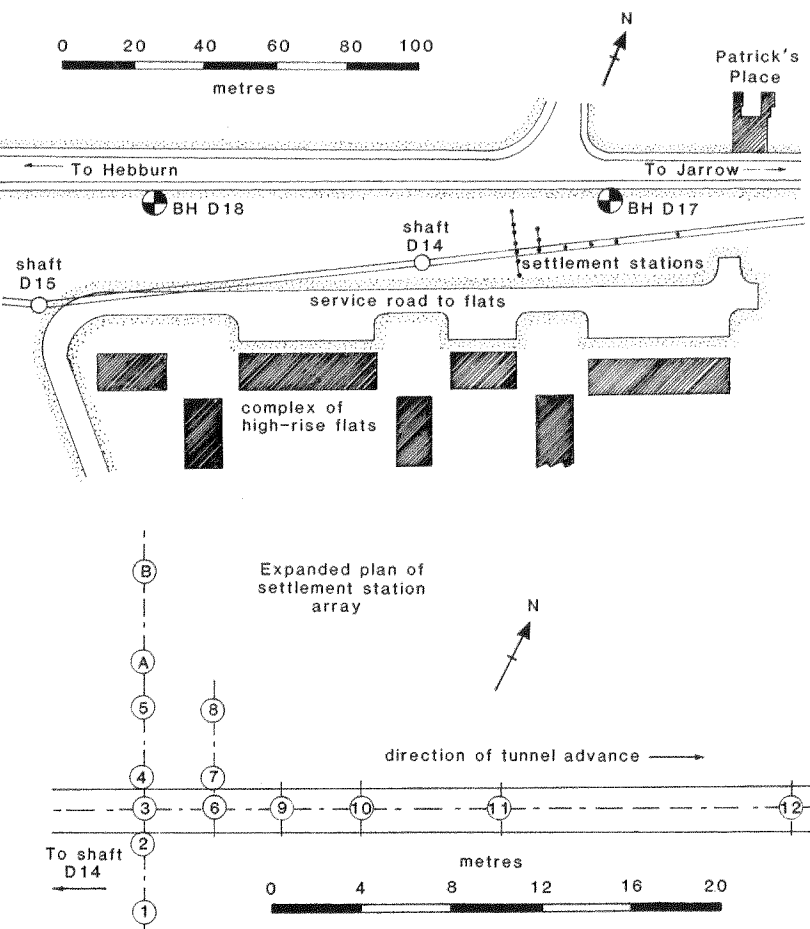


Figure 2.39 Instrumentation array for ground movement monitoring at Hebburn, north-east England. The tunnel forms part of the Northumbrian Water Authority's River Tyne South Bank Interceptor Sewer. Tunnel diameter and depth are 2.024 m (external) and 7.5 m (to axis), respectively, and the tunnel face was in stony/laminated clay. The tunnel, shield-driven in free air, runs approximately parallel to the river, and ground surface at the measurement array slopes at only about 2° northwards. Locations 1 to 12 inclusive represent boreholes containing inclinometer access tubes and magnetic monitors for in-ground settlement. Locations A and B are for surface settlement measurement only.

to extend the information density over a greater zone of tunnelling influence. A settlement station array used by Attewell and Farmer (1973) is shown in Figure 2.39.

Operationally, the base of the levelling staff rests on the domed head of the stainless steel rod. A temporary bench mark can be established from a permanent Ordnance Survey benchmark in close proximity to the settlement point array but outside the influence of any settlement trough. Because the changes in level above and to the sides of the tunnel centre line will often be very small, the demands for careful and precise measurement must be accompanied by equally careful choice of temporary bench mark location on an established rigid structure, minimally affected by environmental changes. A measurement accuracy of ± 0.2 mm must be aimed at.

As emphasized earlier, by the ground-loss equations in section 2.4 for example, there are horizontal movements and strains at ground surface. Such movements, integrated over the distances between levelling stations, have been measured as part of Programme 2 research by University of Durham research teams operating mainly on Northumbrian Water Authority tunnelling contracts in north-east England. Measurements have been taken by steel bands, tensioned (10 kg) by using a spring balance, between indents machined into the centres of the domed heads on the station rods. However, because there are inevitably few measurement stations and because the horizontal movements are much smaller than the vertical movements, the errors are higher than those related to surface levelling. The data are also insufficient to define horizontal movement and strain profiles, particularly in those places either side of the tunnel where the transverse strain changes from compression to tension. Corrections must be made for air temperature, and there may be slight banding errors caused by undulations on the ground surface. Under ideal conditions the limit of accuracy of such a measuring system is the sum of the observational errors, approximately ± 0.6 mm, but since in most cases the operational conditions are far from perfect the total error may be of the order of ± 1 mm.

Measurement of in-ground movement is accomplished first by sinking cased vertical boreholes 150 mm or 200 mm in diameter at specified measuring locations (see, for example, Figure 2.39). The base of each borehole is sunk to such a depth that it experiences no movement from the tunnel excavation (but movement due to any groundwater lowering cannot, unfortunately, be precluded). To extruded aluminium (or sometimes plastic) inclinometer access tubes, having flexibility normal to their long axes and each of assembled length equal to the depth of its particular hole, are attached magnetic settlement rings with spring 'spiders', each ring being located at a predetermined hole depth. The intention is for one of these magnetic ring monitors always to be positioned just above the tunnel crown so that it escapes excavation and continues to monitor the settlement there for comparison with the centre line settlement at ground surface (see section 2.3). It is wise to terminate this

particular access tube just above the tunnel crown, for if the tube passes into the tunnel face section any vibration that occurs when the tube is sawn off in the tunnel might affect the accuracy of the crown settlement readings. After lowering each tube with its magnetic rings into its hole, the annulus between tube and casing is then filled with cement–bentonite grout designed to have a 28-day set strength equal to that of the surrounding undisturbed soil. Following grout pouring, the casing is then drawn and the grout topped up. One of the settlement rings is set to the bottom of each access tube line in order to act as a stable reference datum (see qualifying comment above). The authors have used a special removable 'dolly' insert to the inclinometer tubes for acting as the reference head upon which the staff for precise levelling can rest. A temporary bench mark and the deep settlement ring thus act as stable independent references for surface and in-ground settlement measurements.

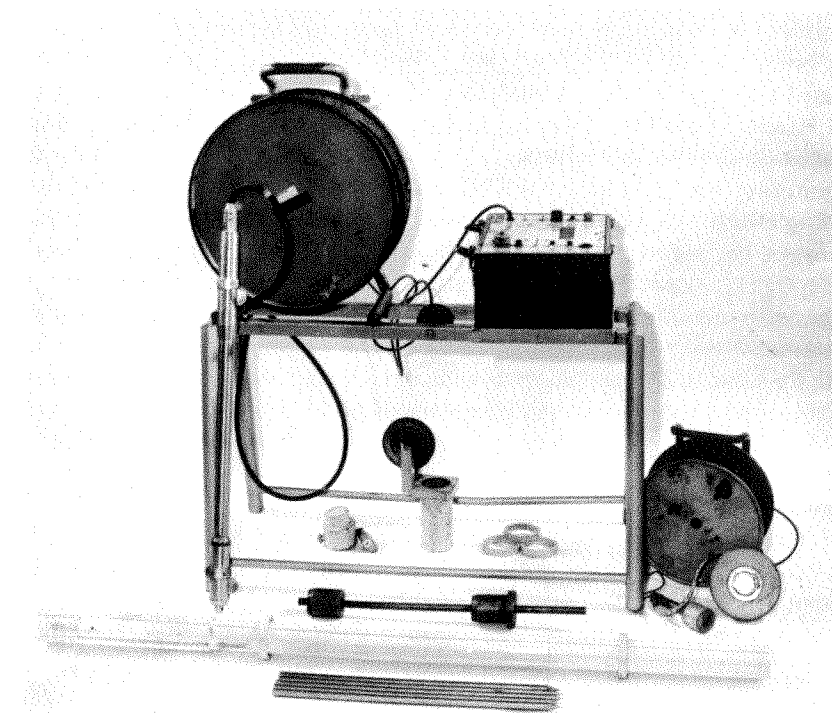


Figure 2.40 Some equipment used for measuring ground movements. Foreground: steel pins for ground surface movement (see Figure 2.38), inclinometer access tubing with two (unattached) magnetic settlement rings, 'dolly' for insertion into top of inclinometer tube and upon which the levelling staff is laid. Resting against the inclinometer support frame is an inclinometer torpedo which is lowered down the access tubing to measure horizontal ground movements. On top of the frame is the inclinometer cable drum and read-out system. Beneath the frame is a lockable top cap for access tubing and more magnetic settlement rings. To the right of the frame is the settlement ring monitor system.

Typical equipment used for measuring ground movements is shown in Figure 2.40. The principle of operation is that the magnetic settlement rings and the inclinometer access tube move according to the movements of the ground into which they are bedded. In spite of the lateral translations of the tubes to which they are attached, the magnetic rings are assumed always to measure vertical movement. Change of ring position is recorded by lowering a probe down the tube and noting the precise depths from the top of the tube at which the probe enters and leaves the ring's magnetic field, as indicated by an audible signal. Such probings require great care in order to achieve sufficient accuracy. The same person should always be designated to take the readings, and for each ring the magnetic field should be entered and exited on both an upward and downward transit. Access tubes contain orthogonal keyways along which a torpedo transducer is lowered for measuring horizontal movement. The torpedo produces an electrical signal, the strength of which is related to the inclination of the torpedo from the vertical. This signal is readily expressed as a horizontal displacement in a known direction, as determined by the orientation of the access tube keyways, and as an absolute magnitude related first to the stable base of the tube and secondly to some fixed surface datum via the top of the tube. Figure 2.4b shows an example of the deflections as measured by an inclinometer system. There is a steel measuring tape for monitoring torpedo depth, and in operation the torpedo is lowered and raised through the full depth of the access tube four times—once for each of the four keyways. Using a torpedo 1 m long, readings are taken at every 1 m increment of depth. Data from each incremental depth and for all four keyways are then reduced by computer to provide a suite of depth-dependent ground-movement vectors in a horizontal plane. These movements are then merged with the settlement ring data to provide three-dimensional ground-movement vectors at the locations of the access tubes.

Modern biaxial sensors record inclination simultaneously in the planes of the two orthogonal keyways, and so separate readings using both sets of keyways are not usually needed. Incremental data are displayed digitally and also recorded on cassette. A microcomputer/floppy disk/line printer system can then be used on-site to process the data and produce graphs of the form shown in Figure 2.4b.

In deep holes, summated twist over numerous sections of jointed inclinometer tube can lead to serious errors. Even with a manufacturer's tolerance on keyway straightness of within 1° per 3 m segment length, a 40 m deep hole could incur an integrated twist error of 13°. Inclinometer holes have been taken to four times this depth, and so it is sensible to incorporate a twist-correction procedure in the processing program. Such correction requires detailed measurement of changes of magnetic bearing with depth across two of the inclinometer tube keyways.

Clearly this type of measurement programme is lengthy, and very much of a research nature, aimed at establishing criteria upon which future predictions

of ground movements can be based. The number of instrumented holes will never be deemed sufficient to present an acceptable three-dimensional picture of the movements. On the other hand, with a very large number of access tubes and settlement rings to probe very carefully as a tunnel face passes, it might prove difficult to accomplish a full data-gathering exercise in the available time. For such work it is sensible to have three inclinometer torpedo systems on site, each precalibrated in the holes before any tunnelling-induced ground movement occurs. One torpedo system can be used for measurement, and it should be presumed that one system could be off-site, perhaps at the manufacturer's works undergoing repair. The third system would then be on standby. Similarly, three magnetic ring probe systems should be assigned to each measurement job.

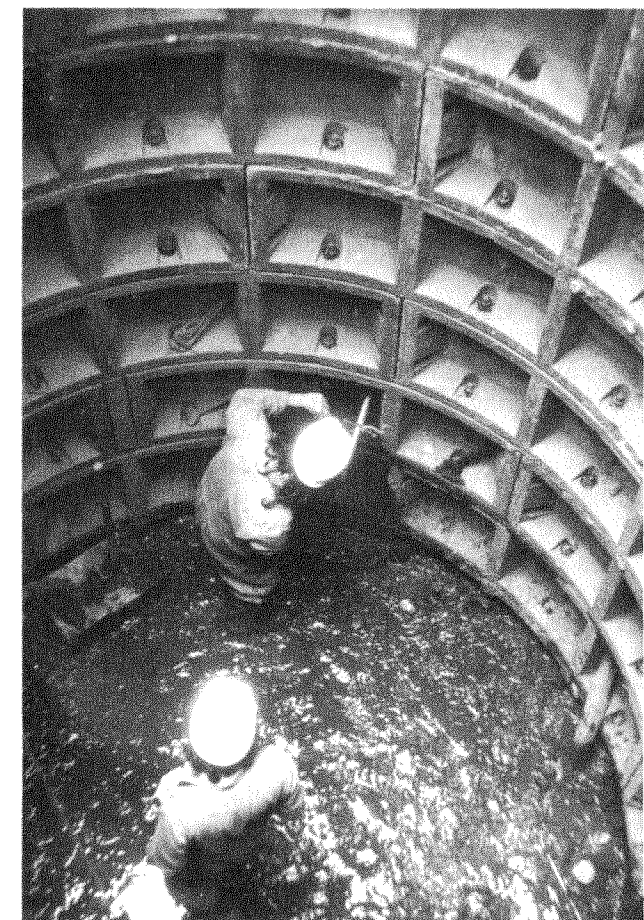


Figure 2.41 (a) Installing a horizontal ground anchor and magnetic ring system at the bottom of a shaft.

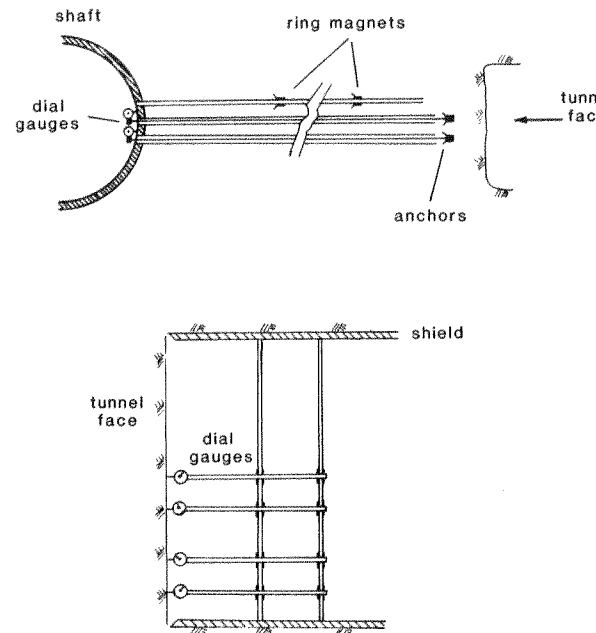


Figure 2.41 (b) Plan views of face movement measurements.

The importance of soil relaxation rate has been stressed in section 2.1.1. Laboratory measurements of deformation rate have been shown to accord with measurements taken in the ground. Deformation rates in London Clay have been measured using a ring magnet installed just above a tunnel crown. An alternative system of monitoring rates of inward face movement, which has been used by the authors, is shown photographically and diagrammatically in Figures 2.41a and b. If a shaft has been sunk in advance of an approaching tunnel face then the results from this system of monitoring may be directly compared with those from the model extrusion test. The system also has the advantage that the inward deformation profile over the tunnel face section may be described.

Adapting this method, three 50 mm diameter auger holes were drilled from the bottom of access shaft D 14 (see Figure 2.39) along the line of the approaching tunnel. Two of these holes were lined with metal tube for a distance of about 6 m. A steel rod having a ground anchor at the far end ran through two of these tubes. The ground anchors were so constructed that, on emerging from the end of the lining, three spring-loaded wings projected from the collar of the anchor. Although the anchor could be pushed into the clay soil, when slight tension was applied to the rods the wings were forced outwards and keyed the anchor into the ground. Where the rods projected into the access shaft they were equipped with dial gauges bearing on to a stainless steel plate which was rigidly fixed to the concrete lining of the shaft. The rods were supported in their tubes

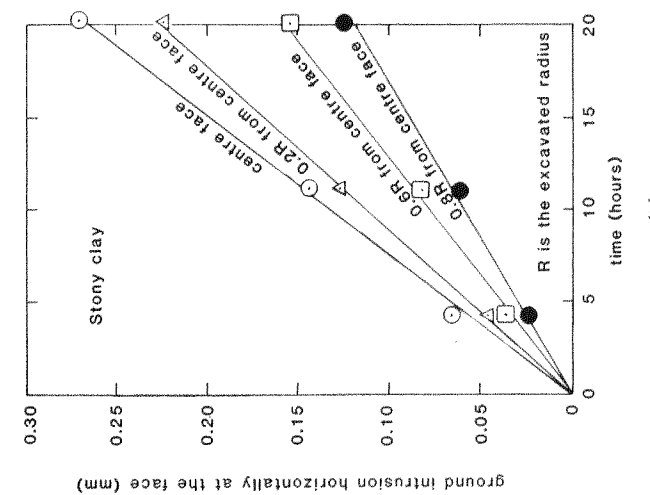
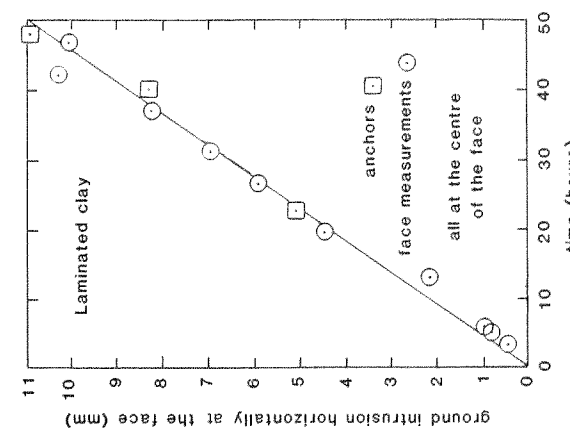


Figure 2.42 Rate of ground intrusion at the tunnel face.



(a)

by nylon bearings and the two ground anchors were installed at distances of 6.274 m and 6.223 m from the actual shaft wall. Time-dependent movement of the anchors into the tunnel face as it approached was directly monitored by the dial gauges in the shaft. The third hole contained a small-bore plastic tube with magnetic rings around its circumference at distances of 2 m and 5 m from the shaft wall. An audible reed switch of the type used for monitoring the same form of settlement ring installed on vertical access tubing for an inclinometer was for this work mounted on a stainless steel rod.

Measurements of clay soil intrusion of the face have also been made using dial gauges mounted on extension rods within the shield itself (Figure 2.41b). The extension rods were clamped to bars passing across the mouth of the shield and the gauges bore on to aluminium plates wedged into the tunnel face immediately following the end of excavation for the week.

Figure 2.42a is an example plot of the magnitude of soil inward movement against time from two ground-anchor experiments and two direct-face experiments performed in a tunnel in laminated clay. The points relate to the centre of the face where the intrusion rate is highest; they produce a good straight-line fit having a gradient (intrusion rate) of 0.221 mm/h. This figure agrees closely with the extrusion rate value of 0.218 mm/h derived from laboratory extrusion tests made on undisturbed samples of this same clay from the same location at the same overburden pressure.

Figure 2.42b is a plot of soil intrusion against time related to four points on a tunnel face in stony clay. In this case, data were obtained from four dial gauges located across the horizontal radius of the face (Figure 2.41b). Although the data are limited, the increase in intrusion rate towards the centre of the face is clear, indicating that the clay soil has tended to develop a dome-like form at the face of the shield rather than shearing around the cutting edge and intruding as a plane-ended cylinder. This feature is quite consistent with observations made on laboratory extrusion tests (Figures 2.3a, b) where the face 'domes' until failure, at which point the clay begins to extrude as a cylindrical plug by shearing around the circumference of the aperture. There was no evidence of direct shear at the tunnel face proper. The intrusive doming effect may be accommodated in any ground-loss analysis by the application of equation (2.1) in section 2.1. It is noted that the dial gauge at the centre of the face in stony clay indicated a maximum soil intrusion rate of 0.0134 mm/h, which was much lower than the intrusion rate for laminated clay.

2.12 Measurements on structures

Pipelines. Movements in the surrounding ground will be transferred in part to the pipe bedding material and thence to the pipe itself. Pipe strains may be resolved into direct (axial) compressive or tensile strain, to longitudinal bending strains having components in the vertical and horizontal planes, and to ring bending. Vibrating-wire strain gauges seem to be the most suitable for

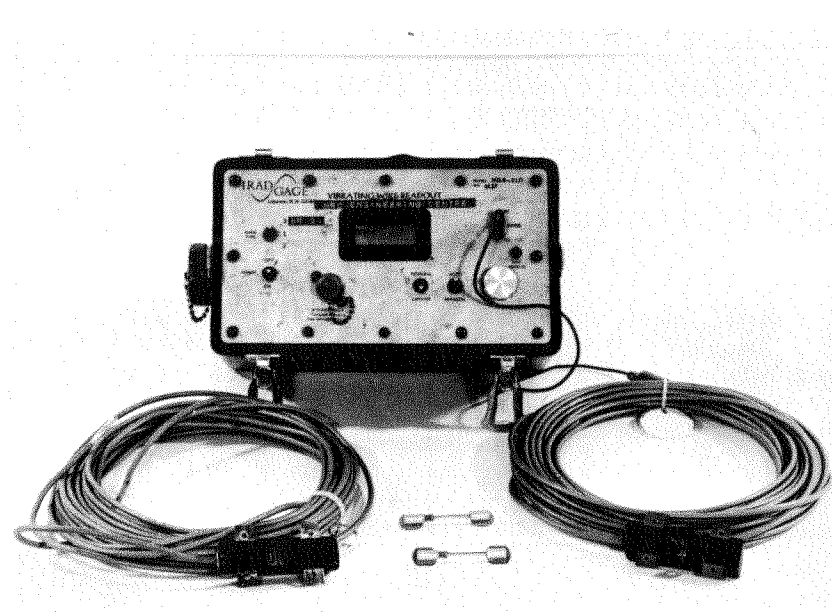


Figure 2.43 Vibrating wire strain gauges for resolving induced strain distribution in buried pipelines.

measuring pipe strains, having long-term stability and inherent robustness. IRAD and Gage Technique vibrating wire acoustic gauges have been used for this purpose (see Figure 2.43).

Before the approach of the tunnel face, the ground at the chosen location is excavated down to the crown of the pipe and just down to the pipe axis on one side. The minimum of ground is disturbed to allow man-entry for fixing the gauges. It may be necessary to cut away corrosion protection applied to the extrados of the pipe in order to attach the gauges. A firm screwed attachment of gauge to pipe is ideal, but in many cases a statutory undertaker will not permit this, and a strong epoxy-type adhesive must be used. In order to resolve an imposed state of strain a minimum requirement is for two gauges mutually at right angles in both the crown and axis locations. One gauge of each pair is aligned axially along the pipe and the other is aligned circumferentially. After mounting and attaching lead-out wires for the conditioning unit, any exposed pipe must be reprotected, as must be the complete gauge assembly. The access trench is then carefully backfilled and recompacted.

Buildings. Two systems of measurement have been used by the authors. First, tiltmeters have been installed in basements of buildings likely to experience some rotation as a result of nearby tunnelling. Two meters are most

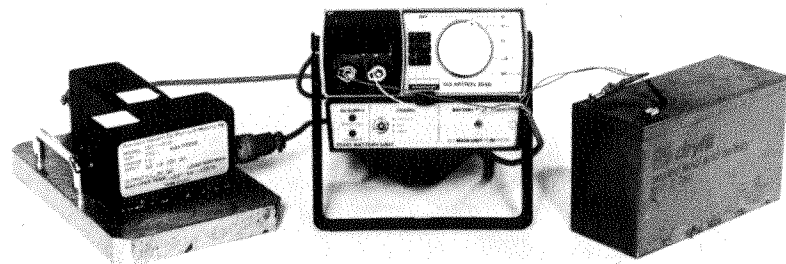


Figure 2.44 Two tiltmeters, set at right angles, for recording rotational movements in buildings.

conveniently arranged at right angles to one another (Figure 2.44) so that the magnitude and direction of changes in slope can be resolved in relation to the tunnel face position. These meters are powered by a stable DC voltage and the output, precalibrated in terms of angular rotation (tilt), may be read on a millivoltmeter or recorded either on a chart recorder or on magnetic tape.

The second system involves the fixing of Demec points, usually on the inside or outside walls of buildings likely to be affected by tunnelling and on both sides of pre-existing cracks. Demec points are small stainless steel discs, 6.6 mm in diameter and 1.64 mm thick, containing a drilled-out centre hole into which the locating pins both of the standard setting gauge and of the measuring gauge fit accurately (Figure 2.45). The setting gauge is used to locate pairs of pins an exact predetermined distance apart, the pins being fixed to the wall by means of epoxy resin. Any change in distance between a pair of points preset to standard is then indicated on the dial of the measuring gauge and quantified as a strain via a manufacturer's (W. H. Mayes and Son (Windsor) Ltd) calibration factor. Readings down to 20 microstrains are theoretically possible, but it is perhaps inadvisable to quote to an accuracy of more than 100 microstrains. In some instances, information on relative *displacement* between points can be rather more valuable, in which case the resolved strain should simply be multiplied by the standard gauge length. It is advisable to correct readings for any temperature variations that may occur on the wall at the different times and dates of reading.

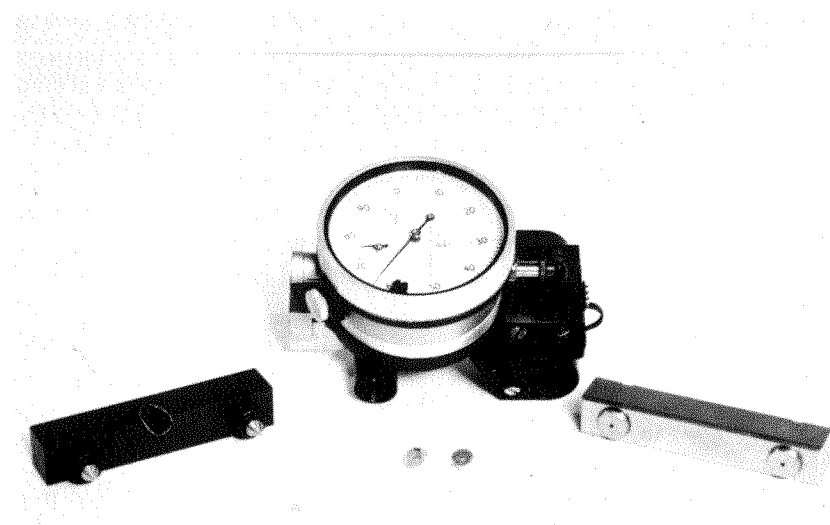


Figure 2.45 Demec gauge and points.

It is likely that future developments in laser technology will allow remote monitoring of structural deformation (Wilson, 1984). It is less likely that strain gauges of the wire or foil resistance type, in say a 45° rosette configuration, will be used for deformation measurements on buildings, but there may be occasions when strain-gauge-based load cells can be inserted between structural members in order to measure changes in tunnelling-induced loads.

2.13 Shafts

Although this book is concerned with ground movements and tunnelling, the fact that shaft construction for access to tunnels, for manholes and for ventilation purposes is an essential part of the overall tunnelling operation suggests the inclusion of some brief notes on the most usual shaft-construction methods.

Underpinning. Bolted segments are sequentially hung from an initially erected ring of segments which are secured against sinking by grouting or by use of a suitable collar at ground surface. During excavation at the base of the shaft only sufficient ground is taken out for the assembly of a complete ring of segments before lifting and bolting to the ring above. This method is attractive for construction in poor ground since the unsupported excavation area can be restricted to that sufficient to erect and bolt one segment to the ring above.

Excavation continues in this manner, ring by ring, until formation level is reached. It is important for the rings to be grouted frequently, otherwise downdrag forces on the outside of the segments can cause high tensile forces to develop around the rings, leading to cracking of the segments and fracturing of the bolts. This is a quick, traditional method of construction suitable in cohesive soils and dry granular soils.

Permeable strata and/or lenses of water-bearing granular soil may be encountered during sinking. Groundwater must be removed, most conveniently by pumping from a sump dug in the base of the excavation, so that construction can proceed in sensibly dry conditions. If this proves to be inadequate, then vacuum ejectors may have to be installed around and outside the perimeter of the deepening shaft.

The shaft base must be sufficiently thick so that, together with the weight of the lining rings (adjusted for wall friction), the total weight exceeds the maximum likely hydrostatic uplift forces on the base. If a base thinner than that calculated must be used, bleed wells are normally incorporated into the construction to allow the hydrostatic pressures to be continuously dissipated.

Caisson method. Precast concrete rings are sunk under their own weight or by the application of kentledge, the soil either being grabbed out by bucket in the dry or under water. Skin friction may be reduced by the application of bentonite mud maintained in an annulus above a choker ring, itself above the cutting edge.

Problems with water inflow and blowing at the excavation base can be removed by using mechanical excavation under water. Calculations for base heave, involving shaft-wall weight, should take no account of frictional resistance if a bentonite lubricant is used.

Construction within a sheet-piled cofferdam. Lateral transmission of groundwater can be cut off by driving a sheet-piled cofferdam to a suitable distance below the base of the excavation. If the piles are to be incorporated into the permanent works the base slab will be fastened to them. On the other hand, the shaft can be constructed within the cofferdam and the sheet piles withdrawn when the base slab is cast. In either case, control of the hydrostatic pressure beneath the base slab must be maintained until the weight of the shaft exceeds the maximum hydrostatic uplift force. Any friction between sheet piles forming part of the permanent works and the surrounding soil can be used to resist hydrostatic uplift pressure and should be entered into the calculations.

Ideally, and if available at a convenient depth, the sheet-pile toes will be seated in a less permeable and firmer horizon. If not, then a suitable cut-off depth can most simply be estimated by flow-net analysis involving the hand-sketching of flow lines and equipotential lines.

Diaphragm wall method. Instead of sheet piling, a diaphragm wall—say of hexagonal or pentagonal shape—can be used to support the excavation, and the wall can be incorporated into the permanent works. Construction of such a wall, using bentonite for temporary support with fluid concrete being tremied in at the base to surround a reinforcement cage while displacing the bentonite upwards and out of the trench, is usually a specialist operation.

Jet grouting method. For shaft construction, jet grouting involves the formation *in situ* of contiguous panels of replacement material, usually a cement slurry, for soil removed (see Figure 2.46). Initially, two guide holes, nominally 150 mm diameter, are sunk to the depth at which the panel wall is to be formed. A monitor containing two jet orifices is lowered to the base of one hole, the other hole serving as a disposal route for the soil slurry that is replaced. The upper, soil-excavating, jet relies for its power on water expelled under very high pressure through a very fine nozzle directed towards the spoil-removal hole. The water jet is surrounded by a concentric collar of compressed air which concentrates the jet, particularly below the water table. Cement slurry is injected through the lower jet into the space created by the removal of the soil fines as the monitor is progressively lifted. Adjacent panels of set cement slurry are linked to form continuous walls of low permeability.

Shaft base. A shaft base should be cast on to a clean gravel blanket and contain bleed wells which must be maintained in an effective condition until such time as the weight of the base and the walls exceeds the total hydrostatic uplift forces. The excavation will create an immediate, quasi-elastic heave of the

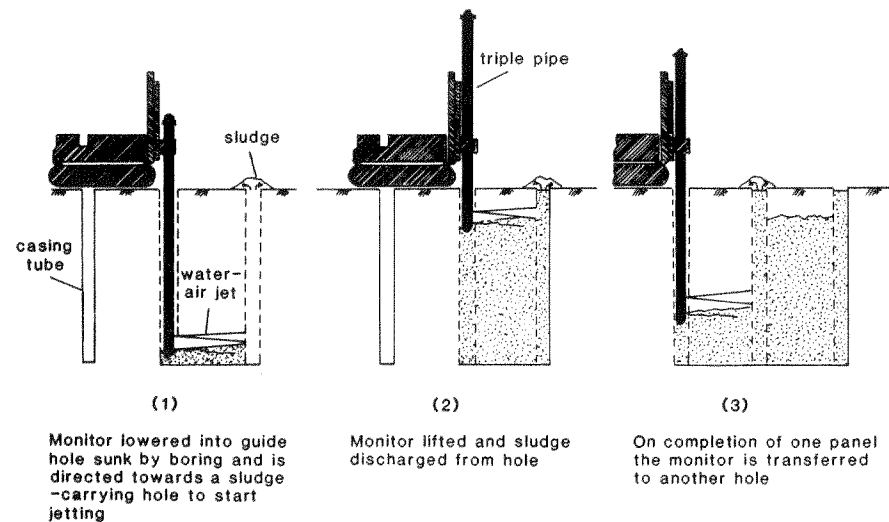


Figure 2.46 GKN Keller Jet Grouting for panel construction.

base—more in the centre than at the sides, which are contained by the shaft walls. Added to this heave there is usually swelling over a period of time in a clay soil. Progressive excavation will obscure the immediate heave and some of the swelling will be resisted by early placement of the base slab, itself to be reduced by subsequent consolidation settlement. The consolidation settlement cannot exceed the degree of swell, and the side friction along the walls of the shaft will tend to reduce load applied by the base. When the calculated weight of the emplaced construction material exceeds the total hydraulic uplift, the wells can be shut off. The original groundwater table will then be progressively restored, resulting in upward elastic and time-dependent movements at the shaft. Side-wall friction at the shaft will restrict this movement, the magnitude of which will in any case be less than the total settlement experienced by the shaft construction before bleed-well closure. Connections between tunnels and shaft should either be of rigid design to resist differential movements between the two or should be flexible enough to accommodate them. It is, in any case, advisable to complete the shaft and base construction some time before making the tunnel connections so that most movement will have ceased.

Buried services. There are several options, including the following.

Isolation: Excavation around an old cast iron main in a carefully staged operation and replacement of the original, compacted backfill with a more deformable material such as blast-furnace coke. If the trench excavation is in a busy street, then the trench must be bridged by cast iron sheeting. After ground movements have ceased, the temporary backfill material must be removed and replaced by specified backfill recompacted to standard. For very old mains, where considerable corrosion may have taken place, this isolation operation may not be feasible, and in any case the movements accompanying exposure could exceed those caused by tunnelling. Almost certainly, the opportunity would be taken to replace the main with a new polyethylene pipe.

Replacement: Replace with less brittle, polyethylene pipe.

Insertion: Renovate old cast iron pipelines of 75 mm and 100 mm diameter by forced insertion of thermoplastic polyethylene. A machine is drawn through the old main, expanding and fracturing it progressively and pulling through a replacement PVC sleeve. A polyethylene pipe is then placed within this protective sleeve. Longitudinal slip movement can be accommodated between pipe and soil.

2.14 Pretunnelling protection of structures

There are several methods whereby building foundations can be isolated, or partially isolated, from ground that is expected to deform around them. These

include diaphragm walling, underpinning (with provision for progressive jacking to overcome settlements), grouting (to render soil adjacent to the structural foundation less prone to deform), sheet piling (although perhaps with the penalty of some vibration damage and weakening of the foundation soil) and contiguous bored-pile walls.

Such methods may be only partially successful and, in view of their expense, should be given very careful consideration before adoption. Most of the methods, and particularly underpinning, are really only applicable with vertical movements in view, whereas lateral distortions can be potentially severe. As noted above (particularly with respect to sheet piling, although it applies to all protective measures) the protective engineering operations could well induce more structural damage than might have been caused by the tunnelling-induced ground movements without the protection.